Vol. L. FEBRUARY, 1924. No. 2.

AMERICAN SOCIETY OF CIVIL ENGINEERS

INSTITUTED 1852

REPORTS, PAPERS, DISCUSSIONS, AND MEMOIRS

CONTENTS

For Index to all Papers, the discussion of which is current in *Proceedings*, see the second page of the cover.

ANALYSIS OF THE STRESSES IN THE RING OF A CONCRETE SKEW ARCH

By J. Charles Rathbun,* M. Am. Soc. C. E.

To Be Presented February 6, 1924.

Synopsis

Although the skew arch is at best an awkward structure, it frequently furnishes the most advantageous solution of an engineering problem.

This paper presents a mathematical analysis of the stresses in a skew arch with fixed ends, and gives examples of the application of the formulas derived. The writer does not claim that this is an exact solution, but does think that the errors involved are no greater than are customary in such work, particularly in the case of a spandrel-filled arch where the load distribution is problematical. Two examples of the application of the formulas are given: First, an analysis of the live and dead load stresses for a spandrel-filled arch; and, second, the effect of a concentrated vertical load on a small model arch. In the first instance, particular attention is paid to the horizontal loads due to the earth thrust with respect not only to its pressure on the arch ring directly, but also to the reaction of the spandrel walls caused by it.

The ring of a concrete skew arch is a statically indeterminate structure containing forces and moments in such positions that in general all cannot be made parallel to a single plane. It must be analyzed, therefore, in three dimensions instead of in the two used with a right arch. However, if all the loads are vertical, symmetrically placed, and lie in a plane that is midway between the spandrel walls, a section parallel to this plane and to the walls can be used for the purpose of a trial analysis.

The assumption of this position of the forces is likely to be in error as is the assumption that the arch thrust against the abutment is eccentric, which eccentricity results in greater compression on the obtuse corner. If the loads do not lie in this plane, it is difficult to foresee the stress distribution and it is possible to have the greatest thrust at the acute end of the abutment.

Formulas are developed for computing the stresses in amount and location for any given arch.

The method of application in its simplest form is given for two cases of flat arches (slabs) in order to present the general outline of procedure free from the lengthy arithmetical computations involved in the design of real arches.

Note.—This paper is issued before the date set for presentation and discussion. Correspondence is invited and may be sent by mail to the Secretary. Discussion on the paper will be closed in May, 1924, and, when finally closed, the paper, with discussion in full, will be published in *Transactions*.

* Asst. Prof., Civ. Eng., Univ. of Washington, Seattle, Wash.

The paper is divided into four parts as follows:

First.—An introduction.

Second.—An outline of the theory, with a statement of the simultaneous equations that define the forces and moments at the crown; also, a simple application of the method.

Third.—An application of the theory to two cases, including an existing arch.

Fourth.—As an Appendix, the development of the theory and the derivation of the equations and loading terms for typical loads.

Introduction

An examination of engineering literature relating to skew arches shows that it is customary to divide the arch ring into laminas by means of planes parallel to the spandrel walls, and to treat these parts as if there were no skew, on the assumption that this method gives safe results because it uses the longest possible span. Several years ago, the writer designed and built a skew arch based on this method of analysis. Cracks appeared later, giving evidence of faulty design. An arch similarly designed and built in a neighboring city a few years afterward recently failed,* indicating tension where the analysis showed compression. The reasoning leading to the approximate solution is questionable as it neglects many forces and moments entirely, particularly the horizontal forces.

When skew crossings are unavoidable, an arch, properly designed, is frequently the most satisfactory and artistic structure available. The skew introduces certain forces and moments not present at all in right arches or present only to a small degree. These factors have not been discussed in published data of past designs, and, therefore, a study of their magnitude and effect on the stresses in the arch ring is desirable.

It is hoped that the discussion of this paper will lead to more practical methods, in case the solution given here does not appeal to bridge designers. It is admitted that the work is laborious, but by the aid of a slide rule and calculating machine, the required time is brought within reason. The formulas submitted include the effect of direct thrust and the deformation due to shear, but the work can be shortened somewhat by following the usual practice of neglecting these factors. In general, those terms that contain the moment of inertia of the section about the normal also can be neglected. A designer experienced in this class of work should be able to foresee, after the first trial design, what terms may be dropped in the case of a particular arch.

It is customary in analyzing a right arch to take a section of unit width. In the case of the skew arch, the width has important properties and the whole arch ring must be considered. In doing this, it is assumed that the load is distributed over the width of the ring, otherwise, some error is involved.

* *Engineering News-Record*, February 22, 1923.

as, for example, when the arch is of the open spandrel type and the load from the roadway is transferred to the ring by posts, in which case it is assumed here that provision is made to distribute this load across the ring parallel to the barrel of the arch.

Outline of Theory

Consider the arch ring as divided into two sections by a plane parallel to the axis of the barrel. This plane should be perpendicular to the surface of the arch ring at the line of intersection. Each section will be considered as a curved cantilever beam (see Fig. 1), rigidly supported at the abutments and subjected to outside forces (the loads), as well as to the force and moment developed at the plane of intersection by the other half. The problem becomes one of determining what force and moment on this plane will account for the movement of the two parts, such as will keep them coincident at their plane of intersection. In general, the lines representing both the force and the axis of the moment will be inclined to the plane; the common point at which the two lines intersect this plane will be designated C. If the arch ring is symmetrical about a vertical line through the crown, it will simplify the problem greatly to pass the cutting plane through the line of symmetry, in which case the point where this line intersects the neutral surface can be taken as the point, C.

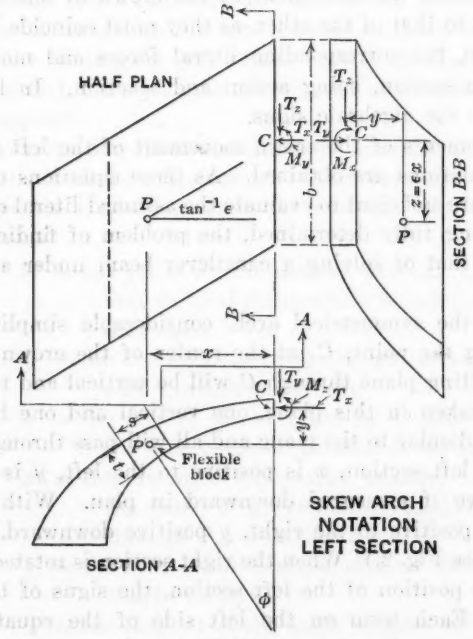

FIG. 1.

The components of the force and of the moment with respect to each of three axes are taken separately, requiring six independent quantities to express completely the crown reaction. These six quantities are expressed as letters

(unknown in value as yet) and thus used when defining the deflection of the crown of either section.

To express completely the deflection of the face cut by the plane through the crown also requires six quantities. These quantities have been taken as the movement of the center point, C, in the direction of each of the three axes and also the angular movement of this face about the same axes. As these six quantities are mutually independent of each other, they may be taken as the six defining quantities. The value of each of these movements for both the left and the right sections can be expressed in terms of the external loads, certain physical characteristics of the arch ring, and the six literal quantities denoting the crown reaction.

Consider the length of ring contained between two planes at a distance, s, apart. (See Fig. 1.) Without serious error this part may be considered as a rectangular parallelopiped. The forces and moments at the crown, together with the external loads, subject this parallelopiped to thrust, shear, moment, and torsion, distorting it and thereby displacing the crown relative to the abutment. The entire section is composed of a number of these blocks, each acting under the influence of a set of forces.

At the same time, the right section of the arch is being acted on by another set of forces and moments which displaces its crown face. The abutments being fixed, of necessity the movement of the crown of one section must be equal in magnitude to that of the other, as they must coincide both before and after loading. Also, the corresponding literal forces and moments have the same value on each section, being action and reaction. In both cases, care must be taken as to the algebraic signs.

Equating the elements of the crown movement of the left section to those of the right, six equations are obtained. As these equations are independent of each other, they are sufficient to evaluate the assumed literal quantities. The crown reactions being fully determined, the problem of finding the stress at any point becomes that of solving a cantilever beam under a given loading. (See Fig. 1.)

In the case of the symmetrical arch, considerable simplification can be effected by choosing the point, C, at the center of the crown on the line of symmetry. The cutting plane through C will be vertical and two of the three axes may then be taken in this plane, one vertical and one horizontal. The third will be perpendicular to the plane and all will pass through the point, C. In considering the left section, x is positive to the left, y is positive downward, and z positive if measured downward in plan. With the right section, however, x is positive to the right, y positive downward, and z positive upward in plan. (See Fig. 2.) When the right section is rotated about the line of symmetry to the position of the left section, the signs of the co-ordinates will be the same. Each term on the left side of the equations as found previously has a corresponding term on the right side, except in the case of the loading, which may be unsymmetrical. These corresponding terms either cancel or combine, depending on the algebraic sign. This materially shortens the formulas and the work of analysis. In this paper, the case of the sym-

metrical arch ring only has been considered; formulas for the unsymmetrical case can be developed similarly, but they are considerably longer and not of sufficient use to warrant the necessary study.

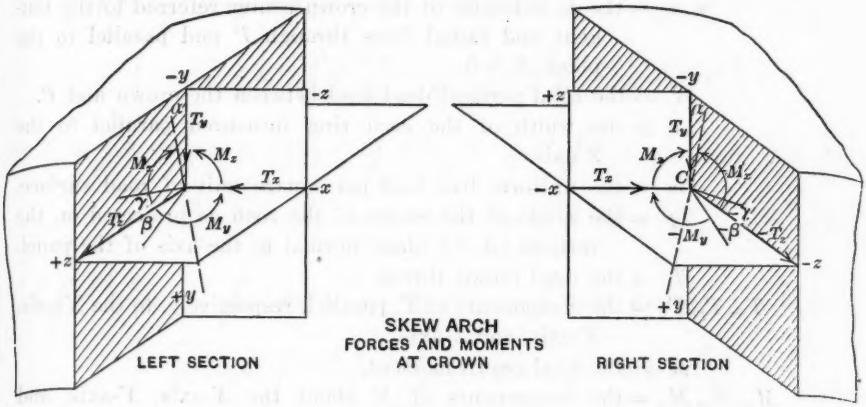

FIG. 2.

The solution of the six equations with six unknowns is not as formidable a task as at first appears. The work is divided into two groups, one containing two equations with two unknowns, and the other, four equations with four unknowns. The latter group quickly reduces to three equations with three unknowns. If the loading as well as the arch is symmetrical (as for a dead load with a level fill), the equations are reduced still further in number, as the first group disappears.

The nomenclature for these simultaneous equations is here given. Care must be used in substituting in these and other formulas in this paper, to use consistent units; in a practical case, the foot and kip will probably be the most advantageous:

P = any point on the neutral axis of the arch ring lying in that vertical plane which is half way between the spandrel walls.

x, y = the co-ordinates of P referred to vertical and horizontal axes through the crown.

A = the area of the arch cut by a plane through P radial to the arch ring and parallel to the axis of the arch panel.

$\bar{x}$ = the distance (measured parallel to the X-axis) from the center of gravity of the load, W, to a vertical plane through P. (See Fig. 5.)

λ = the ratio between the moduli of elasticity in compression and in shear.

ϵ = the tangent of the angle of skew of the arch.

ϕ = the angle of slope of a plane tangent to the neutral surface of the arch at P.

I_y = the moment of inertia of the area, A, about the line through P normal to the neutral surface.

I_z = the moment of inertia of the area, A, about a horizontal line through P parallel to the Z-axis.

F = the factor of torsion, described later. (See page 140.)

u, v = the co-ordinates of the crown center referred to the tangent and radial lines through P and parallel to the plane, $Z = 0$.

W = the total vertical dead load between the crown and P.

b = the width of the arch ring measured parallel to the Z-axis.

w = the uniform live load per square unit of road surface.

g = the grade of the crown of the road as projected on the vertical (X-Y) plane normal to the axis of the panel.

T = the total crown thrust.

T_x, T_y, T_z = the components of T, parallel, respectively, to the X-axis, Y-axis, and Z-axis.

M = the total crown moment.

M_x, M_y, M_z = the components of M about the X-axis, Y-axis, and Z-axis, respectively.

f = the depth of fill over the arch at the line of symmetry. (See Fig. 5.)

e_c = one-half the thickness of the arch at the crown.

t = the thickness of the arch, measured radially at the point, P.

$e = \frac{1}{2}\, t \cos \phi$. (See Fig. 5.)

ω = the weight of the fill per cubic unit.

n = the difference between the elevations of the fill at the spandrel walls on either side at the crown. (See Fig. 5.)

η_d = the ratio between the horizontal and the vertical earth pressures due to the dead load.

η_l = the ratio between the horizontal and the vertical earth pressures due to the live load.

Simultaneous Equations.—The required equations for the symmetrical arch under a dead and a uniform load over the entire road surface are as follows, where the integrations are taken over the half arch ring from the crown to the abutment:

$$\left(\int y^2 \frac{d\,s}{I_z} + \varepsilon^2 \lambda \int x^2 \sin^2 \phi \frac{d\,s}{F}\right) T_x - \left(\varepsilon \lambda \int u\, x \sin \phi \frac{d\,s}{F}\right) T_z$$

$$+ \left(\int y \frac{d\,s}{I_z}\right) M_z - \left(\varepsilon \lambda \int x \sin \phi \cos \phi \frac{d\,s}{F}\right) M_x = W \bar{x}\, y \frac{d\,s}{I_z}$$

$$+ \varepsilon^2 \lambda \int W \bar{x}\, x \sin \phi \cos \phi \frac{d\,s}{F} + \frac{1}{2}\, b\, w \int x^2\, y \frac{d\,s}{I_z}$$

$$+ \frac{1}{2}\, \varepsilon^2 \lambda\, b\, w \int x^3 \sin \phi \cos \phi \frac{d\,s}{F} + \eta_a\, b\, \omega \left\{ - \frac{1}{6}\, b\, n\, \lambda\, \varepsilon \int x\, y \sin^2 \phi \frac{d\,s}{F}\right.$$

$$+\frac{1}{6}\ b\ n\ \lambda\ \varepsilon\int e\,x\sin^2\phi\,\frac{d\,s}{F}-\varepsilon^2\left(\frac{1}{2}\ f^2-f\ e_c+\frac{1}{6}\ n^2\right)\int x^2\sin^2\phi\,\frac{d\,s}{F}$$
$$+\frac{1}{6}\int y^4\,\frac{d\,s}{I_z}+\frac{1}{2}\ f\int y^3\,\frac{d\,s}{I_z}+\frac{1}{2}\ g^2\int x^2\,y^2\,\frac{d\,s}{I_z}+\frac{1}{2}\ f\,g^2\int x^2\,y\,\frac{d\,s}{I_z}$$
$$+\left(f\ e_c-\frac{1}{2}\ e_c^2\right)\int y^2\,\frac{d\,s}{I_z}-\frac{1}{2}\ f\int e^2\,y\,\frac{d\,s}{I_z}-\frac{1}{2}\int y^2\,e^2\,\frac{d\,s}{I_z}$$
$$-f^2\,e_c\int y\,\frac{d\,s}{I_z}\Big\}+\eta_l\ b\ w\left\{\frac{1}{2}\int y^3\,\frac{d\,s}{I_z}+\frac{1}{2}\ g^2\int x^2\,y\,\frac{d\,s}{I_z}+\ e_c\int y^2\,\frac{d\,s}{I_z}\right.$$
$$\left.-\frac{1}{2}\int e^2\,y\,\frac{d\,s}{I_z}-\varepsilon^2\,\lambda\,(f-e_c)\int x^2\sin^2\phi\,\frac{d\,s}{F}\right\}\ \ldots\ldots\ldots(1a)$$

$$\left(\int x^2\,\frac{d\,s}{I_z}+e^2\,\lambda\int x^2\cos^2\phi\,\frac{d\,s}{F}\right)T_y-\left(\varepsilon\,\lambda\int x\sin\ \phi\cos\phi\,\frac{d\,s}{F}\right)M_y=$$
$$-\frac{1}{6}\ g\ b\ \omega\int x^4\,\frac{d\,s}{I_z}-\frac{1}{6}\ \varepsilon^2\,\lambda\,g\,b\,\omega\int x^4\cos^2\phi\,\frac{d\,s}{F}$$
$$+\frac{1}{6}\ \varepsilon\,\lambda\,b^2\,n\,\omega\int x^2\cos^2\phi\,\frac{d\,s}{F}+\eta_a\,b\,\omega\left\{\frac{1}{6}\ b\,n\,g\,\varepsilon\,\lambda\int x^2\sin^2\phi\cos\phi\,\frac{d\,s}{F}\right.$$
$$-\frac{1}{6}\,g^3\int x^4\,\frac{d\,s}{I_z}-\frac{1}{2}\ g\int x^2\,y^2\,\frac{d\,s}{I_z}-f\,g\int x^2\,y\,\frac{d\,s}{I_z}$$
$$\left.-\left(\frac{1}{2}\ f^2+\frac{1}{6}\ n^2\right)g\int x^2\,\frac{d\,s}{I_z}\right\}-\eta_l\,b\,w\left\{g\int x^2\,y\,\frac{d\,s}{I_z}\right.$$
$$\left.+f\,g\int x^2\,\frac{d\,s}{I_z}\right\}\ \ldots\ldots\ldots\ldots\ldots\ldots\ldots(1b)$$

$$\left(-\varepsilon\,\lambda\int u\,x\sin\phi\,\frac{d\,s}{F}\right)T_x+\left(\lambda\int u^2\,\frac{d\,s}{F}\right)T_z+\left(\lambda\int u\cos\phi\,\frac{d\,s}{F}\right)M_x=$$
$$-\varepsilon\,\lambda\int W\,\bar{x}\,u\cos\phi\,\frac{d\,s}{F}-\frac{1}{2}\,\varepsilon\,\lambda\,b\,w\int x^2\,u\cos\phi\,\frac{d\,s}{F}$$
$$+\eta_a\,b\,\omega\left\{\frac{1}{6}\ b\,n\,\lambda\int y\,u\sin\phi\,\frac{d\,s}{F}-\frac{1}{6}\ b\,n\,\lambda\int e\,u\sin\phi\,\frac{d\,s}{F}\right.$$
$$+\frac{1}{6}\ b\,n\,e_c\,\lambda\int u\sin\phi\,\frac{d\,s}{F}+\varepsilon\left(\frac{1}{2}\ f^2-f\,e_c+\frac{1}{6}\ n^2\right)\int x\,u\sin\phi\,\frac{d\,s}{F}\Big\}$$
$$\left.+\eta_l\,b\,w\Big\{\varepsilon\,\lambda\,(f-e_c)\int u\ x\ \sin\phi\,\frac{d\,s}{F}\right\}\ \ldots\ldots\ldots\ldots(1c)$$

$$\left(\int y\,\frac{d\,s}{I_z}\right)T_x+\left(\int\frac{d\,s}{I_z}\right)M_z=\int W\,\bar{x}\,\frac{d\,s}{I_z}+\frac{1}{2}\ b\,w\int x^2\,\frac{d\,s}{I_z}$$
$$+\eta_a\,b\,\omega\left\{\frac{1}{6}\int y^3\,\frac{d\,s}{I_z}+\frac{1}{2}\ f\int y^2\,\frac{d\,s}{I_z}+\frac{1}{2}\,g^2\int x^2\,y\,\frac{d\,s}{I_z}\right.$$
$$\left.+\frac{1}{2}\,f\,g^2\int x^2\,\frac{d\,s}{I_z}+\left(f\,e_c-\frac{1}{2}\ e_c^2\right)\int y\,\frac{d\,s}{I_z}-\frac{1}{2}\ f\int e^2\,\frac{d\,s}{I_z}\right.$$

$$-\frac{1}{2}\int y\,e^2\frac{d\,s}{I_z}-f^2\,e_c\int\frac{d\,s}{I_z}\Big\}+\eta_l\,b\,w\Big\{\frac{1}{2}\int y^2\frac{d\,s}{I_z}+\frac{1}{2}\,g^2\int x^2\frac{d\,s}{I_z}$$
$$+e_c\int y\frac{d\,s}{I_z}-\frac{1}{2}\int e^2\frac{d\,s}{I_z}\Big\}\quad\ldots\ldots\ldots\ldots\ldots\ldots(1d)$$

$$\Big(-\varepsilon\,\lambda\int x\sin\phi\cos\frac{d\,s}{F}\Big)\,T_y+\Big(\lambda\int\sin^2\phi\frac{d\,s}{F}\Big)\,M_y$$
$$=\frac{1}{6}\,\varepsilon g\,b\,\omega\,\lambda\int x^3\sin\phi\cos\phi\frac{d\,s}{F}-\frac{1}{6}\,\lambda\,b^2\,n\,\omega\int x\sin\phi\cos\phi\frac{d\,s}{F}$$
$$-\eta_a\,b\,\omega\Big\{\frac{1}{6}\,b\,n\,\lambda\,g\int x\sin^2\phi\frac{d\,s}{F}\Big\}\quad\ldots\ldots\ldots\ldots\ldots\ldots(1e)$$

$$\Big(-\varepsilon\,\lambda\int x\sin\phi\cos\phi\frac{d\,s}{F}\Big)\,T_x+\Big(\lambda\int u\cos\phi\frac{d\,s}{F}\Big)\,T_z$$
$$+\Big(\lambda\int\cos^2\phi\frac{d\,s}{F}\Big)\,M_x=-\varepsilon\,\lambda\int W\bar{x}\cos^2\phi\frac{d\,s}{F}$$
$$-\frac{1}{2}\,\varepsilon\,\lambda\,b\,w\int x^2\cos^2\phi\frac{d\,s}{F}+\eta_a\,b\,\omega\Big\{\frac{1}{6}\,b\,n\,\lambda\int y\sin\phi\cos\phi\frac{d\,s}{F}$$
$$-\frac{1}{6}\,b\,n\,\lambda\int e\sin\phi\cos\phi\frac{d\,s}{F}+\frac{1}{6}\,b\,n\,e_c\,\lambda\int\sin\phi\cos\phi\frac{d\,s}{F}$$
$$+\varepsilon\,\lambda\Big(\frac{1}{2}f^2-f\,e_c+\frac{1}{6}\,n^2\Big)\int x\sin\phi\cos\phi\frac{d\,s}{F}\Big\}$$
$$+\eta_l\,b\,w\Big\{\varepsilon\,\lambda\,(f-e_c)\int x\sin\phi\cos\phi\frac{d\,s}{F}\Big\}\quad\ldots\ldots\ldots\ldots(1f)$$

The factor of torsion, F, may be computed from Equation (2):

$$\frac{1}{F}=\frac{205\,\pi\,(t^2+b^2)}{180\,b^3\,t^3}\quad\ldots\ldots\ldots\ldots\ldots\ldots\ldots\ldots(2)$$

As the angular rotation of a circular shaft under stress may be computed by the equation, $\theta=\frac{T\,l}{E_s\,I_p}$, in which, θ is the angular rotation in radians, T, the torsion, l, the length of shaft, E_s, the modulus of elasticity in shear, and I_p, the polar moment of inertia, so with the rectangular shaft the angular rotation may be computed from the formula, $\theta=\frac{T\,l}{E_s\,F}$, in which F has a value dependent on the width and breadth of the shaft. As the value of F enters quite prominently into the final computations, the writer hopes that the discussion will emphasize any difference of opinion regarding its amount.*

In the practical application of the formulas, finite quantities must be used unless a definite mathematical shape is given to the arch ring. If $d\,s$ is taken

* This formula is an approximation from one derived by St. Vennant for the rigidity of rectangular shafts. It is given in numerous works on Mechanics, as well as in Mark's "Handbook". Recent experiments described in *Bulletin No. 3*, Faculty of Applied Science and Engineering School of Engineering Research, University of Toronto, give the formula and also show that the rigidity of concrete in torsion is little affected by reinforcement.

as a constant finite quantity, s, the integrations become summations and all Equations (1) are used as though written in the form:

$$\left(\Sigma \frac{y}{I_z}\right) T_x + \left(\Sigma \frac{1}{I_z}\right) M_x = \Sigma W \bar{x} \frac{1}{I_z} + \ldots\ldots - \frac{1}{2} \sum \frac{e^2}{I_z} \Big\} \ldots (1\,d')$$

The constant, s, enters into each term and, therefore, cancels.

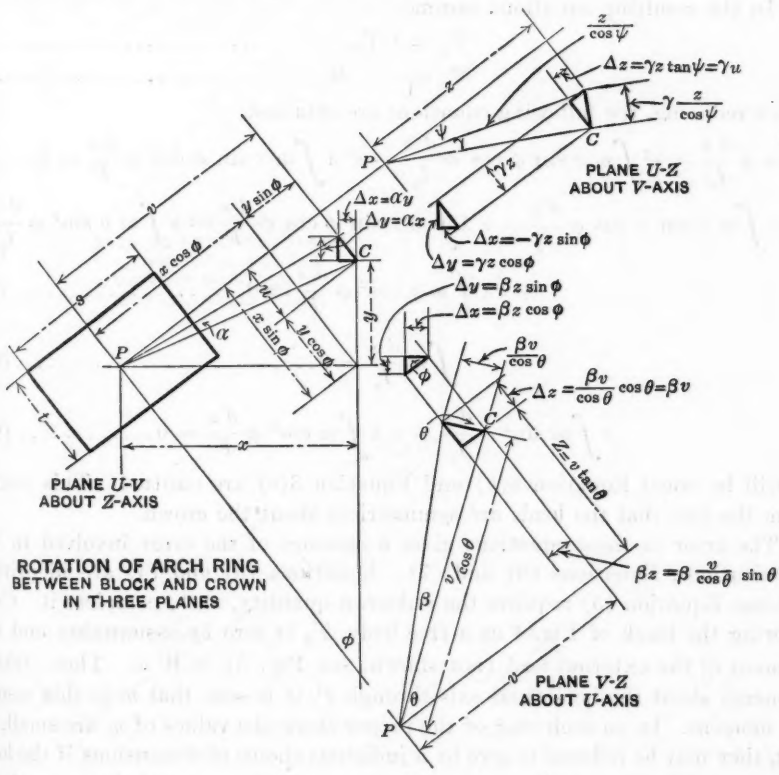

FIG. 3.

It is to be noted that the left side of the equations depends only on the arch ring, whereas the right side is determined by the method of loading. In addition to the loading given, the formulas for the loading terms due to a concentrated vertical load placed at any point on the arch (co-ordinates x', z') have been deduced and are given in the Appendix. As the method used is given in detail, it is felt that any other case that may arise in practice can be treated in the same way.

Error in Approximate Method.—It has been suggested that the approximate method of analysis, that is, by considering lamina parallel to the spandrel walls, is questionable. To estimate the error involved in the approximate method, consider the equations with loading terms for vertical dead load and level grade only. All terms will be considered except those having A in the denominator,

that is, those due to direct thrust and shear, which are usually neglected in arch design. In these equations substitute,

$$v = x \cos \phi + y \sin \phi \quad \ldots\ldots (3)$$

$$u = x \sin \phi - y \cos \phi \quad \ldots\ldots (4)$$

$$W \bar{x} = T_x y + M_z - m \quad \ldots\ldots (5)$$

In the resulting equations assume,

$$T_z = \varepsilon T_x \quad \ldots\ldots (6)$$

$$M_x = - \varepsilon M_z \quad \ldots\ldots (7)$$

After reducing, the following equations are obtained:

$$\int m y \frac{d s}{I_z} - \varepsilon^2 \int m x \sin \phi \cos \phi \frac{d s}{I_y} - \varepsilon^2 \lambda \int m x \sin \phi \cos \phi \frac{d s}{F} = 0 \ldots (8a)$$

$$\varepsilon \int m x \sin \phi \cos \phi \frac{d s}{I_y} + \varepsilon \lambda \int m x \sin \phi \cos \phi \frac{d s}{F} - \varepsilon \int m y \sin^2 \phi \frac{d s}{I_y} + \varepsilon \lambda \int m y \cos^2 \phi \frac{d s}{F} = 0 \quad \ldots\ldots (8c)$$

$$\int m \frac{d s}{I_z} = 0 \quad \ldots\ldots (8d)$$

$$\varepsilon \int m \sin^2 \phi \frac{d s}{I_y} + \varepsilon \lambda \int m \cos^2 \phi \frac{d s}{F} = 0 \quad \ldots\ldots (8f)$$

It will be noted Equation 8(b) and Equation 8(e) are omitted. This results from the fact that the loads are symmetrical about the crown.

The error in these equations gives a measure of the error involved in the substitutions, Equations (6) and (7). Equations (3) and (4) are identities, whereas Equation (5) requires the unknown quantity, m, to complete it. Considering the block of Fig. 4 as a free body, T_y is zero by assumption and the moment of the external load (not shown, see Fig. 5) is $W \bar{x}$. Then, taking moments about the horizontal axis through P, it is seen that m is this resultant moment. In an arch ring of the proper shape the values of m are small, in fact, they may be reduced to zero by a judicious choice of dimensions if the load is definitely known. $W \bar{x}$ may be taken as any loading provided the resultant of all the loads on each block is vertical and lies in a plane midway between the spandrel walls.

To show that the values obtained by the approximate method for T and M are nearly the same as by the more involved one under the assumed limitations of loading, let $\epsilon = 0$ in the original equations for level dead load. Then,

$$\int y^2 \frac{d s}{I_z} T_x + \int y \frac{d s}{I_z} M_z = \int W \bar{x} y \frac{d s}{I_z} \quad \ldots\ldots (9a)$$

$$\int y \frac{d s}{I_z} T_x + \int \frac{d s}{I_z} M_z = \int W \bar{x} \frac{d s}{I_z} \quad \ldots\ldots (9b)$$

which are the equations for a right arch. Assume the arch ring to be re-drawn with the dimensions in the direction of the X-axis increased by a ratio, K. In order that the weight on each block may remain unchanged, the distance between the spandrel walls measured in the Z-direction must be assumed to

be decreased by this same ratio, K. Except for the values of I_z, the terms of the left side of the equations are unchanged, and the value of W is unchanged, but the value of $W\,x$ is multiplied by K, whence the values of both T and M are multiplied by K.

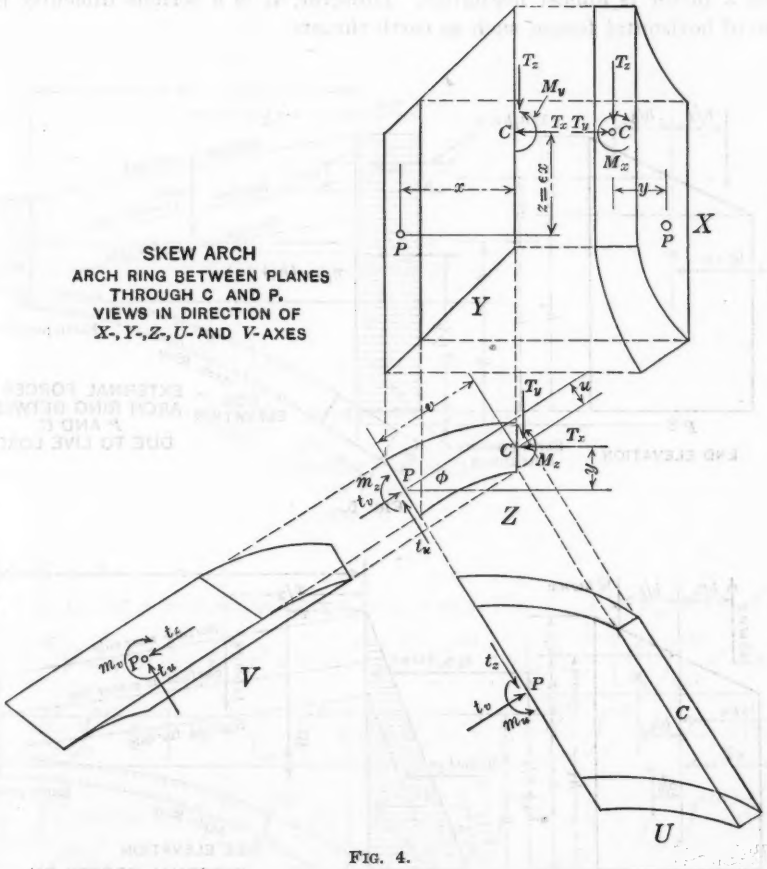

FIG. 4.

This change is exactly the one made when the skew arch is designed by taking laminas parallel to the spandrel walls. In this case, K is equal to the sec. (tan.$^{-1}$ ε) and the results for both T_x and M_x are K times as great as those obtained from the section taken normal to the barrel. The total thrust, T, obtained by analyzing the ring as a skew is,

$$\sqrt{T_x^2 + T_z^2} = \sqrt{1 + \varepsilon^2}\, T_x = K\, T_x \quad \ldots\ldots\ldots\ldots\ldots\ldots (10)$$

and the total moment is,

$$\sqrt{M_x^2 + M_z^2} = K\, M_x \quad \ldots\ldots\ldots\ldots\ldots\ldots\ldots\ldots\ldots\ldots (11)$$

providing the equations of error reduce to identities.

Thus, under certain conditions, the method of design leads to approximately correct results, the approximation depending on the shape of the arch ring. It

is especially to be noted, however, that all the forces must be in one central plane and symmetrically placed about the crown. With respect to vertical forces, this condition is not fulfilled if the surface of the fill is on a grade, as can be seen from the end elevation views in Figs. 5 and 6, but in most designs such a factor is almost negligible. However, it is a serious difficulty in the case of horizontal forces, such as earth thrusts.

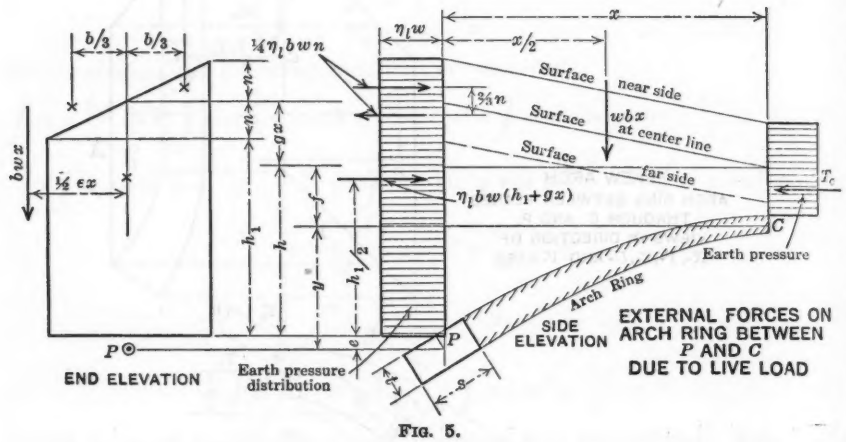

FIG. 5.

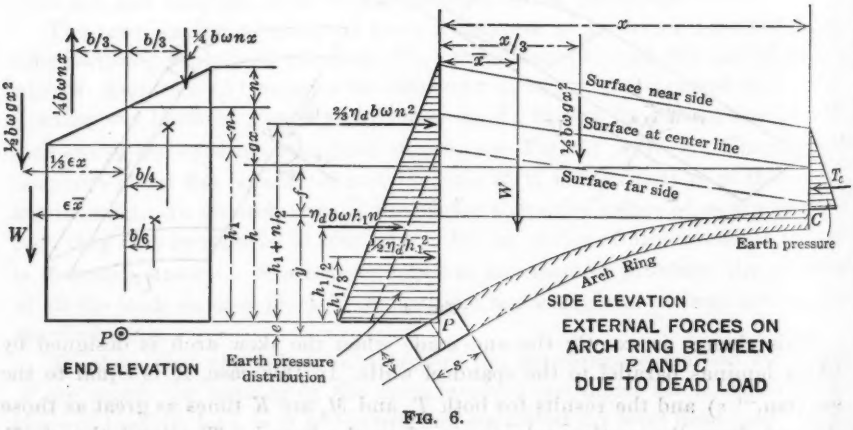

FIG. 6.

Application to a Simple Case.—As an application of Equations (1), let Fig. 7 represent a slab on elastic abutments fixed at the points, A and D. This structure may be treated as an arch and the formulas then used to obtain the reactions along the central plane through the line of symmetry at C. Considering the load to be uniform, the following equations and solution are obtained:

From C to B.

$y = 0, x = x, \cos \phi = 1, \sin \phi = 0, u = 0, v = x, I = I_s, F = F_s, ds = dx.$

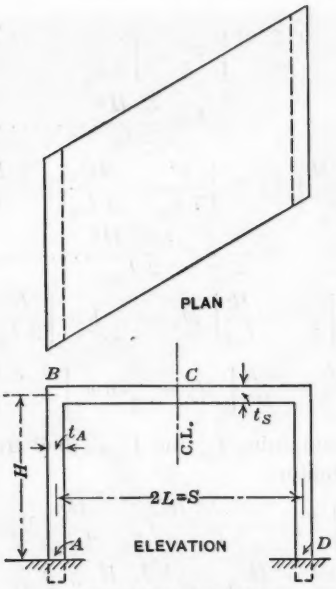

NOTATION FLAT ARCH ON SKEW

FIG. 7.

From B to A:

$y = y,\ x = L,\ \cos\phi = 0,\ \sin\phi = 1,\ u = L,\ v = y,\ I = I_a,\ F = F_a,\ d\,s = d\,y.$

$$\left[\frac{1}{I_{az}}\int_0^H y^2\,d\,y + \frac{\varepsilon^2}{I_{sy}}\int_0^L x^2\,d\,x + \frac{\varepsilon^2\,\lambda\,L^2}{F_a}\int_0^H d\,y\right] T_x - \left[\frac{\varepsilon}{I_{sy}}\int_0^L x^2\,d\,x + \frac{\varepsilon\,\lambda\,L^2}{F_a}\int_0^H d\,y\right] T_z + \frac{1}{I_{az}}\int_0^H y\,d\,y\,M_z = \frac{1}{2}\,b\,w\,\frac{L^2}{I_{az}}\int_0^H y\,d\,y \quad \ldots (12a)$$

$$-\left[\frac{\varepsilon}{I_{sy}}\int_0^L x^2\,d\,x + \frac{\varepsilon\,\lambda\,L^2}{F_a}\int_0^H d\,y\right] T_x + \left[\frac{1}{I_{sy}}\int_0^L x^2\,d\,x + \frac{1}{I_{ay}}\int_0^H y^2\,d\,y + \frac{\lambda\,L^2}{F_a}\int_0^H d\,y\right] T_z - \frac{1}{I_{ay}}\int_0^H y\,d\,y\,M_x = \frac{1}{2}\,b\,w\,\frac{\varepsilon\,L^2}{I_{ay}}\int_0^H y\,d\,y \quad \ldots (12c)$$

$$\left[\frac{1}{I_{az}}\int_0^H y\,d\,y\right] T_x + \left[\frac{1}{I_{sz}}\int_0^L d\,x + \frac{1}{I_{az}}\int_0^H d\,y\right] M_z = \frac{1}{2}\,b\,w\left[\frac{1}{I_{sz}}\int_0^L x^2\,d\,x + \frac{L^2}{I_{az}}\int_0^H d\,y\right] \quad \ldots (12d)$$

$$-\left[\frac{1}{I_{ay}}\int_0^H y\,d\,y\right] T_z + \left[\frac{1}{I_{ay}}\int_0^H d\,y + \frac{\lambda}{F_s}\int_0^L d\,x\right] M_x = \frac{1}{2}\,b\,w\left[\frac{\varepsilon\,L^2}{I_{ay}}\int_0^H d\,y - \frac{\varepsilon\,\lambda}{F_s}\int_0^H x^2\,d\,x\right] \quad \ldots (12f)$$

Integrating:

$$\left[\frac{H^3}{3\,I_{az}}+\frac{\varepsilon^2\,L^2}{3\,I_{sy}}+\frac{\varepsilon^2\,\lambda\,L^2\,H}{F_a}\right]T_x-\left[\frac{\varepsilon\,L^3}{3\,I_{sy}}+\frac{\varepsilon\,\lambda\,L^2\,H}{F_a}\right]T_z+\frac{H^2}{2\,I_{az}}\,M_z$$
$$=\frac{1}{2}\,b\,w\,\frac{L^2\,H^2}{2\,I_{az}}\qquad\text{(13a)}$$

$$-\left[\frac{\varepsilon\,L^3}{3\,I_{sy}}+\frac{\varepsilon\,\lambda\,L^2\,H}{F_a}\right]T_x+\left[\frac{L^3}{3\,I_{sy}}+\frac{H^3}{3\,I_{ay}}+\frac{\lambda\,L^2\,H}{F_a}\right]T_z-\frac{H^2}{2\,I_{ay}}\,M_x$$
$$=\frac{1}{2}\,b\,w\,\frac{\varepsilon\,L^2\,H^2}{2\,I_{ay}}\qquad\text{(13c)}$$

$$\left[\frac{H^2}{2\,I_{az}}\right]T_x+\left[\frac{L}{I_{sz}}+\frac{H}{I_{az}}\right]M_z=\frac{1}{2}\,b\,w\left[\frac{L^3}{3\,I_{sz}}+\frac{L^2\,H}{I_{az}}\right]\qquad\text{(13d)}$$

$$\left[-\frac{H^2}{2\,I_{ay}}\right]T_z+\left[\frac{H}{I_{ay}}+\frac{\lambda\,L}{F_s}\right]M_x=\frac{1}{2}\,b\,w\left[-\frac{\varepsilon\,L^2\,H}{I_{ay}}-\frac{\varepsilon\,\lambda\,L^3}{3\,F_s}\right]\qquad\text{(13f)}$$

Dropping all terms containing I_{ay} and I_{sy} as they are large in numerical value and occur in the denominator:

$$\left[\frac{H^3}{3\,I_{az}}+\frac{\varepsilon\,\lambda\,L^2\,H}{F_a}\right]T_x-\frac{\varepsilon\,\lambda\,L^2\,H}{F_a}\,T_z+\frac{H^2}{2\,I_{az}}\,M_z=\frac{1}{2}\,b\,w\,\frac{L^2\,H^2}{2\,I_{az}}\qquad\text{(14a)}$$

$$-\frac{\varepsilon\,\lambda\,L^2\,H}{F_a}\,T_x+\frac{\lambda\,L^2\,H}{F_a}\,T_z=0\qquad\text{(14c)}$$

$$\frac{H}{2\,I_{az}}\,T_x+\left[\frac{L}{I_{sz}}+\frac{H}{I_{az}}\right]M_z=\frac{1}{2}\,b\,w\left[\frac{L^3}{3\,I_{sz}}+\frac{L^2\,H}{I_{az}}\right]\qquad\text{(14d)}$$

$$\frac{\lambda\,L}{F_s}\,M_x=-\frac{1}{2}\,b\,w\,\frac{\varepsilon\,\lambda\,L^3}{3\,F_s}\qquad\text{(14f)}$$

From Equation 14 (e):

$$\varepsilon\,T_x=T_z\qquad\text{(15)}$$

From Equation 14 (f):

$$M_x=-\frac{\varepsilon\left(\frac{1}{2}\,b\,w\right)L^2}{3}=-\frac{\varepsilon\,b\,w\,S^2}{24}\qquad\text{(16)}$$

Substituting Equation (15) in Equation (14a):

$$\frac{H^3}{3\,I_{az}}\,T_x+\frac{H^2}{2\,I_{az}}\,M_z=\frac{1}{2}\,b\,w\,\frac{L^2\,H^2}{2\,I_{az}}\qquad\text{(17)}$$

From Equations (17) and (14d):

$$\left[\frac{L}{I_{sz}}+\frac{H}{4\,I_{az}}\right]M_z=\frac{1}{2}\,b\,w\left[\frac{L}{3\,I_{sz}}+\frac{H}{4\,I_{az}}\right]L^2\qquad\text{(18)}$$

$$H\left[\frac{L}{I_{sz}}+\frac{H}{4\,I_{az}}\right]T_x=\frac{1}{2}\,b\,w\,\frac{L^3}{I_{sz}}\qquad\text{(19)}$$

It is to be noted that although $T_z=\epsilon\,T_x$ for all values of S and H (Fig. 7), it is not true in general that $M_x=-\epsilon\,M_z$. If H is placed equal to zero, the moment on a slab fixed at the ends becomes $-M_x=\varepsilon\,M_z=\frac{1}{24}\,b\,w\,S^2$; in this

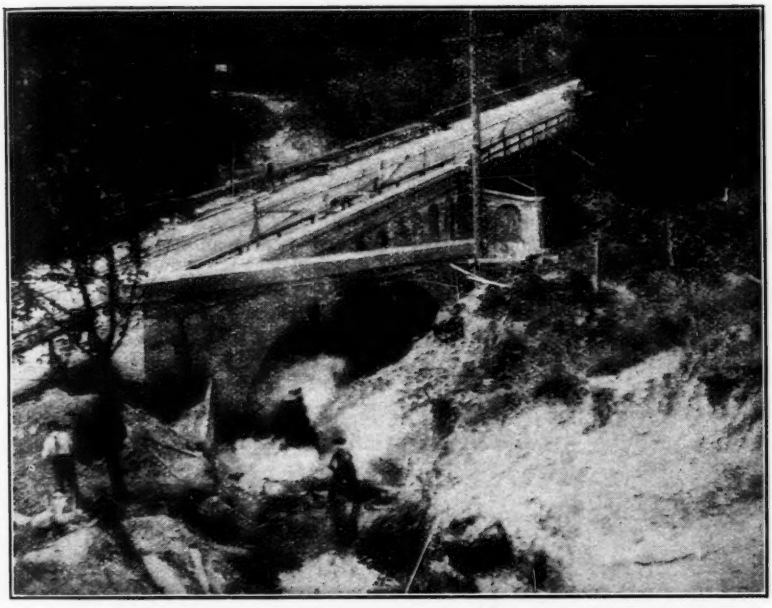

FIG. 8.—VIEW LOOKING DOWN, DURING CONSTRUCTION, OF SKEW ARCH IN LESCHI PARK, SEATTLE, WASH.

FIG. 9.—VIEW LOOKING UP, COMPLETED SKEW ARCH IN LESCHI PARK, SEATTLE, WASH.

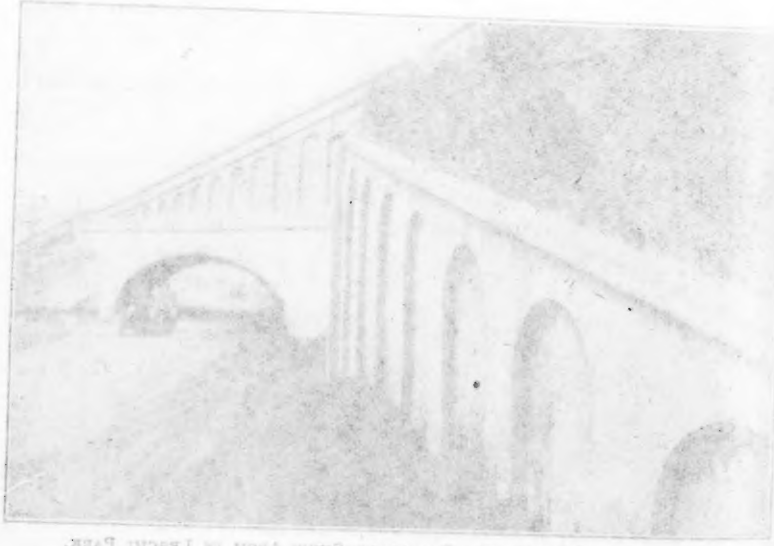

case, the span may be analyzed by taking laminas parallel to the spandrel wall. Incidentally, as $y = 0$ and $\sin \phi = 0$, the terms in all the equations giving the measure of error reduce to zero, except in Equation 14 (d) which reduces to zero from other considerations.

If, however, I_{az} is made very small compared to I_{sz}, $M_z = \frac{1}{8} b w S^2 \ddagger -\frac{M_x}{\varepsilon}$ the latter remaining $-\frac{1}{24} b w S^2$. The equations giving the error are no longer reduced to identities as $\int m \frac{d s}{I_z} \ddagger 0$. This is the case of a flat slab resting on skew abutments, but without fixed ends.

To take a definite example, assume the following dimensions:

$b = 20$ ft.; $t_s = t_a = 1$ ft.; $S = 30$ ft.; $H = 12$ ft.; $w = 0.1$ kip per sq. ft. then,

$$I_z = I_a = \frac{1}{12} (20) (1)^3, \frac{F}{\lambda} = \frac{(1) (20)}{9}$$

$$M_x = -\varepsilon \frac{20}{24} (0.1) (30)^2 = -75 \varepsilon \ldots\ldots\ldots\ldots\ldots\ldots (20)$$

$$[18 + 1.8] M_z = [6 + 1.8] 30^2 \ldots\ldots\ldots\ldots\ldots\ldots (21)$$

$$12 [18 + 1.8] T_x = \frac{12}{20} (30)^3 \ldots\ldots\ldots\ldots\ldots\ldots (22)$$

$$M_z = \frac{13}{11} (75) \ldots\ldots\ldots\ldots\ldots\ldots (23)$$

$$\varepsilon T_x = T_z = \frac{750}{11} \varepsilon \ldots\ldots\ldots\ldots\ldots\ldots (24)$$

Application of Theory

To illustrate the application of the theory to practical cases, two examples will be given, one being that of a model acted on by a concentrated vertical load placed in turn in six different positions, and the other being that of an arch ring (Figs. 8 and 9), under a dead load and a uniform live load over the entire arch. The analysis of the model shows the general effect on the abutment reactions of shifting the position of a concentrated load on the arch. The analysis of the arch shows the method of procedure and amount of work involved in the first approximation for the design. The steel has been omitted in this design, but should be included for the second approximation being placed according to the results of the first. In both examples, as b occurs in the denominator of every term, all equations can be multiplied by this factor. In the second approximation several terms may be omitted, being small as compared with others.

Application to a Spandrel Filled Arch.—The arch ring analyzed has a clear span of 30 ft. and a rise of 14 ft. The fill has a depth at the center point of 9 ft. and a longitudinal grade of 17 per cent. The abutments are 30 ft. apart.

These and other details of the arch ring are shown on Figs. 8 and 9 and Table 1.

The section used in laying out the arch ring is that made by a vertical plane perpendicular to the barrel of the arch rather than parallel to the spandrel walls. After drawing this section to any convenient scale, the arch ring should be divided into an even number of parts equal in length, beginning at the crown. For each of these blocks, the following quantities are obtained by scaling: $\tan \phi$, x, y, and t. (See Fig. 1.) The factor of torsion as well as the moment of inertia about the z-axis and about the normal at the center of each block must be computed. These quantities, together with the angle of skew, $\tan^{-1}\epsilon$, the width, b, the depth, f, and the moduli of elasticity of the material, both in compression and shear, are the only quantities required for the solution under any system of loading. In computing the moment of inertia, the effect of the steel must be taken into account by substituting for the area of the steel an area of concrete which would have an equivalent effect, that is, the steel area multiplied by the ratio of

$$\frac{\text{Modulus of elasticity of steel}}{\text{Modulus of elasticity of concrete}}.$$

The remainder of the work consists in substituting in Equations (1) and solving the six simultaneous equations thus obtained.

In order that the amount of work required for a trial analysis may be estimated, the complete solution for obtaining crown reactions is given. Table 1 shows the computations for the approximate values of the integrations. Table 2 gives the substitutions in the formulas with the reduction to the simultaneous equations, which, in turn, are solved in Table 3, giving the crown reactions. After these are obtained, the stress at any section is fully determinate.

The method of constructing Table 1 is clear. A table of natural functions and a slide rule are indispensable and in addition a table of squares, cubes, and reciprocals will facilitate the work. A computing machine will greatly diminish the labor of solving the simultaneous equations.

The ring was analyzed for the following loads: (*a*) dead load; (*b*) uniformly distributed live load; (*c*) horizontal earth pressure of the spandrel fill; (*d*) horizontal earth pressure due to a uniform live load; and (*e*) temperature. The five loads have been kept separate in this analysis and are found in the five right-hand columns of Table 3. The equations to the left of the equality sign remain the same, of course, for all five loads.

In the example just given, the reinforcement was disregarded and, as the necessary change is easily followed, it was not considered wise to lengthen the paper by adding the recomputations required after placing the steel in the position indicated by the first set of computations. The changes in the value of A (the area) and I (the moment of inertia), are simple. Recent experiments show that F is changed little by adding reinforcement.

With small arches many of the terms may be omitted, as their influence is negligible compared to that of other terms. This is particularly true in the case of earth pressures. It is with this idea that Equations (1) are con-

TABLE 1.—COMPUTATIONS FOR INTEGRALS.

(All Units in Feet and Kips).

Point	t^*	x^*	y^*	$\tan\phi^*$	$\frac{1}{t^3}$	$\frac{y}{t^3}$	$\frac{y^2}{t^3}$	$\frac{y^3}{t^3}$	$\frac{y^4}{t^3}$	$\frac{x^2}{t^3}$	$\frac{x^2\,y}{t^3}$	$\frac{x^2\,y^2}{t^3}$
1	1.174	1.24	0.04	0.055	0.619	0.03	....	....	.....	0.95	0.04	.....
2	1.20	3.74	0.36	0.213	0.579	0.21	0.08	0.03	0.01	8.06	2.91	1.1
3	1.24	6.14	1.04	0.340	0.523	0.54	0.57	0.60	0.62	19.70	20.50	21.3
4	1.28	8.45	1.975	0.495	0.476	0.94	1.86	3.67	7.25	34.00	66.8	131.9
5	1.36	10.65	3.255	0.710	0.397	1.29	4.21	13.70	44.60	45.00	146.7	477.5
6	1.575	12.55	4.85	0.940	0.257	1.24	6.01	29.15	141.37	40.25	196.0	950.6
7	1.95	14.20	6.72	1.232	0.136	0.91	6.11	41.06	275.92	27.20	183.2	1 231.1
8	2.52	15.60	8.88	1.70	0.062	0.55	4.85	42.83	378.15	15.15	134.0	1 183.2
9	3.68	16.68	11.02	2.25	0.020	0.22	2.43	26.78	295.10	5.57	61.4	676.6
10	5.44	17.70	13.36	2.55	0.006	0.08	1.07	14.30	191.00	1.97	26.4	352.7
Abutment	6.00	18.00	14.00	....	.....	....	....	.....	.....	.....	.....	.....
Totals	.....	.....	.....	....	3.075	6.01	27.19	172.12	1 334.02	197.85	887.94	5 026.0

Point	$\frac{x^4}{t^3}$	$\sin\phi$	$\cos\phi$	u	v	$\frac{u^2}{t^3}$	$\frac{\sin^2\phi}{t^3}$	$\frac{x\sin^2\phi}{t^3}$	$\frac{x^2\sin^2\phi}{t^3}$	$\frac{u\cos\phi}{t^3}$
1	2	0.055	0.998	0.03	1.23	....	0.002	.....	.....	0.02
2	118	0.208	0.978	0.42	4.73	0.10	0.025	0.094	0.35	0.24
3	741	0.322	0.947	1.00	6.16	0.52	0.054	0.333	2.05	0.48
4	2 426	0.444	0.896	1.99	8.46	1.89	0.093	0.795	6.72	0.85
5	5 100	0.579	0.815	3.50	10.55	4.89	0.133	1.416	15.06	1.14
6	6 350	0.685	0.729	5.05	12.45	6.54	0.120	1.510	18.91	0.94
7	5 480	0.776	0.630	6.82	14.14	6.27	0.081	1.152	16.36	0.58
8	3 690	0.862	0.507	8.98	15.50	5.02	0.046	0.728	11.26	0.29
9	1 548	0.914	0.406	9.77	16.85	2.33	0.016	0.280	4.67	0.09
10	616	0.931	0.365	11.59	18.90	0.83	0.005	0.095	1.69	0.03
Totals	26 066	.....	.....	....	.....	28.39	0.575	6.403	77.07	4.66

*Obtained by scaling.

TABLE 1.—(*Continued*).

Point	$\frac{\cos^2\phi}{t^3}$	$\frac{x^2\cos^2\phi}{t^3}$	$\frac{x\sin\phi\cos\phi}{t^3}$	$\frac{x^2\sin\phi\cos\phi}{t^3}$	$\frac{x^3\sin\phi\cos\phi}{t^3}$	$\frac{u\,x\sin\phi}{t^3}$	$\frac{u\,x^2\cos\phi}{t^3}$	$\frac{x^4\cos^2\phi}{t^3}$
1.....	0.615	0.95	0.04	0.06	0.1	.....	0.04	1
2.....	0.552	7.75	0.44	1.65	6.2	0.19	3.30	109
3.....	0.470	17.72	0.98	6.01	36.9	1.04	18.08	666
4.....	0.383	27.40	1.61	18.58	114.8	3.56	60.67	1 959
5.....	0.264	29.95	2.00	21.30	227.1	6.57	128.76	3 401
6.....	0.186	21.41	1.61	20.04	251.5	11.13	148.35	3 370
7.....	0.054	10.76	0.94	13.25	188.3	10.10	116.50	2 170
8.....	0.016	3.89	0.43	6.70	104.7	7.53	69.44	946
9.....	0.003	0.91	0.12	2.07	34.5	3.30	24.44	254
10.....	0.001	0.25	0.04	0.66	11.7	1.18	8.25	80
Totals....	2.494	120.99	8.21	85.32	975.8	46.60	577.83	12 956

Point	$\frac{y\sin^2\phi}{t^3}$	$\frac{x\,y\sin\phi\cos\phi}{t^3}$	Wt. Fill	Wt. conc.	Total	ΔW	W	Δx	$\Delta W\bar{x}$	$W\bar{x}$
1.....	.....	....	2 250	450	2 700	162	.....	....	.....	.....
2.....	0.009	0.16	2 260	450	2 710	163	162	2.5	405	405
3.....	0.056	1.02	2 340	470	2 810	169	325	2.4	780	1 185
4.....	0.184	3.18	2 430	490	2 920	175.5	494	2.31	1 141	2 326
5.....	0.433	6.51	2 430	525	2 955	177.5	669.5	2.18	1 460	3 786
6.....	0.584	7.81	2 350	600	2 950	177	847	1.92	1 623	5 409
7.....	0.544	6.32	2 260	730	2 990	179.5	1 024	1.65	1 690	7 099
8.....	0.406	3.80	2 030	950	2 980	179	1 203.5	1.40	1 686	8 785
9.....	0.176	1.32	1 770	1 385	3 155	189.2	1 382.5	1.10	1 523	10 308
10.....	0.067	0.53	1 690	2 069	3 750	225	1 571.5	1.00	1 572	11 880
Abutment....	.....	....	.....	.....	.....	.....	.....	0.30	539	12 419
Totals....	2.459	30.65	.....	.....	.....	.....	1 796.5	....	.....	.....

TABLE 1.—(*Continued*).

Point	$\frac{W\bar{x}}{t^3}$	$\frac{Wxy}{t^3}$	$\frac{W\bar{x}\cos^2\phi}{t^3}$	$\frac{W\bar{x}u\cos^2\phi}{t^3}$	$\frac{W\bar{x}y\sin\phi\cos\phi}{t^3}$	$\frac{\sin\phi\cos\phi}{t^3}$	$\frac{u\sin\phi}{t^3}$	e
1.....	.....	.....	.....	.....	.....	0.034	.....	0.586
2.....	234	85	224	95.5	178	0.118	0.049	0.586
3.....	621	640	557	570.7	1 164	0.160	0.169	0.585
4.....	1 108	2 190	889	1 974.5	3 734	0.190	0.420	0.573
5.....	1 505	4 880	1 002	4 298.2	7 555	0.187	0.805	0.554
6.....	1 390	6 700	735	5 095.5	8 702	0.129	0.886	0.573
7.....	965	6 450	380	4 102.6	6 647	0.066	0.715	0.613
8.....	545	4 830	140	2 503.8	3 776	0.028	0.484	0.636
9.....	206	2 270	34	904.6	1 285	0.007	0.198	0.715
10.....	71	950	10	313.2	447	0.002	0.067	0.993
Totals....	6 645	28 995	3 971	19 858.6	33 488	0.921	3.793	.....

Point	$\frac{y\sin\phi\cos\phi}{t^3}$	$\frac{xy\sin^2\phi}{t^3}$	$\frac{uy\sin\phi}{t^3}$	$\frac{e\sin\phi\cos\phi}{t^3}$	$\frac{ex\sin^2}{t^3}$	$\frac{eu\sin\phi}{t^3}$	$\frac{e^2y^2}{t^3}$
1.....	0.001	.....	.....	0.019	.....	.....	.....
2.....	0.042	0.034	0.017	0.069	0.054	0.030	0.026
3.....	0.166	0.346	0.176	0.093	0.168	0.098	0.194
4.....	0.375	1.630	0.834	0.109	0.186	0.456	0.609
5.....	0.610	4.610	2.625	0.104	0.785	0.446	1.300
6.....	0.623	7.320	4.320	0.074	0.865	0.626	2.000
7.....	0.443	7.750	4.790	0.040	0.706	0.443	2.310
8.....	0.244	6.39	4.275	0.018	0.462	0.309	1.980
9.....	0.082	3.09	2.180	0.006	0.210	0.148	1.370
10....	0.002	1.28	0.890	0.002	0.095	0.067	1.023
Totals....	2.588	31.715	20.107	0.534	3.431	2.623	10.812

TABLE 2.—Computations.

$\lambda = 2.5$; $\varepsilon = 1.53$; $b = 60$ ft.; $w = 0.1$ kips per sq. ft.; grade = 17%

$f = 9$ ft.; $e_c = 0.59$ ft.; $\omega = 0.1$ kip per cu. ft.; $\eta_d = \eta_l = \frac{1}{3}$

$d\,s = 2.5$ ft.; $E = (2)\ (10^3)\ (144)$ kips per sq. ft.

$g = (0.17)\ \sec.\ \tan^{-1}\varepsilon = (0\ 17)\ (1.828) = 0.31$
$n = (0.5)\ (0.17)\ (b)\ \sin\tan^{-1}\varepsilon = (0.5)\ (0.17)\ (60)\ (0.84) = 4.27$
$F = \left[(2.5)\ (205)\ \frac{(\pi)}{(180)}\right]\left[\frac{1}{b\ t^3} + \frac{1}{b^3\ t}\right] = 8.9448\left(\frac{1}{b\ t^3} + \frac{1}{b^3\ t}\right)$

Arch Coefficients:

(a). $[(12)\ (27.19) + \varepsilon^2\ (8.945)\ (77.07)]\ T_x - [(\varepsilon)\ (8.945)\ (46.60)]\ Tz + (12)\ (6.01)\ Mz + \varepsilon\ (8.945)\ (8.21)\ M_x = [(326.28) + \varepsilon^2\ (689.38)]\ T_x + \varepsilon\ 416.83\ Tz - \varepsilon\ 73.44\ M_x = 1\ 939.05\ T_x - 637.75\ T_z + 72.12\ M_y - 112.4\ M_z$
(b). $[(12)\ (197.85) + \varepsilon^2\ (8.945)\ (120.99)]\ T_y = (2\ 374.20 + \varepsilon^2\ 1\ 082.23)\ T_y = 4\ 907.6\ T_y$
(c). $(8.945)\ (28\ 89)\ Tz + (8.945)\ (4.66)\ M_x = 2^{\prime}3.94\ Tz + 41.68\ M_x$
(d). $(12)\ (3.075)\ M_z = 36.90\ M_z$
(e). $(8.945)\ (0.575)\ M_y = 5.14\ M_y$
(f). $(8.945)\ (2.494)\ M_x = 22.31\ M_x$

Dead Loading Terms:

(a). $-(12)\ (28\ 995) - \varepsilon^2\ (8.945)\ (33\ 488) = -347\ 940 - 299\ 544\ \varepsilon^2 = -1\ 049\ 142.55$
(b). $(0.31)\ (26\ 066.1)\ (12) + \varepsilon^2\ (8.945)\ (0.31)\ (12\ 956) - \varepsilon\ (4.27)\ (60)\ (8.945)\ (120.99) = +96\ 965.89 + 35\ 925.55\ \varepsilon^2 - 277\ 268.20\ \varepsilon = -245\ 156.34$
(c). $\varepsilon\ (8.945)\ (19\ 858.6) = 177\ 631.3\ \varepsilon = 271\ 775.89$
(d). $-(12)\ (6\ 645) = -79\ 740$
(e). $-\varepsilon\ (0.31)\ (8.945)\ (975.8) + (4.27)\ (8.945)\ (60)\ (8.21) = -2\ 705.79\ \varepsilon + 18\ 814.52 = 14\ 674.66$
(f). $\varepsilon\ (8.945)\ (3\ 971) = 35\ 519.82\ \varepsilon = 54\ 345.32$

Live Loading Terms:

(a). $-(36)\ (837\ 96) - \varepsilon^2\ (3)\ (8.945)\ (975.8) = -30\ 166.56 - 25\ 185.02\ \varepsilon^2 = -89\ 122.7$
(c). $(3)\ (8.945)\ (577.83)\ \varepsilon = 15\ 505.74\ \varepsilon = 23\ 723.78$
(d). $-(36)\ (197.85) = -7\ 122.60$
(f). $(3)\ (8.945)\ (120.99)\ \varepsilon = 3\ 246.70\ \varepsilon = 4\ 967.45$

Horizontal Earth Pressure, Dead Load:

$$\eta d = \frac{1}{3},\ \text{or}\ \eta d\ b\ \omega = 2$$

(a). $2\ [-(42.7)\ (\varepsilon)\ (8.945)\ (31.71) + (4.27)\ (\varepsilon)\ (8.945)\ (3.431) - (40.5 - 5.31 + 3.03)\ (\varepsilon^2)\ (77.07)\ (8.945) + (2)\ (1\ 334.0) + (6)\ (9)\ (172.12) + (6)\ (0.312)\ (5\ 026.0) + (6)\ (9)\ (0.312^2)\ (837.96) + (5.31 - 0.17)\ (12)\ (27.19) - (6)\ (9)\ (2.15) - (6)\ (10.812) + (6.01)\ (12)\ (47.79)] = 2\ [-18\ 530.5 + 2\ 005.0 - 61\ 677.9 + 2\ 668.2 + 9\ 294.5 + 2\ 898.0 + 4\ 348.5 + 1\ 677.1 - 116.1 - 64.9 - 3\ 446.6] = 2\ [-55\ 797.2 = -113\ 537.4]$
(b). $2\ [(42.7)\ (\varepsilon)\ (8.945)\ (0.31)\ (55.32) - (2)\ (0.312^2)\ (26\ 066.1) - (6)\ (0.31)\ (5\ 026) - (12)\ (9)\ (0.31)\ (837.96) - (0.31)\ (197.85)\ (12)\ (40.5 + 3.03)] = 2\ [15\ 456.2 - 1\ 558.0 - 9\ 348.4 - 28\ 054.9 - 32\ 038.2] = 2\ [-55\ 538.3] = -111\ 076\ 6$
(c). $2\ [(42.7)\ (8.945)\ (20.107) - (42.7)\ (8.945)\ (2.623) + (42.7)\ (0.59)\ (8.945)\ (3.793) + (\varepsilon)\ (38.20)\ (8.945)\ (46.60)] = 2\ [7\ 679.7 - 1\ 001.9 + 854.76 + 24\ 494.45] = 2\ [+32\ 027.1] = 64\ 054.2$
(d). $2\ [(2)\ (172.12) + (6)\ (9)\ (27.19) + (6)\ (0.312)\ (837.96) + (6)\ (9)\ (0.312^2)\ (197.85) + (5.14)\ (6.01)\ (12) - (6)\ (9)\ (0.841) - (3)\ (2.15) + (12)\ (9)\ (0.59)\ (3.075)] = 2\ [344.2 + 1\ 468 + 482 + 1\ 027 + 371 - 45.4 + 12.9 + 1\ 710.7] = 2\ [5\ 344.6] = 10\ 689.2$
(e). $2\ [-(42.7)\ (0.31)\ (8.945)\ (6.403)] = 2\ [-758.13] = -1\ 516.2$
(f). $2\ [(42.7)\ (8.945)\ (2.588) - (42.7)\ (0.534)\ (8.945) + (42.7)\ (0.59)\ (8.945)\ (0.921) + (\varepsilon)\ (8.945)\ (38.2)\ (8.21)] = 2\ [=988.5 - 204.0 + 207.5 + 4\ 292.1] = 2\ [5\ 284.1] = 10\ 568.2$

Horizontal Earth Pressures, Live Load;

$$\eta l = \frac{1}{3},\ \text{or}\ \eta l\ b\ w = 2$$

(a). $2\ [(6)\ (172.12) + (6)\ (0.312)\ (837.96) + (12)\ (0.59)\ (27.19) - (6)\ (2.15) - \varepsilon^2\ (8.945)\ (8.41)\ (77.07)] = 2\ [1\ 032.4 + 483.2 + 192.5 - 12.9 - 13\ 571.7] = 2\ [-11\ 876.5] = -23\ 753.0$
(b). $2\ [-(12)\ (0.31)\ (837.96) - (12)\ (9)\ (0.31)\ (197.85)] = 2\ [-3\ 117.2 - 662.4] = 2\ [-3\ 779.6] = -7\ 559.$
(c). $2\ [\varepsilon\ (8.41)\ (8.945)\ (46.60)] = 2\ [5\ 363.4] = +10\ 726.8$
(d). $2\ [(6)\ (27.19) + (6)\ (0.312)\ (197.85) + (12)\ (0.59)\ (6.01 - (6)\ (0.841)] = 2\ [163.1 + 114.8 + 42.6 - 5.0] = 2\ [315\ 5] = 631.0$
(f). $2\ [\varepsilon\ (8.945)\ (8.41)\ (8.21)] = 2\ [944\ .9] = 1\ 889.8$

Temperature Stresses 25° Change:

(a). $\frac{60}{2.5}\ (18)\ (25)\ (0.0000065)\ (2\ 000)\ (144) = 2\ 020$
(c). $\varepsilon\ (2\ 020) = 3\ 095$

TABLE 3.—SOLUTION OF SIMULTANEOUS EQUATIONS.

Equations.	Dead load. (a).	Live load. (b).	Horizontal Thrust. Dead. (c).	Horizontal Thrust. Live. (d).	Temperature. (e).
(b) +4 907.60 T_y − 112.40 M_y	= + 243 156.34	.....	−111 076.60	− 7 559.2	.....
(β) − 112.4 T_y + 5.14 M_y	= − 14 674.66	.....	− 1 516.2	.....	.....
−2 457.98 T_y + 112.4 M_y	= − 320 901.21	.....	− 33 155.8	.....	.....
+2 449.67 T_y	= − 77 744.87	.....	−144 232.4	− 7 559.2	.....
T_y	= − 31.7868	.....	− 58.878	− 3.086	.....
+4 907.6 T_y	= − 155 751.88	.....	−288 951.1	−15 143.9	.....
− 112.4 M_y	= + 398 908.22	.....	+178 185.1	+ 7 584.7	.....
M_y	= − 3 549.00	....	− 1 585.28	− 67.48	.....
(∞) + 72.12 T_x +36.90 M_z	= + 79 740.00	+ 7 122.60	+ 10 689.2	+ 621.0	.....
+ 140.96 T_x +72.12 M_z	= + 155 849.56	+ 13 920.92	+ 20 891.7	+ 1 233.3	.....
(α) +1 989.05 T_x − 637.75 T_z +72.12 M_z −112.4 M_c	= +1 049 142.55	+ 89 122.17	−113 594.4	−23 753.0	+ 2 021.8
+1 798.07 T_x − 637.75 T_z −112.4 M_c	= + 893 293.99	+ 75 201.25	−134 846.1	−24 986.6	+ 2 021.8
(c) − 637.75 T_x + 253.90 T_z + 41.7 M_c	= − 271 775.89	− 23 723.78	+ 64 054.2	+10 726.8	+ 3 093.3
(γ) − 112.4 T_x + 41.7 T_z + 22.31 M_x	= − 54 345.32	− 4 967.45	+ 10 568.2	+ 1 889.8	.....
−1 719.02 T_x + 684.37 T_z −112.40 M_x	= − 732 556.72	− 63 946.12	+172 654.5	+28 913.5	+ 8 337.8
− 566.28 T_x + 210.09 T_z +112.40 M_x	= − 223 416.16	− 25 026.51	+ 53 243.6	+ 9 521.0	.....
+ 79.02 T_x + 46.62 T_z	= + 160 737.27	+ 11 255.13	+ 38 168.4	+ 3 927.2	+ 10 359.6
+1 232.81 T_x − 427.66 T_z	= + 669 877.83	+ 50 174.74	− 81 242.5	−15 465.3	+ 2 021.8
+ 725.33 T_x + 427.66 T_z	= +1 474 494.00	+103 246.88	+350 130.8	+36 025.5	+ 94.979.6
+1 958.14 T_x	= +2 144 371.83	+ 153 421.62	+268 898.8	+20 680.2	+ 97 001.4
T_x	= + 1 095.1	+ 78.351	+ 137.323	+ 10.561	+ 49.5
+1 232.81 T_x + 726.87 T_z	= +2 506 114.95	+175 488.00	+595 098.0	+61 230.5	+161 519.6
+1 154.53 T_z	= +1 886 237.12	+125 308.26	+676 340 5	+76 695.8	+159 497.8
T_z	= + 1 590.46	+ 108.54	+ 585.81	+ 66.430	+ 138.2
+ 112.4 T_x	= + 123 089.99	+ 8 806.62	+ 15 435.1	+ 1 187.1	+ 5 568.0
− 41.7 T_z	= − 66 322.30	− 4 525.96	− 24 428.5	− 2 770.1	− 5 762.6
22.32 M_x	= − 2 422.37	− 686.79	+ 1 574.9	+ 306.8	− 194.6
M_c	= − 108.53	− 30.77	+ 70.56	+ 13.746	− 8.6
− 72.12 T_x	= − 78 979.09	− 5 650.65	+ 9 908.8	− 761.7	− 357.3
+36.90 M_z	= + 760.91	+ 1 471.95	+ 1 785.4	− 130.7	− 357.3
M_z	= + 20.6	+ 39.89	+ 483.84	− 3.54	− 96.8
Summary: T_x	= + 1 095.1	+ 78.35	+ 137.3	+ 10.6	+ 49.5
T_y	= − 31.7	.....	− 58.9	− 3.1	.....
T_z	= + 1 590.5	+ 108.5	+ 585.8	+ 66.4	+ 138.2
M_z	= + 20.6	+ 39.9	+ 483.8	− 3.5	− 96.8
M_y	= − 3 549.0	.....	− 1 585.3	− 67.5	.....
M_x	= − 108.5	− 30.8	+ 70.6	+ 13.7	− 8.6

densed from those obtained in outlining the theory by dropping some of these minor terms. That the significance of some of these omitted terms may be estimated, Table 4 has been prepared, in which the equations are solved with none of the terms omitted. This gives an idea of the error involved in this case in which both the skew and the grade are larger than will usually be found. It was partly with this idea in mind that the abnormal grade of 17% was used.

TABLE 4.

ARCH COEFFICIENTS, INCLUDING TERMS OMITTED IN TABLE 2:

(*a*). $[4.19 + 4.52 + 326.28 + 0.93\,\epsilon^2 + 0.84\,\epsilon^2 + 689.38\,\epsilon^2]\ T_X - [1.325\,\epsilon + 0.547\,\epsilon + 416.83\,\epsilon]\ T_Z + 72.12\ M_Y + [0.072\,\epsilon - 0.054\,\epsilon - 73.44\,\epsilon]\ M = [334.99 + 691.14\,\epsilon^2]\ T_X - 41\,870\,\epsilon\ T_Z + 72.12\ M_Z - 73.42\,\epsilon\ M_X = 1\,952.88\ T_X - 640.61\ T_Z + 72.12\ M_Z - 112.33\ M_X$

(*b*). $[1.808 + 10.48 + 2\,374.20 + 1.12\,\epsilon^2 + 0.69\,\epsilon^2 + 1\,082.23\,\epsilon^2]\ T_Y = 2\,386.49 + 1\,081.80\,\epsilon^2 = 4\,918.87$

(*c*). $[0.207 + 0.035 + 253.94]\ T_Z - [0.011 - 0.003 - 41.68]\ M_X = 254.18\ T_Z + 41.67\ M_X$

(*e*). $[0.014 + 0.004 + 5.14]\ M_Y = 5.15\ M_Y$

(*f*). $[0.006 + 0.011 + 22.31]\ M_Z = 22.32\ M_Z$

DEAD LOADING TERMS:

(*a*). $[-2\,203.2 - 347\,940 + 412.02\,\epsilon^2 - 299\,544\,\epsilon^2 - 307.10\,\epsilon^2 = -350\,143 - 299\,649\,\epsilon^2 = -1\,057\,591.34$

(*b*). $[312.72 + 647.91 + 96\,965.89 + 77.21\,\epsilon^2 - 287.16\,\epsilon^2 + 35\,925.55\,\epsilon^2 - 177.39\,\epsilon - 277\,268.2\,\epsilon] = 97\,926.52 - 277\,732.75\,\epsilon + 36\,304.1\,\epsilon^2 = -242\,020.32$

(*c*). $[-743.76 + 193.46 + 177\,631.30]\,\epsilon = 177\,081\,\epsilon = 270\,933.93$

(*e*). $[3.61 - 2.70 - 2\,705.79]\,\epsilon - 18.44 + 13.75 - 18\,814\,52 = -2\,704.69\,\epsilon + 18\,809.83 = 14\,671.65$

(*f*). $[40.0 + 23.34 + 35\,519.82]\,\epsilon = 35\,583.16\,\epsilon = 54\,442.23$

LIVE LOADING TERMS:

(*a*). $[-194\,40 - 30\,166.56 + (34.93 - 26.04 - 25\,185.021)\,\epsilon^2] = -30\,360.96 - 25\,176.13\,\epsilon^2 = -89\,122.17$

(*c*). $[-62.31 + 14.71 + 15\,505\,74]\,\epsilon = 15\,468.14\,\epsilon = 23\,650.95$

(*f*). $[3\,37 + 2.08 + 3\,246.70]\,\epsilon = 3\,252.14\,\epsilon = 4\,975.77$

HORIZONTAL EARTH PRESSURE, DEAD LOAD:

(*a*). $-2\,[27.7 + 77.4 - 5\,2 - 22.0 + 0.7 + 13.4 + 21.5 + 129 + 268.5 - 20.9 - 26.2 + 1.0 + 40.5 + 23\,2 - 21\,5 + 3.7 - 3.7 + 83.5 - 29.1 + 10.4 - 2.3 - 44.3 - 18\,530.5 + 2\,005.0 - 198.2 - 61\,677.9 + 2\,668.2 + 9\,294.5 + 2\,898.0 + 4\,348.5 + 1\,677.1 - 116.1 + 5.9 - 64.9 + 3\,343.6] = -2\,(-53\,821.5) = 107\,643.0$

(*b*). $-2\,[-55.6 + 90.6 + 6.2 - 17.8 + 13\,3 + 15\,436.2 - 1\,553.0 - 9\,348.4 - 28\,054.9 + 129.2 - 32\,038.2] = -2\,(-55\,372.4) = 110\,744\,8$

(*c*). $-2\,[23.0 - 3.1 + 3.1 + 77.9 + 12.6 - 4.6 + 1.1 + 31.6 + 7\,679.7 - 1\,001.9 + 854.8 + 24\,494.5] = -2\,(32\,168.7) = -64\,337.4$

(*d*). $-2\,[344.2 + 1\,468.0 + 482 + 1\,027.0 + 371.0 - 45.4 + 2.0 - 12.9 + 1\,710.7] = -2\,(5\,346.6) = 10\,693\,2$

(*e*). $-2\,[-1.3 - 0.8 - 758.1] = -2\,(-760\,2) = 1\,520.4$

(*f*). $-2\,[-1.2 - 0.2 - 4.2 + 0.9 - 0.2 + 0.1 + 3.1 + 988.5 - 204.0 + 207.5 + 4\,292.1] = -2\,(5\,282.4) = -10\,564.8$

HORIZONTAL EARTH PRESSURE, LIVE LOAD:

(*a*). $-2\,[8.6 - 2.4 + 2.5 + 29.8 - 2.9 + 2.7 + 1\,032.4 + 483.2 + 192.5 + 12\,6 - 12.9 - 18.3 - 19.6 - 13\,571.7 = -2\,(-11\,863.5) = 23\,727$

(*b*). $-2\,[-10.0 - 3\,117.2 - 662.4] = -2\,(-3\,789.6) = 7\,579.2$

(*c*). $-2\,(17.1 + 6.9 + 5\,363.4) = -2\,(5\,387.4) = -10\,774.8$

(*d*). $-2\,[163.1 + 114\,8 + 42.6 + 6.4 - 5.0] = -2\,(321\,9) = -643.8$

(*f*). $-2\,(-0.9 + 0.7 + 944.93) = -2\,(944.7) = -1\,889.4$

The solution of the resulting equations is given in Table 5.

TABLE 5.

	Dead load.	Live load.	Horizontal dead load.	Horizontal live load.	Temperature.
T_X	+ 1 073.4	+ 78.6	+ 173.3	+ 11.5	+ 49.3
T_Y	− 31.6	.....	+ 57.9	− 3.1	.....
T_Z	+ 1 662.5	+ 110.7	+ 676.4	+ 69.2	+ 137.5
M_Z	+ 63.0	+ 39.4	− 49.0	− 207.1	− 96.3
M_Y	− 3 587.8	.....	− 1 548.9	− 67.0	.....
M_X	− 140.8	− 33.8	+ 82.9	+ 13.4	− 8.5

Application to a Model with a Concentrated Load.—The writer had hoped to make a model of steel and to conduct a series of tests to check his theory. Practical difficulties have arisen to prevent this. The computations have been made and merely the results showing the change in crown and abutment reactions as the load is moved about, are indicated on Fig. 10. The model investi-

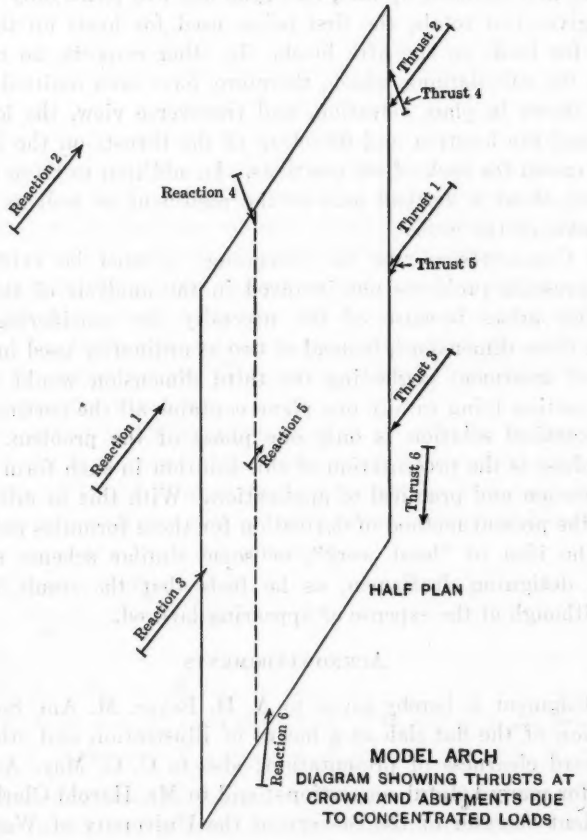

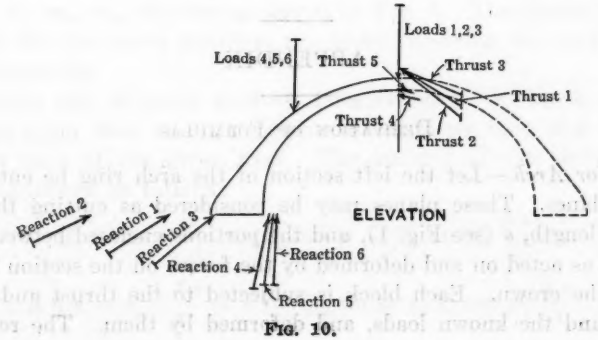

FIG. 10.

gated had a clear span of 11¼ in. measured perpendicularly between abutments; in fact, it is a model of the larger arch ring to a scale of ⅜ in. = 1 ft. The perpendicular distance between spandrel walls is taken as 12 in.

In obtaining the loading terms the integrals are taken for the blocks between the load and the abutment only. The columns corresponding to Table 1 were first summed up and, later, the last five terms only were summed up. This gives two totals, the first being used for loads on the crown and the second for loads on the fifth block. In other respects, no new ideas are involved in the calculations, which, therefore, have been omitted.

Fig. 10 shows in plan, elevation, and transverse view, the left section of the model and the location and direction of the thrusts on the left abutment and on the crown for each of six positions. In addition to these thrusts, there is a moment about a vertical axis at the abutment as well as one about a horizontal axis at the crown.

General Comments.—From the foregoing, it must be evident that the skew arch presents problems not involved in the analysis of the right arch. The difficulty arises because of the necessity for considering forces and moments in three dimensions, instead of two as ordinarily used in arch design. A method of treatment neglecting the third dimension would be unreliable because no section lying in any one plane contains all the pertinent factors.

The theoretical solution is only one phase of the problem. An equally important phase is the presentation of this solution in such form as to be easy of comprehension and practical of application. With this in mind, the writer has chosen the present method of derivation for these formulas rather than one involving the idea of "least work", or some similar scheme not generally familiar to designing draftsmen, as he feels that the result is a gain in clearness, although at the expense of appearing labored.

Acknowledgments

Acknowledgment is hereby given to A. H. Beyer, M. Am. Soc. C. E., for the suggestion of the flat slab as a means of illustration and other criticisms leading toward clearness of presentation; also to C. C. May, Assoc. M. Am. Soc. C. E., for many helpful suggestions; and to Mr. Harold Clarke, a member of the Student Chapter of the Society of the University of Washington, for checking the algebra and arithmetic in the first draft of the paper.

APPENDIX

Derivation of Formulas

Terms for Arch.—Let the left section of the arch ring be cut by a series of radial planes. These planes may be considered as cutting the ring into blocks of a length, s (see Fig. 1), and the portions enclosed between two adjacent planes as acted on and deformed by the forces on the section between the block and the crown. Each block is subjected to the thrust and moment at the crown and the known loads, and deformed by them. The resulting def-

ormation of the block deflects the crown; the total crown deflection is the sum of the deflections due to all the block deformations. In order that the crown faces of the left section and of the right section shall coincide, it is necessary that the following equations be satisfied:

$$\Delta x_L = -\Delta x_R \quad (25a)$$
$$\Delta y_L = \Delta y_R \quad (25b)$$
$$\Delta z_L = -\Delta z_R \quad (25c)$$
$$\Delta \alpha_L = -\Delta \alpha_R \quad (25d)$$
$$\Delta \beta_L = \Delta \beta_R \quad (25e)$$
$$\Delta \gamma_L = -\Delta \gamma_R \quad (25f)$$

where Δx_L, Δy_L, and Δz_L equal the components of the deflection of the crown center of the left section in the x, y, and z-directions, respectively; $\Delta \alpha_L$, $\Delta \beta_L$, and $\Delta \gamma_L$ equal the rotation of the left crown face about the z, y, and x-axes, respectively; and, similarly, for the right section.

It is necessary to find: First, the forces and moments acting on the blocks in terms of the loads and of the six unknowns at the crown; second, the deformation of the block due to these forces; and, third, the deflection at the crown due to this deformation. The result will give the values to be substituted in the preceding equations.

To find the forces and moments acting on a block the center of which is P, the part of the arch between the crown and this block is taken as a free body. (See Fig. 4.) As it must be in equilibrium, the sum of the forces parallel to each axis and the sum of the moments about each axis are equal to zero as shown in the following equations:

$$t_v = T_x \cos \phi + T_y \sin \phi \quad (26a)$$
$$t_u = -T_x \sin \phi + T_y \cos \phi \quad (26b)$$
$$t_z = T_z \quad (26c)$$
$$m_z = T_x y - T_y x + M_z \quad (26d)$$
$$m_u = T_x z \cos \phi + T_y z \sin \phi - T_z v + M_y \cos \phi + M_x \sin \phi \quad (26e)$$
$$m_v = -T_x z \sin \phi + T_y z \cos \phi + T_z u - M_y \sin \phi + M_x \cos \phi \quad (26f)$$

Axes are assumed through the point, P, one normal to the arch ring, one parallel to the barrel of the arch, and the third perpendicular to these two, and the forces and moments are referred to these axes. The meanings of the terms t_v, t_u, t_z, m_z, m_u, m_v, are as shown in Fig. 4. The formulas will first be developed for the crown reaction, the terms involving the load to be considered subsequently.

These forces and moments produce deformation of the block causing the center of its upper face to shift relative to the lower face, and the face to rotate about each of the given axes. The amount of this deformation or rotation is expressed as follows:

$$E\,d\,v = t_v \frac{d\,s}{A} = (T_x \cos \phi + T_y \sin \phi) \frac{d\,s}{A} \quad (27a)$$

$$E\,d\,u = t_u \frac{\lambda\,d\,s}{A} = \lambda\,(-T_x \sin \phi + T_y \cos \phi) \frac{d\,s}{A} \quad (27b)$$

$$E\,d\,z = t_z \frac{\lambda\,d\,s}{A} = \lambda\,T_z \frac{d\,s}{A} \quad \ldots\ldots\ldots\ldots\ldots\ldots\ldots\ldots (27c)$$

$$E\,d\,\alpha = m_z \frac{d\,s}{I_z} = (T_x\,y - T_y\,x + M_z) \frac{d\,s}{I_z} \quad \ldots\ldots\ldots\ldots\ldots (27d)$$

$$E\,d\,\beta = m_u \frac{d\,s}{I_y} = (T_x\,\varepsilon\,x\cos\phi + T_y\,\varepsilon\,x\sin\phi - T_z\,v + M_y\cos\phi + M_x\sin\phi) \frac{d\,s}{I_y} \quad \ldots\ldots\ldots\ldots\ldots\ldots\ldots (27e)$$

$$E\,d\,\gamma = m_v \frac{\lambda\,d\,s}{F} = \lambda\,(-T_x\,\varepsilon\,x\sin\phi + T_y\,\varepsilon\,x\cos\phi + T_z\,u - M_y\sin\phi + M_x\cos\phi) \frac{d\,s}{F} \quad \ldots\ldots\ldots\ldots\ldots\ldots\ldots (27f)$$

where E is the modulus of elasticity and α, β, and γ are the rotation of the upper face of the block relative to the lower about the z, u, and v-axes, respectively.

The sections of the arch ring, that is, the faces of the blocks at the cutting planes, are not, in general, symmetrical about the two axes of reference. The vertical plane will cut the arch ring in a rectangular section, but any inclined plane will cut the ring in an oblique parallelogram the angles of which are functions of the skew. A slight error is introduced by assuming that the normal and horizontal axes are conjugate.

The usual assumption in the theory of flexure was made, namely, that a straight line perpendicular to the neutral surface remains straight during deformation.

The rotation of the line joining the points, C and P, due to the deformation of the block, is shown in Fig. 3, in three planes, relative to the z-axis, u-axis, and v-axis the angular movements being α, β, and γ, respectively. During the movement, the line, $C\,P$, is assumed to remain straight and of constant length, that is, this part of the arch is assumed to be rigid. The resultant movement of C is shown in Table 6.

TABLE 6.—Movement of Point C Due to Deformation at Point P.

Movement of block at Point P.	Components of Movement at Point C.					
	$d\,x_0$	$d\,y_0$	$d\,z_0$	$d\,\alpha_0$	$d\,\beta_0$	$d\,\gamma_0$
$d\,v$	$d\,v\cos\phi$	$d\,v\sin\phi$	.....	....	.....	.....
$d\,u$	$-d\,u\sin\phi$	$d\,u\cos\phi$	.....	....	.....	.....
$d\,z$	.....	.....	$d\,z$	...	.....	.....
$d\,\alpha$	$d\,\alpha\,y$	$-d\,\alpha\,x$	.....	$d\,\alpha$	.....	.....
$d\,\beta$	$d\,\beta\,z\cos\phi$	$d\,\beta\,z\sin\phi$	$-d\,\beta\,v$	....	$d\,\beta\cos\phi$	$d\,\beta\sin\phi$
$d\,\gamma$	$-d\,\gamma\,z\sin\phi$	$d\,\gamma\,z\cos\phi$	$d\,\gamma\,u$	....	$-d\,\gamma\sin\phi$	$d\,\gamma\cos\phi$

It should be noted that the movement of the point, P, is referred to perpendicular axes, one being parallel to the barrel and the others being tangent and normal to the neutral surface at P, whereas, in some cases, the movement of C is referred to these same axes and, in some cases to the axes, x and

y. The first set of co-ordinates are referred to as v and u and z. The relationships between x, y, and u, v, Equations (3) and (4), are fundamental equations of trigonometry.

To find the horizontal movement, Δx, of the point in the direction of x, due to all crown forces and moments deforming one block, the sum of the terms of the column, $d\,x$, should be taken. The values of $d\,v$, $d\,u$, etc., already obtained, are then substituted.

The term, L_x, denotes the deflection of the crown in the direction of the x-axis, due to the external loads only, when the left half of the arch is considered as a cantilever; likewise, for the remaining terms involving L.

$$E\,\Delta x = \left\{ \cos^2\phi\,\frac{d\,s}{A} + \lambda \sin^2\phi\,\frac{d\,s}{A} + y^2\,\frac{d\,s}{I_z} + z^2\cos^2\phi\,\frac{d\,s}{I_y} + \lambda\,z^2\sin^2\phi\,\frac{d\,s}{F} \right\} T_x$$

$$+ \left\{ (1-\lambda)\sin\phi\cos\phi\,\frac{d\,s}{A} - x\,y\,\frac{d\,s}{I_z} + z^2\sin\phi\cos\phi\,\frac{d\,s}{I_y} - \lambda\,z^2\sin\phi\cos\phi\,\frac{d\,s}{F} \right\} T_y - \left\{ v\,z\cos\phi\,\frac{d\,s}{I_y} + \lambda\,u\,z\sin\phi\,\frac{d\,s}{F} \right\} T_z$$

$$+ \left\{ y\,\frac{d\,s}{I_z} \right\} M_z + \left\{ z\cos^2\phi\,\frac{d\,s}{I_y} + \lambda\,z\sin^2\phi\,\frac{d\,s}{F} \right\} M_y$$

$$+ \left\{ z\sin\phi\cos\phi\,\frac{d\,s}{I_y} - \lambda\,z\sin\phi\cos\phi\,\frac{d\,s}{F} \right\} M_x + L_x \ldots\ldots (28a)$$

$$E\,\Delta y = \left\{ (1-\lambda)\sin\phi\cos\phi\,\frac{d\,s}{A} - x\,y\,\frac{d\,s}{I_z} + z^2\sin\phi\cos\phi\,\frac{d\,s}{I_y} - \lambda\,z^2\sin\phi\cos\phi\,\frac{d\,s}{F} \right\} T_x + \left\{ \sin^2\phi\,\frac{d\,s}{A} + \lambda\cos^2\phi\,\frac{d\,s}{A} + x^2\,\frac{d\,s}{I_z} + z^2\sin^2\phi\,\frac{d\,s}{I_y} + \lambda\,z^2\cos^2\phi\,\frac{d\,s}{F} \right\} T_y + \left\{ -v\,z\sin\phi\,\frac{d\,s}{I_y} + \lambda\,u\,z\cos\phi\,\frac{d\,s}{F} \right\} T_z - \left\{ x\,\frac{d\,s}{I_z} \right\} M_z + \left\{ z\sin\phi\cos\phi\,\frac{d\,s}{I_y} - \lambda\,z\sin\phi\cos\phi\,\frac{d\,s}{F} \right\} M_y + \left\{ z\sin^2\phi\,\frac{d\,s}{I_y} + \lambda\,z\cos^2\phi\,\frac{d\,s}{F} \right\} M_x + L\,y \ldots (28b)$$

$$E\,\Delta z = -\left\{ v\,z\cos\phi\,\frac{d\,s}{I_y} + \lambda\,u\,z\sin\phi\,\frac{d\,s}{F} \right\} T_x - \left\{ v\,z\sin\phi\,\frac{d\,s}{I_y} - \lambda\,u\,z\cos\phi\,\frac{d\,s}{F} \right\} T_y + \left\{ \lambda\,\frac{d\,s}{A} + v^2\,\frac{d\,s}{I_y} + \lambda\,u^2\,\frac{d\,s}{F} \right\} T_z - \left\{ v\cos\phi\,\frac{d\,s}{I_y} + \lambda\,u\sin\phi\,\frac{d\,s}{F} \right\} M_y - \left\{ v\sin\phi\,\frac{d\,s}{I_y} - \lambda\,u\cos\phi\,\frac{d\,s}{F} \right\} M_x + L\,z\,. \quad (28c)$$

$$E\,\Delta\alpha = \left\{ y\,\frac{d\,s}{I_z} \right\} T_x - \left\{ x\,\frac{d\,s}{I_z} \right\} T_y + \left\{ \frac{d\,s}{I_z} \right\} M_z + L\,\alpha \ldots\ldots (28d)$$

$$E \Delta \beta = \left\{ z \cos^2 \phi \frac{d s}{I_y} + \lambda z \sin^2 \phi \frac{d s}{F} \right\} T_x + \left\{ z \sin \phi \cos \phi \frac{d s}{I_y} - \lambda z \sin \phi \cos \phi \frac{d s}{F} \right\} T_y - \left\{ v \cos \phi \frac{d s}{I_y} + \lambda u \sin \phi \frac{d s}{F} \right\} T_z + \left\{ \cos^2 \phi \frac{d s}{I_y} + \lambda \sin^2 \phi \frac{d s}{F} \right\} M_y + \left\{ \sin \phi \cos \phi \frac{d s}{I_y} - \lambda \sin \phi \cos \phi \frac{d s}{F} \right\} M_x + L \beta \quad \ldots\ldots\ldots\ldots\ldots\ldots (28e)$$

$$E \Delta \gamma = \left\{ z \sin \phi \cos \phi \frac{d s}{I_y} - \lambda z \sin \phi \cos \phi \frac{d s}{F} \right\} T_x + \left\{ z \sin^2 \phi \frac{d s}{I_y} + \lambda z \cos^2 \phi \frac{d s}{F} \right\} T_y - \left\{ v \sin \phi \frac{d s}{I_y} - \lambda u \cos \phi \frac{d s}{F} \right\} T_z + \left\{ \sin \phi \cos \phi \frac{d s}{I_y} - \lambda \sin \phi \cos \phi \frac{d s}{F} \right\} M_y + \left\{ \sin^2 \phi \frac{d s}{I_y} + \lambda \cos^2 \phi \frac{d s}{F} \right\} M_x + L \gamma \quad \ldots\ldots (28f)$$

As each block acts independently, the sum of the partial deflections due to each deformation should be taken to find the total deflection of the crown along and around each axis. If the blocks are considered of infinitesimal length, the terms of Equations (28) can be written as integrals. In practice, however, the arch ring should be divided into blocks of uniform length, s. The following equations are then obtained:

$$E \Delta x = \left\{ \int \cos^2 \phi \frac{d s}{A} + \lambda \int \sin^2 \phi \frac{d s}{A} + \int y^2 \frac{d s}{I_z} + \varepsilon^2 \int x^2 \cos^2 \phi \frac{d s}{I_y} + \varepsilon^2 \lambda \int x^2 \sin^2 \phi \frac{d s}{F} \right\} T_x + \left\{ (1 - \lambda) \int \sin \phi \cos \phi \frac{d s}{A} - \int x y \frac{d s}{I_z} + \varepsilon^2 \int \left(\frac{1}{I_y} - \frac{\lambda}{F} \right) x^2 \sin \phi \cos \phi \, d s \right\} T_y - \left\{ \varepsilon \int v x \cos \phi \frac{d s}{I_y} + \varepsilon \lambda \int u x \sin \phi \frac{d s}{F} \right\} T_z + \left\{ \int y \frac{d s}{I_z} \right\} M_z + \left\{ \varepsilon \int x \cos^2 \phi \frac{d s}{I_y} + \varepsilon \lambda \int x \sin^2 \phi \frac{d s}{F} \right\} M_y + \left\{ \varepsilon \int \left(\frac{1}{I_y} - \frac{\lambda}{F} \right) x \sin \phi \cos \phi \, d s \right\} M_x + L_x \quad \ldots\ldots\ldots\ldots\ldots\ldots\ldots\ldots\ldots\ldots (29a)$$

$$E \Delta y = \left\{ (1 - \lambda) \int \sin \phi \cos \phi \frac{d s}{A} - \int x y \frac{d s}{I_z} + \varepsilon^2 \int \left(\frac{1}{I_y} - \frac{\lambda}{F} \right) x^2 \sin \phi \cos \phi \, d s \right\} T_x + \left\{ \int \sin^2 \phi \frac{d s}{A} + \lambda \int \cos^2 \phi \frac{d s}{A} + \int x^2 \frac{d s}{I_z} + \varepsilon^2 \int x^2 \sin^2 \phi \frac{d s}{I_y} + \varepsilon^2 \lambda \int x^2 \cos^2 \phi \frac{d s}{F} \right\} T_y - \left\{ \varepsilon \int v x \sin \phi \frac{d s}{I_y} - \varepsilon \lambda \int u x \cos \phi \frac{d s}{F} \right\} T_z - \left\{ \int x \frac{d s}{I_z} \right\} M_z$$

$$+\left\{\varepsilon\int\left(\frac{1}{I_z}-\frac{\lambda}{F}\right)x\sin\phi\cos\phi\,ds\right\}M_y+\left\{\varepsilon\int x\sin^2\phi\,\frac{ds}{I_y}+\varepsilon\lambda\int x\cos^2\phi\,\frac{ds}{F}\right\}M_x+Ly \quad\ldots\ldots(29b)$$

$$E\,\Delta z=-\left\{\varepsilon\int v\,x\cos\phi\,\frac{ds}{I_y}+\varepsilon\lambda\int u\,x\sin\phi\,\frac{ds}{F}\right\}T_x-\left\{\varepsilon\int v\,x\sin\phi\,\frac{ds}{I_y}-\varepsilon\lambda\int u\,x\cos\phi\,\frac{ds}{F}\right\}T_y+\left\{\lambda\int\frac{ds}{A}+\int v^2\,\frac{ds}{I_y}+\lambda\int u^2\,\frac{ds}{F}\right\}T_z-\left\{\int v\cos\phi\,\frac{ds}{I_y}+\lambda\int u\sin\phi\,\frac{ds}{F}\right\}M_y-\left\{\int v\sin\phi\,\frac{ds}{I_y}-\lambda\int u\cos\phi\,\frac{ds}{F}\right\}M_x+Lz \quad\ldots\ldots(29c)$$

$$E\,\Delta\alpha=\left\{\int y\,\frac{ds}{I_z}\right\}T_x-\left\{\int x\,\frac{ds}{I_z}\right\}T_y+\left\{\int\frac{ds}{I_z}\right\}M_z+L\alpha \quad\ldots..(29d)$$

$$E\,\Delta\beta=\left\{\varepsilon\int x\cos^2\phi\,\frac{ds}{I_y}+\varepsilon\lambda\int x\sin^2\phi\,\frac{ds}{F}\right\}T_x+\left\{\varepsilon\int\left(\frac{1}{I_y}-\frac{\lambda}{F}\right)x\sin\phi\cos\phi\,ds\right\}T_y-\left\{\int v\cos\phi\,\frac{ds}{I_y}+\lambda\int u\sin\phi\,\frac{ds}{F}\right\}T_z+\left\{\int\cos^2\phi\,\frac{ds}{I_y}+\lambda\int\sin^2\phi\,\frac{ds}{F}\right\}M_y+\left\{\int\left(\frac{1}{I_y}-\frac{\lambda}{F}\right)\sin\phi\cos\phi\,ds\right\}M_x+L\beta \quad\ldots\ldots(29e)$$

$$E\,\Delta\gamma=\left\{\varepsilon\int\left(\frac{1}{I_z}-\frac{\lambda}{F}\right)x\sin\phi\cos\phi\,ds\right\}T_x+\left\{\varepsilon\int x\sin^2\phi\,\frac{ds}{I_y}+\varepsilon\lambda\int x\cos^2\phi\,\frac{ds}{F}\right\}T_y-\left\{\int v\sin\phi\,\frac{ds}{I_y}-\lambda\int u\cos\phi\,\frac{ds}{F}\right\}T_z+\left\{\int\left(\frac{1}{I_y}-\frac{\lambda}{F}\right)\sin\phi\cos\phi\right\}M_y+\left\{\int\sin^2\phi\,\frac{ds}{I_y}+\lambda\int\cos^2\phi\,\frac{ds}{F}\right\}M_x+L\gamma \quad\ldots\ldots(29f)$$

The deflection of the right-hand section likewise may be found, considering the crown as the origin and noting that the arch is symmetrical about the center of the crown. In this case, the equations will be the same, term by term, for both sides of the arch, except the loading terms and the sign of V and M. Substituting these values for Δx_L, Δx_R, etc., in the first set of Equations (25), there results:

$$\left\{\int\cos^2\phi\,\frac{ds}{A}+\lambda\int\sin^2\phi\,\frac{ds}{A}+\int y^2\,\frac{ds}{I_z}+\varepsilon^2\int x^2\cos^2\phi\,\frac{ds}{I_y}+\varepsilon^2\lambda\int x^2\sin^2\phi\,\frac{ds}{F}\right\}T_x-\left\{\varepsilon\int v\,x\cos\phi\,\frac{ds}{I_y}+\varepsilon\lambda\int u\,x\sin\phi\,\frac{ds}{F}\right\}T_z$$

$$+\left\{\int y\frac{d\,s}{I_z}\right\}M_z+\left\{\varepsilon\int\left(\frac{1}{I_y}-\frac{\lambda}{F}\right)x\sin\phi\cos\phi\,d\,s\right\}M_x=$$
$$-\frac{1}{2}(L\,x+R\,x)\ldots\ldots\ldots\ldots\ldots\ldots\ldots\ldots(30a)$$

$$\left\{\int\sin^2\phi\frac{d\,s}{A}+\lambda\int\cos^2\phi\frac{d\,s}{A}+\int x^2\frac{d\,s}{I_z}+\varepsilon^2\int x^2\sin^2\phi\frac{d\,s}{I_y}\right.$$
$$\left.+\varepsilon^2\lambda\int x^2\cos^2\phi\frac{d\,s}{F}\right\}T_y+\left\{\varepsilon\int\left(\frac{1}{I_y}-\frac{\lambda}{F}\right)x\sin\phi\cos\phi\,d\,s\right\}M_y=$$
$$-\frac{1}{2}(L\,y-R\,y)\ldots\ldots\ldots\ldots\ldots\ldots\ldots\ldots(30b)$$

$$-\left\{\varepsilon\int v\,x\cos\phi\frac{d\,s}{I_y}+\varepsilon\lambda\int u\,x\sin\phi\frac{d\,s}{F}\right\}T_x+\left\{\int v^2\frac{d\,s}{I_y}\right.$$
$$\left.+\lambda\int u^2\frac{d\,s}{F}+\lambda\int\frac{d\,s}{A}\right\}T_z-\left\{v\sin\phi\frac{d\,s}{I_y}-\lambda\int u\cos\phi\frac{d\,s}{F}\right\}M_x=$$
$$-\frac{1}{2}(L\,z+R\,z)\ldots\ldots\ldots\ldots\ldots\ldots\ldots\ldots(30c)$$

$$\left\{\int y\frac{d\,s}{I_z}\right\}T_x+\left\{\int\frac{d\,s}{I_z}\right\}M_z=-\frac{1}{2}(L\,\alpha+R\,\alpha)\ldots\ldots(30d)$$

$$\left\{\varepsilon\int\left(\frac{1}{I_y}-\frac{\lambda}{F}\right)x\sin\phi\cos\phi\,d\,s\right\}T_y+\left\{\int\cos^2\phi\frac{d\,s}{I_y}\right.$$
$$\left.+\lambda\int\sin^2\phi\frac{d\,s}{F}\right\}M_y=-\frac{1}{2}(L\,\beta-R\,\beta)\ldots\ldots\ldots(30e)$$

$$\left\{\varepsilon\int\left(\frac{1}{I_y}-\frac{\lambda}{F}\right)x\sin\phi\cos\phi\,d\,s\right\}T_x-\left\{\int v\sin\phi\frac{d\,s}{I_y}\right.$$
$$\left.-\lambda\int u\cos\phi\frac{d\,s}{F}\right\}T_z+\left\{\int\sin^2\phi\frac{d\,s}{I_y}+\lambda\int\cos^2\phi\frac{d\,s}{F}\right\}M_x=$$
$$-\frac{1}{2}(L\,\lambda+R\,\lambda)\ldots\ldots\ldots\ldots\ldots\ldots\ldots(30f)$$

The solution of Equations (30) will give the forces and moments at the crown, due to the loads on the arch ring represented by the loading terms, after which the stresses at any point are obtained.

The error due to assuming s as finite, may be reduced by taking a large number of blocks or by plotting the terms as a curve and taking the area under it.

Temperature Loading Terms.—As the loading terms are equal in quantity to the deflection of the crown of the section acting as a cantilever supported at the abutment, the terms for temperature can be written immediately and are as follows:

$$\frac{1}{2}(L\,x+R\,x)=x_a\,t^\circ\,e\,E\ldots\ldots\ldots\ldots\ldots\ldots(31a)$$

$$\frac{1}{2}(L\,y - R\,y) = \frac{1}{2}(L\,\beta + R\,\beta) = 0 \ldots (31b) \text{ and } (31e)$$

$$\frac{1}{2}(L\,z + R\,z) = \varepsilon\, x_a\, t^\circ\, e\, E \ldots\ldots\ldots\ldots\ldots\ldots (31c)$$

$$\frac{1}{2}(L\,\alpha + R\,\alpha) = \frac{1}{2}(L\,\gamma + R\,\gamma) = 0 \ldots (31d) \text{ and } (31f)$$

in which,

x_a = value of x for center of abutment;
t° = change in temperature from normal; and
e = coefficient of expansion.

If a finite summation is made and the terms are divided by the constant, Δs, the temperature terms also should be divided by this constant.

The principal loads of interest in arch design are the dead load, the uniform live load, and the concentrated load. If the road is on a grade and the cross-section is taken parallel to the barrel of the arch, the upper line of the fill is not level. This causes complications in the terms involving grade. The constant terms, E and s, can be cancelled, as they occur in every term.

Concentrated Loading Terms.—Equations for the loading terms have been written for a concentrated load, W, placed at the point, x', z', and acting vertically. These equations are derived by placing two equal and opposite forces at the crown and also two at the point, $x = o$, $z = z'$. One of these crown forces acts in the same manner as T_y in the equations already derived, the other, together with one at the point, o, z' produces a moment, Wz', equal to M_x, but opposite in sign, whereas, the original load and the second force at o, z' produce a moment, $W\,x'$, corresponding to M_z. Substituting $T_y = W$, $M_z = W\,x'$ and $M_x = -W\,z'$ in the equations for deflection, the following terms are produced for a vertical load of magnitude, W, placed at the point, x', z'. It is to be noted that the summation should be carried only from the abutment to the load, as the ring between the load and the crown is deformed only by the crown reactions.

$$L\,x = \left\{(1-\lambda)\int_A^C \sin\phi\cos\phi\,\frac{d\,s}{A} - \int_A^C x\,y\,\frac{d\,s}{I_z}\right.$$
$$\left. + \varepsilon^2\int_A^C x^2\sin\phi\cos\phi\left(\frac{1}{I_y} - \frac{\lambda}{F}\right)d\,s\right\} W + \left\{\int_A^C y\,\frac{d\,s}{I_z}\right\} W\,x'$$
$$- \left\{\varepsilon\int_A^C x\sin\phi\cos\phi\left(\frac{1}{I_y} - \frac{\lambda}{F}\right)d\,s\right\} W\,z' \ldots\ldots\ldots (32a)$$

$$L\,y = \left\{\int_A^C \sin^2\phi\,\frac{d\,s}{A} + \lambda\int_A^C \cos^2\phi\,\frac{d\,s}{A} + \int_A^C x^2\,\frac{d\,s}{I_z} + \varepsilon^2\int_A^C x^2\sin^2\phi\,\frac{d\,s}{I_y}\right.$$
$$\left. + \varepsilon^2\,\lambda\int_A^C x^2\cos^2\phi\,\frac{d\,s}{F}\right\} W - \left\{\int_A^C x\,\frac{d\,s}{I_z}\right\} W\,x'$$
$$- \left\{\varepsilon\int_A^C x\sin^2\phi\,\frac{d\,s}{I_y} + \varepsilon\,\lambda\int_A^C x\cos^2\phi\,\frac{d\,s}{F}\right\} W\,z' \ldots\ldots\ldots (32b)$$

$$L\,z = -\left\{\varepsilon\int_A^C v\,x\sin\phi\,\frac{d\,s}{I_y} - \varepsilon\,\lambda\int_A^C u\,x\cos\phi\,\frac{d\,s}{F}\right\}W + \left\{\int_A^C v\sin\phi\,\frac{d\,s}{I_y}\right.$$
$$\left. - \lambda\int_A^C u\cos\phi\,\frac{d\,s}{F}\right\}W\,z' \quad\ldots\ldots(32c)$$

$$L\,\alpha = -\left\{\int_A^C x\,\frac{d\,s}{I_z}\right\}W + \left\{\int_A^C \frac{d\,s}{I_z}\right\}W\,x' \quad\ldots\ldots(32d)$$

$$L\,\beta = \left\{\varepsilon\int_A^C\left(\frac{1}{I_y}-\frac{\lambda}{F}\right)x\sin\phi\cos\phi\,d\,s\right\}W$$
$$-\left\{\int_A^C\left(\frac{1}{I_y}-\frac{\lambda}{F}\right)\sin\phi\cos\phi\,d\,s\right\}W\,z' \quad\ldots\ldots(32e)$$

$$L\,\gamma = \left\{\varepsilon\int_A^C x\sin^2\phi\,\frac{d\,s}{I_y} + \varepsilon\,\lambda\int_A^C x\cos^2\phi\,\frac{d\,s}{F}\right\}W$$
$$-\left\{\int_A^C \sin^2\phi\,\frac{d\,s}{I_y} + \lambda\int_A^C \cos^2\phi\,\frac{d\,s}{F}\right\}W\,z' \quad\ldots\ldots(32f)$$

Dead Loading Terms.—In Fig. 5 are shown the forces acting on the left hand section of ring and fill contained between two vertical planes parallel to the barrel of the arch, one through the crown and the other through the point, P. The vertical forces are the weight of the arch ring, and of the inclined fill, which is separated for convenience into ten parts by a horizontal plane through the surface above the point of symmetry. A similar oblique wedge-shaped part due to the grade will have a like effect for the right half of the arch, but opposite in sign. The constant, η_d, denotes the ratio between intensities of horizontal and vertical earth pressures.

Taking moments and forces at the point, P, the following equations may be written:

$$E\,d\,v = \frac{1}{2}\,b\,\omega\,g\,x^2\sin\phi\,\frac{d\,s}{A} + W\sin\phi\,\frac{d\,s}{A} - \eta_d\,b\,\omega\,T\cos\phi\,\frac{d\,s}{A} \quad\ldots\ldots(33a)$$

$$E\,d\,u = \frac{1}{2}\lambda\,b\,\omega\,g\,x^2\cos\phi\,\frac{d\,s}{A} + \lambda\,W\cos\phi\,\frac{d\,s}{A} + \eta_d\,b\,\omega\,\lambda\,T\sin\phi\,\frac{d\,s}{A} \quad\ldots(33b)$$

$$E\,d\,z = 0 \quad\ldots\ldots(33c)$$

$$E\,d\,\alpha = -\frac{1}{6}\,b\,\omega\,g\,x^3\,\frac{d\,s}{I_z} - W\bar{x}\,\frac{d\,s}{I_z} - \eta_d\,b\,\omega\,R\,\frac{d\,s}{I_z} \quad\ldots\ldots(33d)$$

$$E\,d\,\beta = \frac{1}{6}\,\varepsilon\,b\,\omega\,g\,x^3\sin\phi\,\frac{d\,s}{I_y} + \varepsilon\,W\bar{x}\sin\phi\,\frac{d\,s}{I_y} - \frac{1}{6}\,n\,b^2\,\omega\,x\sin\phi\,\frac{d\,s}{I_y}$$
$$+\eta_d\,b\,\omega\,Q\cos\phi\,\frac{d\,s}{I_y} \quad\ldots\ldots(33e)$$

$$E\,d\,\gamma = \frac{1}{6}\,\lambda\,\varepsilon\,b\,\omega\,g\,x^3\cos\phi\,\frac{d\,s}{F} + \lambda\,\varepsilon\,W\bar{x}\cos\phi\,\frac{d\,s}{F} - \frac{1}{6}\lambda\,n\,b^2\,\omega\,x\cos\phi\,\frac{d\,s}{F}$$
$$-\eta_d\,b\,\omega\,\lambda\,Q\sin\phi\,\frac{d\,s}{F} \quad\ldots\ldots(33f)$$

in which the values, T, Q, and R are written to shorten the formulas. They represent the horizontal thrust, moment about the vertical through P and the moment about an axis through P parallel to the z-axis, respectively, due to horizontal earth action when $\eta_a\, b\, \omega$ is unity.

As to the other symbols used in Fig. 5, $\bar{x}$ is the horizontal distance from the plane through P to the center of gravity of the dead load, W.

Inserting these values in Table 6, the following equations are obtained which represent the loading terms for the left half of the arch:

$$E \Delta x = \frac{1}{2} b \omega g (1-\lambda) \int x^2 \sin\phi \cos\phi \frac{ds}{A}$$
$$+ (1-\lambda) \int W \sin\phi \cos\phi \frac{ds}{A} - \frac{1}{6} b \omega g \int x^3 y \frac{ds}{I_z} - \int W \bar{x} y \frac{ds}{I_z}$$
$$+ \frac{1}{6} \varepsilon^2 b \omega g \int x^4 \sin\phi \cos\phi \frac{ds}{I_y} - \frac{1}{6} \varepsilon^2 b \omega g \lambda \int x^4 \sin\phi \cos\phi \frac{ds}{F}$$
$$+ \varepsilon^2 \int W \bar{x} x \sin\phi \cos\phi \frac{ds}{I_y} - \varepsilon^2 \lambda \int W \bar{x} x \sin\phi \cos\phi \frac{ds}{F}$$
$$- \frac{1}{6} \varepsilon n b^2 \omega \int x^2 \sin\phi \cos\phi \frac{ds}{I_y} + \frac{1}{6} \varepsilon n \lambda b^2 \omega \int x^2 \sin\phi \cos\phi \frac{ds}{F}$$
$$+ \eta_a b \omega \Big\{ - T \cos^2\phi \frac{ds}{A} - \lambda \int T \sin^2\phi \frac{ds}{A} + \varepsilon \int Q x \cos^2\phi \frac{ds}{I_y}$$
$$+ \varepsilon \lambda \int Q x \sin^2\phi \frac{ds}{F} - \int R y \frac{ds}{I_z} \Big\} \quad \ldots\ldots\ldots\ldots\ldots\ldots (34a)$$

$$E \Delta y = \frac{1}{2} b \omega g \int x^2 \sin^2\phi \frac{ds}{A} + \frac{1}{2} \lambda b \omega g \int x^2 \cos^2\phi \frac{ds}{A}$$
$$+ \int W \sin^2\phi \frac{ds}{A} + \lambda \int W \cos^2\phi \frac{ds}{A} + \frac{1}{6} b \omega g \int x^4 \frac{ds}{I_z} + \int W \bar{x} x \frac{ds}{I_z}$$
$$+ \frac{1}{6} \varepsilon^2 b \omega g \int x^4 \sin^2\phi \frac{ds}{I_y} + \varepsilon^2 \int W \bar{x} x \sin^2\phi \frac{ds}{I_y}$$
$$- \frac{1}{6} \varepsilon n b^2 \omega \int x^2 \sin^2\phi \frac{ds}{I_y} + \frac{1}{6} \varepsilon^2 \lambda b \omega g \int x^4 \cos^2\phi \frac{ds}{F}$$
$$+ \varepsilon^2 \lambda \int W \bar{x} x \cos^2 \frac{ds}{F} - \frac{1}{6} \lambda \varepsilon n b^2 \omega \int x^2 \cos^2\phi \frac{ds}{F}$$
$$+ \eta_a b \omega \Big\{ - (1-\lambda) T \sin\phi \cos\phi \frac{ds}{A} + \varepsilon \int Q x \sin\phi \cos\phi \frac{ds}{I_y}$$
$$- \varepsilon \lambda \int Q x \sin\phi \cos\phi \frac{ds}{F} + \int R x \frac{ds}{I_z} \Big\} \quad \ldots\ldots\ldots\ldots (34b)$$

$$E \Delta z = - \frac{1}{6} \varepsilon b \omega g \int v x^3 \sin\phi \frac{ds}{I_y} - \varepsilon \int W \bar{x} v \sin\phi \frac{ds}{I_y}$$
$$+ \frac{1}{6} n b^2 \omega \int x v \sin\phi \frac{ds}{I_y} - \frac{1}{6} \lambda n b^2 \omega \int x u \cos\phi \frac{ds}{F}$$

$$+\frac{1}{6}\,\varepsilon\,\lambda\,b\,\omega\,g\int u\,x^3\cos\phi\,\frac{d\,s}{F}+\varepsilon\,\lambda\int W\,\bar{x}\,u\cos\phi\,\frac{d\,s}{F}$$

$$-\eta_d\,b\,\omega\left\{\int Q\,v\cos\phi\,\frac{d\,s}{I_y}+\lambda\int Q\,u\sin\phi\,\frac{d\,s}{F}\right\}\quad\ldots\ldots\ldots(34c)$$

$$E\,\Delta\,\alpha=-\frac{1}{6}\,b\,\omega\,g\int x^3\,\frac{d\,s}{I_z}-\int W\,\bar{x}\,\frac{d\,s}{I_z}-\eta_d\,b\,\omega\left\{\int R\,\frac{d\,s}{I_z}\right\}\quad\ldots\ldots(34d)$$

$$E\,\Delta\,\beta=\frac{1}{6}\,\varepsilon\,b\,\omega\,g\int x^3\sin\phi\cos\phi\,\frac{d\,s}{I_y}-\frac{1}{6}\,\varepsilon\,\lambda\,b\,\omega\,g\int x^3\sin\phi\cos\phi\,\frac{d\,s}{F}$$

$$+\varepsilon\int W\,\bar{x}\sin\phi\cos\phi\,\frac{d\,s}{I_y}-\varepsilon\,\lambda\int W\,\bar{x}\sin\phi\cos\phi\,\frac{d\,s}{F}$$

$$-\frac{1}{6}\,n\,b^2\,\omega\int x\sin\phi\cos\phi\,\frac{d\,s}{I_y}+\frac{1}{6}\,\lambda\,b^2\,\omega\,n\int x\sin\phi\cos\phi\,\frac{d\,s}{F}$$

$$+\eta_d\,b\,\omega\left\{\int Q\cos^2\phi\,\frac{d\,s}{I_y}+\lambda\int Q\sin^2\phi\,\frac{d\,s}{F}\right\}\quad\ldots\ldots\ldots\ldots(34e)$$

$$E\,\Delta\,\gamma=\frac{1}{6}\,\varepsilon\,b\,\omega\,g\int x^3\sin^2\phi\,\frac{d\,s}{I_y}+\varepsilon\int W\,x\sin^2\phi\,\frac{d\,s}{I_y}$$

$$-\frac{1}{6}\,n\,b^2\,\omega\int x\sin^2\phi\,\frac{d\,s}{I_y}+\frac{1}{6}\,\varepsilon\,\lambda\,b\,\omega\,g\int x^3\cos^2\phi\,\frac{d\,s}{F}$$

$$+\varepsilon\,\lambda\int W\,x\cos^2\phi\,\frac{d\,s}{F}-\frac{1}{6}\,\lambda\,n\,b^2\,\omega\int x\cos^2\phi\,\frac{d\,s}{F}$$

$$+\eta_d\,b\,\omega\left\{\int Q\sin\phi\cos\phi\,\frac{d\,s}{I_y}-\lambda\int Q\sin\phi\cos\phi\,\frac{d\,s}{F}\right\}\quad\ldots\ldots(34f)$$

The loading terms for the right side are the same, except for the sign of g and n. Equating the left side to the right and, combining or cancelling terms, Equations (35) are obtained:

$$\frac{1}{2}\,E\,(\Delta\,x_L+\Delta\,x_R)=(1-\lambda)\int W\sin\phi\cos\phi\,\frac{d\,s}{A}-\int W\,x\,y\,\frac{d\,s}{I_z}$$

$$+\varepsilon^2\int W\,x\,x\sin\phi\cos\phi\,\frac{d\,s}{I_y}-\varepsilon^2\,\lambda\int W\,\bar{x}\,x\sin\phi\cos\phi\,\frac{d\,s}{F}$$

$$+\eta_d\,b\,\omega\left\{-\int\frac{1}{2}\,(T_L+T_R)\cos^2\phi\,\frac{d\,s}{A}-\lambda\int\frac{1}{2}\,(T_L+T_R)\sin^2\phi\,\frac{d\,s}{A}\right.$$

$$+\varepsilon\int\frac{1}{2}\,(Q_L+Q_R)\,x\cos^2\phi\,\frac{d\,s}{I_y}+\varepsilon\,\lambda\int\frac{1}{2}\,(Q_L+Q_R)\,x\sin^2\phi\,\frac{d\,s}{F}$$

$$\left.-\int\frac{1}{2}\,(R_L+R_R)\,y\,\frac{d\,s}{I_z}\right\}\quad\ldots\ldots\ldots\ldots\ldots(35a)$$

$$\frac{1}{2}\,E\,(\Delta\,y_L-\Delta\,y_R)=\frac{1}{2}\,b\,\omega\,g\int x^2\sin^2\phi\,\frac{d\,s}{A}+\frac{1}{2}\,\lambda\,b\,\omega\,g\int x^2\cos^2\phi\,\frac{d\,s}{A}$$

$$+\frac{1}{6}\,b\,\omega\,g\int x^4\,\frac{d\,s}{I_z}+\frac{1}{6}\,\varepsilon^2\,b\,\omega\,g\int x^4\sin^2\phi\,\frac{d\,s}{I_y}-\frac{1}{6}\,\varepsilon\,n\,b^2\,\omega\int x^2\sin^2\phi\,\frac{d\,s}{I_y}$$

$$+\frac{1}{6}\,\lambda\,\varepsilon^2\,b\,\omega\,g\int x^4\cos^2\phi\,\frac{d\,s}{F}-\frac{1}{6}\,\varepsilon\,\lambda\,n\,b^2\,\omega\int x^2\cos^2\phi\,\frac{d\,s}{F}$$

$$+ \eta_a\, b\, \omega \Big\{ - (1-\lambda) \int \frac{1}{2} (T_L - T_R) \sin\phi \cos\phi \frac{d\,s}{A_s}$$

$$+ \varepsilon \int \frac{1}{2} (Q_L - Q_R)\, x \sin\phi \cos\phi \frac{d\,s}{I_y} - \varepsilon\, \lambda \int \frac{1}{2} (Q_L - Q_R)\, x \sin\phi \cos\phi \frac{d\,s}{F}$$

$$+ \int \frac{1}{2} (R_L - R_R)\, x \frac{d\,s}{I_z} \Big\} \quad \ldots\ldots\ldots\ldots\ldots\ldots (35b)$$

$$\frac{1}{2} E (\Delta z_L + \Delta z_R) = - \varepsilon \int W \bar{x}\, v \sin\phi \frac{d\,s}{I_y} + \varepsilon\, \lambda \int W \bar{x}\, u \cos\phi \frac{d\,s}{F}$$

$$- \eta_a\, b\, \omega \Big\{ \int \frac{1}{2} (Q_L + Q_R)\, v \cos\phi \frac{d\,s}{I_y} + \lambda \int \frac{1}{2} (Q_L + Q_R)\, u \sin\phi \frac{d\,s}{F} \Big\} \quad (35c)$$

$$\frac{1}{2} E (\Delta \alpha_L + \Delta \alpha_R) = - \int W \bar{x} \frac{d\,s}{I_z} - \eta_a\, b\, \omega \Big\{ \int \frac{1}{2} (R_L + R_R) \frac{d\,s}{I_z} \Big\} \quad (35d)$$

$$\frac{1}{2} E (\Delta \beta_L - \Delta \beta_R) = \frac{1}{6} \varepsilon\, b\, \omega\, g \int x^3 \sin\phi \cos\phi \frac{d\,s}{I_y}$$

$$- \frac{1}{6} \varepsilon\, b\, \omega\, g\, \lambda \int x^3 \sin\phi \cos\phi \frac{d\,s}{F} - \frac{1}{6} n\, b^2\, \omega \int x \sin\phi \cos\phi \frac{d\,s}{I_y}$$

$$+ \frac{1}{6} \lambda\, n\, b^2\, \omega \int x \sin\phi \cos\phi \frac{d\,s}{F} + \eta_a\, b\, \omega \Big\{ \int \frac{1}{2} (Q_L - Q_R) \cos^2\phi \frac{d\,s}{I_y}$$

$$+ \lambda \int \frac{1}{2} (Q_L - Q_R) \sin^2\phi \frac{d\,s}{F} \Big\} \quad \ldots\ldots\ldots\ldots\ldots (35e)$$

$$\frac{1}{2} E (\Delta \gamma_L + \Delta \gamma_R) = \varepsilon \int W \bar{x} \sin^2\phi \frac{d\,s}{I_y} + \varepsilon\, \lambda \int W \bar{x} \cos^2\phi \frac{d\,s}{F}$$

$$+ \eta_a\, b\, \omega \Big\{ \int \frac{1}{2} (Q_L + Q_R) \sin\phi \cos\phi \frac{d\,s}{I_y}$$

$$- \lambda \int \frac{1}{2} (Q_L + Q_R) \sin\phi \cos\phi \frac{d\,s}{F} \Big\} \quad \ldots\ldots\ldots\ldots\ldots (35f)$$

Such quantities as $\frac{1}{2} (T_L + T_R)$ are evaluated as follows:

From Fig. 5, direct:

$$T = \frac{1}{2} h_1 + h_1 n + \frac{2}{3} n^2 - T_c \quad \ldots\ldots\ldots\ldots\ldots (36)$$

$$Q = \frac{1}{6} h_1 n\, b + \frac{1}{6} n^2 b + \varepsilon\, T_c\, x - Q_c \quad \ldots\ldots\ldots\ldots\ldots (37)$$

$$R = \frac{1}{6} h_1 + \frac{1}{2} h_1^2 n + \frac{2}{3} h_1 n^2 + \frac{1}{6} n^3 + T\, e + T_c\, y - R_c - T_e\, e_e \quad \ldots (38)$$

Substituting the value of $h_1 = h + g\, x - n$:

$$T = \frac{1}{2} h^2 + g\, x\, h + \frac{1}{2} g^2 x^2 + \frac{1}{6} n^2 - T_c \quad \ldots\ldots\ldots\ldots (39)$$

$$Q = \frac{1}{6} b\, n\, h + \frac{1}{6} b\, n\, g\, x + \varepsilon\, T_c\, x - Q_c \quad \ldots\ldots\ldots\ldots (40)$$

$$R = \frac{1}{6} h^3 + \frac{1}{6} g^3 x^3 + \frac{1}{2} g x h^2 + \frac{1}{6} h n^2 + \frac{1}{2} g^2 x^2 h$$

$$+ \frac{1}{6} g x n^2 + T e - T y - R_c - T_c e_c \ldots\ldots\ldots\ldots\ldots (41)$$

Placing $x = 0, y = 0, h = f - e_c$

$$T_c = \frac{1}{2} f^2 + \frac{1}{2} e_c^2 - f e_c + \frac{1}{6} n^2 \ldots\ldots\ldots\ldots\ldots (42)$$

$$Q_c = \frac{1}{6} b n (f - e_c) \ldots\ldots\ldots\ldots\ldots (43)$$

$$R_c = \frac{1}{6} f^3 + \frac{1}{2} f^2 e_c + \frac{1}{2} f e_c^2 + \frac{1}{6} e_c^3 + \frac{1}{6} f n^2$$

$$- \frac{1}{6} n^2 e_c - \frac{1}{6} n^3 \ldots\ldots\ldots\ldots\ldots (44)$$

Changing the sign of g and n and adding or subtracting the left section from the right, the following results after substituting for h its equivalent $y + f - e$:

$$\frac{1}{2} (T_L + T_R) = \frac{1}{2} y^2 + f y - y e - f e + \frac{1}{2} e^2 + \frac{1}{2} g^2 x^2$$

$$- \frac{1}{2} e_c^2 + f e_c \ldots\ldots\ldots\ldots\ldots (45)$$

$$\frac{1}{2} (T_L - T_R) = g x y + f g x - g x e \ldots\ldots\ldots\ldots\ldots (46)$$

$$\frac{1}{2} (Q_L + Q_R) = \frac{1}{6} b n y - \frac{1}{6} b n e + \frac{1}{6} b n e_c + \varepsilon \left(\frac{1}{2} f^2 - f e_c \right.$$

$$\left. + \frac{1}{2} e_c^2 + \frac{1}{6} n^2 \right) x \ldots\ldots\ldots\ldots\ldots (47)$$

$$\frac{1}{2} (Q_L - Q_R) = \frac{1}{6} b n g x \ldots\ldots\ldots\ldots\ldots (48)$$

$$\frac{1}{2} (R_L + R_R) = \frac{1}{6} y^3 + \frac{1}{2} f y^2 + \frac{1}{2} g^2 x^2 y + \frac{1}{2} f g^2 x^2 + f e_c y$$

$$- \frac{1}{2} e_c^2 y - \frac{1}{2} f e^2 + \frac{1}{3} e^3 - \frac{2}{3} e_c^3 + \frac{1}{2} f e_c^2 - \frac{1}{2} y e^2 - f^2 e_c \ldots (49)$$

$$\frac{1}{2} (R_L - R_R) = \frac{1}{6} g^3 x^3 + \frac{1}{2} g x y^2 + g x f y - \frac{1}{2} g x e^2$$

$$+ \frac{1}{2} f^2 g x + \frac{1}{6} n^2 g x \ldots\ldots\ldots\ldots\ldots (50)$$

The loading terms for a level grade are obtained by placing g and n equal to zero and are as follows:

$$\frac{1}{2} E (\Delta x_L + \Delta x_R) = (1 - \lambda) \int W \sin \phi \cos \phi \frac{d s}{A} - \int W \bar{x} y \frac{d s}{I_z}$$

$$+ \varepsilon^2 \int W \bar{x}\, x \sin\phi \cos\phi \frac{d\,s}{I_y} - \varepsilon^2 \lambda \int W \bar{x}\, x \sin\phi \cos\phi \frac{d\,s}{F}$$

$$+ \eta_a\, b\, \omega \left\{ - \int \frac{1}{2} (T_L + T_R) \cos^2\phi \frac{d\,s}{A} - \lambda \int \frac{1}{2} (T_L + T_R) \sin^2\phi \frac{d\,s}{A} \right.$$

$$+ \frac{\varepsilon}{2} (Q_L + Q_R) \int x \cos^2\phi \frac{d\,s}{I_y} + \frac{\varepsilon\,\lambda}{2} (Q_L + Q_R) \int x \sin^2\phi \frac{d\,s}{F}$$

$$\left. - \int \frac{1}{2} (R_L + R_R)\, y \frac{d\,s}{I_z} \right\} \ldots\ldots\ldots\ldots\ldots\ldots (51a)$$

$$\frac{1}{2} E (\Delta y_L - \Delta y_R) = 0 \ldots\ldots\ldots\ldots\ldots\ldots (51b)$$

$$\frac{1}{2} E (\Delta z_L + \Delta z_R) = - \varepsilon \int W \bar{x}\, v \sin\phi \frac{d\,s}{I_y} + \varepsilon\,\lambda \int W \bar{x}\, u \cos\phi \frac{d\,s}{F}$$

$$- \eta_a\, b\, \omega \left\{ \frac{1}{2} (Q_L + Q_R) \int v \cos\phi \frac{d\,s}{I_y} \right.$$

$$\left. + \frac{\lambda}{2} (Q_L + Q_R) \int u \sin\phi \frac{d\,s}{F} \right\} \ldots\ldots\ldots\ldots\ldots (51c)$$

$$\frac{1}{2} E (\Delta \alpha_L + \Delta \alpha_R) = - \int W \bar{x} \frac{d\,s}{I_z} - \eta x\, b\, \omega \left\{ \int \frac{1}{2} (R_L + R_R) \frac{d\,s}{I_z} \right\} \quad (51d)$$

$$\frac{1}{2} E (\Delta \beta_L - \Delta \beta_R) = 0 \ldots\ldots\ldots\ldots\ldots\ldots (51e)$$

$$\frac{1}{2} E (\Delta \gamma_L + \Delta \gamma_R) = \varepsilon \int W \bar{x} \sin^2\phi \frac{d\,s}{I_y} + \lambda\,\varepsilon \int W \bar{x} \cos^2\phi \frac{d\,s}{F}$$

$$+ \eta_a\, b\, \omega \left\{ \frac{1}{2} (Q_L + Q_R) \int \sin\phi \cos\phi \frac{d\,s}{I_y} \right.$$

$$\left. - \frac{\lambda}{2} (Q_L + Q_R) \int \sin\phi \cos\phi \frac{d\,s}{F} \right\} \ldots\ldots\ldots\ldots (51f)$$

in which the values of the horizontal earth reactions become:

$$\frac{1}{2} (T_L + T_R) = \frac{1}{2} y^2 + f\,y + y\,e - f\,e + \frac{1}{2} e^2 + f\,e_c + \frac{1}{2} e_c^2 \ldots (52)$$

$$\frac{1}{2} (R_L + R_R) = \frac{1}{6} y^3 + \frac{1}{2} f\,y^2 + \left(f\,e_c - \frac{1}{2} e_c^2 \right) y - \frac{1}{2} f\,e^2 - \frac{1}{3} e^3$$

$$- \frac{2}{3} e_c + \frac{1}{2} f\,e_c^2 - \frac{1}{2} y\,e^2 - f^2 e_c \ldots\ldots\ldots\ldots\ldots (53)$$

$$\frac{1}{2} (Q_L + Q_R) = + \varepsilon \left(\frac{1}{2} f^2 - f\,e_c + \frac{1}{2} e_c^2 \right) x \ldots\ldots\ldots (54)$$

Uniform Loading Terms.—The loading terms for a load uniformly distributed over either half or all of the arch are obtained in an exactly analogous manner from Fig. 6. The following equations are taken at once from the diagram:

$$E\,d\,v = b\,w\,x \sin\phi \frac{d\,s}{A} - \eta_1\, b\, w\, T \cos\varphi \frac{d\,s}{A} \ldots\ldots\ldots (55a)$$

$$E\,d\,u = \lambda\,b\,w\,x\cos\phi\,\frac{d\,s}{A} + \eta_l\,b\,w\,\lambda\,T\sin\phi\,\frac{d\,s}{A} \quad \ldots\ldots (55b)$$

$$E\,d\,z = 0 \quad \ldots\ldots (55c)$$

$$E\,d\,\alpha = -\frac{1}{2}\,b\,w\,x^2\,\frac{d\,s}{I_z} - \eta_l\,b\,w\,R\,\frac{d\,s}{I_z} \quad \ldots\ldots (55d)$$

$$E\,d\,\beta = \frac{1}{2}\,\varepsilon\,b\,w\,x^2\sin\phi\,\frac{d\,s}{I_y} + \eta_l\,b\,w\,Q\cos\phi\,\frac{d\,s}{I_y} \quad \ldots\ldots (55e)$$

$$E\,d\,\gamma = \frac{1}{2}\,\varepsilon\,\lambda\,b\,w\,x^2\cos\phi\,\frac{d\,s}{F} - \eta_l\,b\,w\,\lambda\,Q\sin\phi\,\frac{d\,s}{F} \quad \ldots\ldots (55f)$$

in which the earth pressure terms are:

$$T = h_1 + g\,x - f_c + e_c \quad \ldots\ldots (56)$$

$$Q = \frac{1}{6}\,b\,n + \varepsilon\,f_c\,x - \varepsilon\,e_c\,x - \frac{1}{6}\,b\,n = \varepsilon\,(f - e_c)\,x \quad \ldots\ldots (57)$$

$$R = \frac{1}{2}\,(h + g\,x)^2 - \frac{1}{2}\,(f - e_c)^2 + (h + g\,x)\,e - (f - e_c)\,(y + e_c) \quad \ldots\ldots (58)$$

Substituting these values in Table 6, the loading terms for the arch loaded on one section only becomes:

$$\begin{aligned} E\,\Delta\,x = {} & b\,w\,(1-\lambda)\int x\sin\phi\cos\phi\,\frac{d\,s}{A} - \frac{1}{2}\,b\,w\int x^2\,y\,\frac{d\,s}{I_z} \\ & + \frac{1}{2}\,\varepsilon^2\,b\,w\int x^3\sin\phi\cos\phi\,\frac{d\,s}{I_y} - \frac{1}{2}\,\varepsilon^2\,b\,w\,\lambda\int x^3\sin\phi\cos\phi\,\frac{d\,s}{F} \\ & + \eta_l\,b\,w\left\{-\int T\cos^2\phi\,\frac{d\,s}{A} - \lambda\int T\sin^2\phi\,\frac{d\,s}{A} - R\,y\,\frac{d\,s}{I_z}\right. \\ & \left. + \varepsilon\int Q\,x\cos^2\phi\,\frac{d\,s}{I_y} + \varepsilon\,\lambda\int Q\,x\sin^2\phi\,\frac{d\,s}{F}\right\} \quad \ldots\ldots (59a) \end{aligned}$$

$$\begin{aligned} E\,\Delta\,y = {} & b\,w\int x\sin^2\phi\,\frac{d\,s}{A} + \lambda\,b\,w\int x\cos^2\phi\,\frac{d\,s}{A} + \frac{1}{2}\,b\,w\int x^3\,\frac{d\,s}{I_z} \\ & + \frac{1}{2}\,\varepsilon^2\,b\,w\int x^3\sin^2\phi\,\frac{d\,s}{I_y} + \frac{1}{2}\,\lambda\,\varepsilon^2\,b\,w\int x^3\cos^2\phi\,\frac{d\,s}{F} \\ & + \eta_l\,b\,w\left\{-(1-\lambda)\int T\sin\phi\cos\phi\,\frac{d\,s}{A} + \int R\,x\,\frac{d\,s}{I_z}\right. \\ & \left. + \varepsilon\int Q\,x\sin\phi\cos\phi\,\frac{d\,s}{I_y} - \varepsilon\,\lambda\int Q\,x\sin\phi\cos\phi\,\frac{d\,s}{F}\right\} \quad \ldots\ldots (59b) \end{aligned}$$

$$\begin{aligned} E\,\Delta\,z = {} & -\frac{1}{2}\,\varepsilon\,\overline{b}\,w\int x^2\,v\sin\phi\,\frac{d\,s}{I_y} + \frac{1}{2}\,\lambda\,\varepsilon\,b\,w\int x^2\,u\cos\phi\,\frac{d\,s}{F} \\ & - \eta_l\,b\,w\left\{\int Q\,v\cos\phi\,\frac{d\,s}{I_y} + \lambda\int Q\,u\sin\phi\,\frac{d\,s}{F}\right\} \quad \ldots\ldots (59c) \end{aligned}$$

$$E\,\Delta\,\alpha = -\frac{1}{2}\,b\,w\int x^2\,\frac{d\,s}{I_z} - \eta_l\,b\,w\left\{R\,\frac{d\,s}{I_z}\right\} \quad \ldots\ldots (59d)$$

$$E \Delta \beta = \frac{1}{2} \varepsilon\, b\, w \int x^2 \sin\phi \cos\phi \frac{d\,s}{I_y} - \frac{1}{2} \varepsilon\, \lambda\, b\, w \int x^2 \sin\phi \cos\phi \frac{d\,s}{F}$$
$$+ \eta_l\, b\, w \left\{ \int Q \cos^2\phi \frac{d\,s}{I_y} + \lambda \int Q \sin^2\phi \frac{d\,s}{F} \right\} \ldots\ldots\ldots (59e)$$

$$E \Delta \gamma = \frac{1}{2} \varepsilon\, b\, w \int x^2 \sin^2\phi \frac{d\,s}{I_y} + \frac{1}{2} \lambda\, \varepsilon\, b\, w \int x^2 \cos^2\phi \frac{d\,s}{F}$$
$$+ \eta_l\, b\, w \left\{ \int Q \sin\phi \cos\phi \frac{d\,s}{I_y} - \lambda \int Q \sin\phi \cos\phi \frac{d\,s}{F} \right\} \ldots\ldots (59f)$$

As before, adding the terms of the left section to the right, after making the proper changes in sign, the equations for full load are obtained:

$$E\,(\Delta x_L + \Delta x_R) = (1-\lambda)\, b\, w \int x \sin\phi \cos\phi \frac{d\,s}{A} - \frac{1}{2}\, b\, w \int x^2\, y \frac{d\,s}{I_z}$$
$$+ \frac{1}{2}\, \varepsilon^2\, b\, w \int x^3 \sin\phi \cos\phi \frac{d\,s}{I_y} - \frac{1}{2}\, \varepsilon^2\, \lambda\, b\, w \int x^3 \sin\varphi \cos\phi \frac{d\,s}{F}$$
$$+ \eta_l\, b\, w \left\{ - \int \frac{1}{2} (T_L + T_R) \cos^2\phi \frac{d\,s}{A} - \lambda \int \frac{1}{2} (T_L + T_R) \sin^2\phi \frac{d\,s}{A} \right.$$
$$- \int \frac{1}{2} (R_L + R_R)\, y \frac{d\,s}{I_z} + \varepsilon^2 (f - e_c) \int x^2 \cos^2\phi \frac{d\,s}{I_y}$$
$$\left. + \lambda\, \varepsilon^2 (f - e_c) \int x^2 \sin^2\phi \frac{d\,s}{F} \right\} \ldots\ldots\ldots\ldots\ldots (60a)$$

$$\frac{1}{2} E\,(\Delta y_L - \Delta y_R) = \eta_l\, b\, w \left\{ - (1-\lambda)\, g \int x \sin\phi \cos\phi \frac{d\,s}{A} \right.$$
$$\left. + g \int x^2\, y \frac{d\,s}{I_z} + g\, f \int x^2 \frac{d\,s}{I_z} \right\} \ldots\ldots\ldots\ldots\ldots (60b)$$

$$\frac{1}{2} E\,(\Delta z_L + \Delta z_R) = - \frac{1}{2}\, \varepsilon\, b\, w \int x^2\, v \sin\phi \frac{d\,s}{I_y}$$
$$+ \frac{1}{2}\, \lambda\, \varepsilon\, b\, w \int x^2\, u \cos\phi \frac{d\,s}{F} - \eta_l\, b\, w \left\{ \varepsilon\, (f - e_c) \int v\, x \cos\phi \frac{d\,s}{I_y} \right.$$
$$\left. + \varepsilon\, \lambda\, (f - e_c) \int u\, x \sin\phi \frac{d\,s}{F} \right\} \ldots\ldots\ldots\ldots\ldots (60c)$$

$$\frac{1}{2} E(\Delta \alpha_L + \Delta \alpha_R) = - \frac{1}{2}\, b\, w \int x^2 \frac{d\,s}{I_z} - \eta_l\, b\, w \left\{ \frac{1}{2} (R_L + R_R) \frac{d\,s}{I_z} \right\} . (60d)$$

$$\frac{1}{2} E\,(\Delta \beta_L - \Delta \beta_R) = 0 \ldots\ldots\ldots\ldots\ldots\ldots\ldots (60e)$$

$$\frac{1}{2} E\,(\Delta \gamma_L + \Delta \gamma_R) = \frac{1}{2}\, \varepsilon\, b\, w \int x^2 \sin^2\phi \frac{d\,s}{I_y} + \frac{1}{2}\, \varepsilon\, \lambda\, b\, w \int x^2 \cos^2\phi \frac{d\,s}{F}$$
$$+ \eta_l\, b\, w \left\{ \varepsilon (f - e_c) \int x \sin\phi \cos\phi \frac{d\,s}{I_y} \right.$$
$$\left. - \varepsilon\, \lambda\, (f - e_c) \int x \sin\phi \cos\phi \frac{d\,s}{F} \right\} \ldots\ldots\ldots\ldots\ldots (60f)$$

in which, the terms due to earth pressure are:

$$\frac{1}{2}(T_L + T_R) = y - e + \frac{1}{2} f_c \quad \ldots\ldots(61)$$

$$\frac{1}{2}(Q_L + Q_R) = \varepsilon (f - e_c)\, x \quad \ldots\ldots(62)$$

$$\frac{1}{2}(R_L + R_R) = \frac{1}{2} y^2 + \frac{1}{2} g^2 x^2 + y\, e_c + \frac{1}{2} e_c^2 - \frac{1}{2} e^2 \quad \ldots\ldots(63)$$

$$\frac{1}{2}(R_L - R_R) = g\, x\, y + g\, x\, f \quad \ldots\ldots(64)$$

$$\frac{1}{2}(T_L - T_R) = g\, x \quad \ldots\ldots(65)$$

If g and n are placed equal to zero, the value of the second loading term reduces to zero; also, one term is dropped from the value of $\frac{1}{2}(R_L + R_R)$, but otherwise the terms are unaffected.

Shortening the Equations.—The equations as obtained are unwieldy for practical use, and an attempt has been made to shorten them without materially sacrificing their accuracy. If the terms due to direct thrust on the arch ring, and due to the deformations from shear and bending about the normal, are omitted, the resulting answer is affected but slightly. These terms are small compared to those due to bending about a horizontal axis and torsion about the line perpendicular to the face of the block.

The equations for determining the crown reactions can then be written, as given in Equations (1). In these equations, the terms that should be omitted in the case of earth thrust will change with the shape of the arch ring. However, the true values of η_d and η_l are very uncertain. As a first approximation, the writer would suggest the ones given.

HIGHWAY RESEARCH IN ILLINOIS*

By Clifford Older,† M. Am. Soc. C. E.

Synopsis

In this paper are described a series of research projects carefully planned to give an insight and understanding of the unsolved problems of rural pavement design.

The principal problems investigated include the drainage of sub-grade soils, the effect of repeated bearing pressures on soils, the effect of temperature changes on pavement surfaces, the position of wheel loads as affecting stresses in pavement slabs, impact resulting from moving wheel loads, and the fatigue effect of repeated loads causing bending stresses in plain concrete.

A test road was constructed so as to eliminate as far as possible the variable factor of sub-grade bearing power. Six groups of test sections were built, each representing a given type of pavement. Each group included a series of sections graduated in thickness and strength from light to heavy, and presumed to be comparable with corresponding sections of the other groups. The test road was subjected to a graduated artificial truck traffic, beginning with wheel loads of 2 500 lb. and ending with wheel loads of 13 000 lb.

In this paper are described briefly the methods used in the investigations, the data obtained, and the tentative conclusions drawn from these studies.

The highway research activities of the Division of Highways, Department of Public Works and Buildings, of Illinois were started in 1920 with an ambitious program. This work centers about a test road constructed by the State near Bates, Ill., popularly called the Bates Test Road. The contemplated expenditure of about $100 000 000 for the paving of a primary road system was the inspiration that gave birth to the intensive research activities of the Department.

For purposes of discussion, this research work will be considered under two classifications:

First.—Carefully controlled special investigations bearing on the most important factors involved in the rational design of pavement surfaces. The principal problems were to determine (*a*) the path of wheel travel resulting in maximum destructive forces; (*b*) the impact effects of wheel loads; (*c*) the safe working stress for certain paving materials; and (*d*) the character of the support afforded the pavement by the sub-grade soil.

Second.—Traffic tests of a variety of pavement sections designed so as to give empirical data for use in confirming any fundamental laws developed.

* Presented at the meeting of the Highway Division, January 17, 1924.

† Chf. Highway Engr., Div. of Highways, Springfield, Ill.

Anticipating possible failure to develop a complete rational method for the design of pavement surfaces, the empirical data were expected to become a valuable guide for future construction. The Bates Test Road was planned with both these general forms of research in mind.

General Plan of the Research Project

In planning the road, an endeavor was made to include as comprehensive a series of test sections as might be necessary to bring out the traffic-supporting characteristics of each of the general types considered to merit a place in the large State paving program then contemplated. Each group of sections representing a given type included ranges of thickness varying from an arbitrary minimum considered suitable for the lightest traffic to a maximum considered as possibly being able to withstand the heaviest units of traffic permitted in Illinois.

As the test sections were completed, special investigations were undertaken, including observations of natural phenomena and a series of carefully controlled load tests designed to throw light on the rational design problem. It was then planned to subject all sections to an artificial truck traffic, beginning with truck loads no greater than those which might be expected on light traffic roads, followed by successive increases of wheel loads until the maximum permitted by law had been reached, or possibly exceeded. It was hoped that this plan of traffic testing would bring out at least roughly the relationship between wheel loads and thickness of pavement for each type used.

Description of Test Sections

Each of the following types was represented by a group of sections:

(*a*) Vitrified brick surfacing with bituminous joint filler on a macadam base;
(*b*) Asphaltic concrete surfacing on a macadam base;
(*c*) Asphaltic concrete surfacing on a concrete base;
(*d*) Vitrified brick with bituminous joint filler on a concrete base;
(*e*) So-called "monolithic" brick, or brick with cement grout filler laid on a concrete base before it had set; and
(*f*) One-course concrete, both plain and with various inclusions of embedded steel.

In Table 1 will be found details of the various sections included in the original construction, grouped by types. Sections 12 to 57, inclusive, were constructed in the fall of 1920. The base of Sections 1 to 11, inclusive, was laid in the spring of 1921. The asphaltic concrete surface on Sections 6 to 22, inclusive, was laid during the spring months of 1921, as was also the brick surfacing on Sections 1 to 5, inclusive, and 23 to 32, inclusive. Concrete Sections 57 to 63, inclusive, were laid in the spring of 1921. Sections 63 and 63B were not included in the original plan, but were added before the completion of the remainder of the sections, profiting by the results obtained from certain preliminary investigations, to be described later.

TABLE 1.—Detailed Description of the Original Test Sections.

(*a*) Vitrified Brick Surfacing with Bituminous Joint Filler on Macadam Base.*

Number of section.	Length, in feet.	Thickness of brick, in inches.	Cushion.	Base course thickness, in inches.	Total thickness, in inches.	Number of courses in base.
1 A	100	3-lug	2-in. sand	4	9	1
B	100	3-lugless	2-in. "	4	9	1
2	100	4-lug	2-in. "	4	10	1
3	100	4- "	2-in. "	4	10	1
4	100	4-lugless	1-in. mastic	8	13	2
5	100	3- "	2-in. "	8	13	2
....	600	.....	.....	..	..	..

(*b*) Asphaltic Concrete Surface on Macadam Base.*

Number of section.	Length, in feet.	Wearing course.	Base course.	Total thickness, in inches.	Number of courses in base.
6	200	2 in. Topeka	10 in. Macadam	12	2
7	200	2 " "	8 " "	10	2
8	200	1½ " " / 1½ " Binder	5 " "	8	1
9	200	2 " Topeka	6 " "	8	1
10	200	2 " "	4 " Novaculite	6	1
11	200	2 " "	4 " Macadam	6	1
..	1 200	.....	.....	..	..

(*c*) Asphaltic Concrete Surface on Concrete Base.†

Number of section.	Length, in feet.	Wearing course, in inches.	Base course thickness, in inches.	Mix.	Total thickness, in inches.
12 A	200	2 in. Topeka	4	1-3-5	6
B	25	2 " "	5	1-3-5	7
13	200	1½ " " / 1½ " Binder	4	1-3-5	7
14	200	2 " Topeka	4	1-2-3½	6
15	200	1½ " " / 1½ " Binder	4	1-2-3½	7
16	200	2 " Topeka	5	1-3-5	7
17	200	2 " "	5	1-2-3½	7
18	200	1½ " " / 1½ " Binder	5	1-2-3½	8
19	200	2 " Topeka	6	1-3-5	8
20	200	2 " "	6	1-2-3½	8
21	200	2 " "	7	1-2-3½	9
22	200	1½ " " / 1½ " Binder	8	1-2-3½	11
....	2 225	.....	..	.....	..

* The coarse aggregate for the macadam base is crushed limestone.

† Crushed limestone used for coarse aggregate.

TABLE 1.—(*Continued*).

(*d*) VITRIFIED BRICK SURFACE WITH BITUMINOUS JOINT FILLER ON CONCRETE BASE.*

Number of section.	Length, in feet.	Thickness of brick, in inches.	Cushion.	Base course thickness, in inches.	Base mix.	Total thickness, in inches.
23 A	100	3-lug	1 sand	6½	1-2-3½	10½
B	100	3-lugless	1 "	6½	"	10½
24	100	3-lug	1 "	5½	"	9½
25	100	3-lugless	1 mastic	5½	"	9½
26 A	100	4-lug	1 sand	4	"	9
B	100	4-lugless	1 "	4	"	9
27	100	3-lug	1 "	4½	"	8½
28	100	3-lugless	1 "	4½	"	8½
29 A	100	3-lug	1 "	4½	1-3-5	8½
B	75	3-lugless	1 "	4½	"	8½
30	125	3-lug	1 "	3½	1-2-3½	7½
31	100	3-lugless	1 sand-cement	3½	"	7½
32 A	100	3-lug	1 sand	3½	1-3-5	7½
B	100	3-lugless	1 "	3½	"	7½
.....	1 400	.....	.....	...	.....	...

(*e*) MONOLITHIC BRICK ON CONCRETE BASE.*

Number of section.	Length, in feet.	Thickness of brick, in inches.	Type.	Base course thickness, in inches.	Base mix.	Total thickness, in inches.
33	200	3	Monolithic	2	1-2-3½	5
34 A	200	3	Semi-monolithic	2	"	5¾ (¾ in. sand cement bed)
35	200	4	Monolithic	2	"	6
36	200	3	"	3	1-3-5	6
37	200	3	"	3	1-2-3½	6
38	200	4	"	3	"	7
39	200	4	"	4	1-3-5	8
.....	1 400	..	.....	..	.....	.....

* Crushed limestone used for coarse aggregate.

TABLE 1.—(*Continued.*)

(*f.*) Portland Cement Concrete*.

Number of section.	Length, in feet.	Thickness, in inches.	Mix.	Special features.
40	200	9	1-2-3½	None.
41	150	8	"	Corrugated transverse joint every 25 ft. Corrugated longitudinal joints full length of section†.
42	150	8	"	None.
43	150	7	"	Corrugated transverse joint every 25 ft. Corrugated longitudinal joints full length of section†.
44	150	7	"	None.
45	100	6	"	Corrugated transverse joint every 25 ft. Corrugated longitudinal joints full length of section†. Pavement reinforced with circumferential reinforcing in 25 by 9 ft. sections‡.
46	100	6	"	Corrugated transverse joint every 25 ft. Corrugated longitudinal joints full length of section†. Pavement reinforced with circumferential reinforcing in 25 by 18 ft. sections. Transverse rods passed through longitudinal joints. No longitudinal rods adjacent to longitudinal joints‡.
47	100	6	"	Corrugated transverse joint every 25 ft. No longitudinal joints†. Pavement reinforced with circumferential reinforcing in 25 by 18 ft. sections.
48	100	5	"	Same as Section 45.
49	100	5	"	" " " 46.
50	100	5	"	" " " 47.
51	100	6	"	Wire mesh reinforcing§.
52	200	6	"	None.
53	100	5	"	Same as Section 51.
54	200	5	"	None.
55	200	5	"	"
56	200	5	"	4% Calcium chloride incorporated in 125 ft. 2½% " " " " 75 ft.
57	200	5	"	Cemite cement used.
58	200	4	"	4-in. rolled-stone base course under slab.
59	200	4	"	Cemite cement used.
60	200	4	"	2½% calcium chloride incorporated.
61A	100	4	"	Hydrated lime, 7½%.
61B	100	4	"	None.
62	200	4	"	‖
63A	150	7	"	‖
63B	50	7	"	‖
....	3 800	....	....	

* Crushed limestone used for coarse aggregate in all sections, except Sections 55 and 63A, in which gravel was used.

† Transverse and longitudinal joints were formed by setting on edge strips of horizontally corrugated galvanized iron. The strips were 6 ft. long and had a width of 1 in. less than the thickness of the pavement. The width of the corrugations was 3 in., and the depth 1 in. The metal was 16-gauge and the weight of galvanizing was 2 oz. per sq. ft.

‡ All bar reinforcing consisted of ¾-in. round deformed dowel bars placed 2 in. from the top of the slab and 6 in. in from the edges of the section, with a 3-in. lap at intersections.

§ The wire mesh reinforcing weighed approximately 45 lb. per 100 sq. ft. The total effective longitudinal sectional area, in square inches per foot of width, was 0.093 and the sectional area of the longitudinals, in square inches per foot of width, was 0.087.

‖ Longitudinal joint full length of section; ⅝-in. deformed bars, 5 ft. long and spaced 10 ft. apart, were placed across longitudinal joint. A ¾-in. plain round painted bar was placed 6 in. from each outside edge of the slab and at one-half its depth. The longitudinal bar along the edge was continuous through Sections 62, 63A, and 63B.

A length of 200 ft. was selected as standard for each primary test section. This dimension should be of such magnitude that in case of the complete failure of an adjacent section, thereby imposing undue stress on the end of the section in question, an additional length would still remain from which to judge the normal effect of traffic on a similar road of indefinite length. It was also considered that the test sections involving the use of concrete should be of suffi-

cient length to include one construction joint and at least one natural transverse contraction crack before the artificial truck traffic was started.

In each section involving the use of concrete, a construction joint was placed at a distance of 25 ft. from the east end of the section. A number of Goldbeck pressure cells were placed in many of the sections as the pavement was laid. About 600 iron pipes of a length equal to the depth of the pavement were also set at various places, the tops being closed by water-tight plugs. The purpose of these pipes was to enable observers to secure samples of the sub-grade soil for moisture determinations and to facilitate observation of contact between the under surface of the pavement slab and the sub-grade soil.

Inasmuch as the soil throughout a large part of the State exhibits fairly uniform physical characteristics and considering the fact that the relative behavior of the various sections could not be judged if the nature of the foundation varied materially, a site was selected where sub-grade conditions would be as nearly uniform as possible. Practically all unprejudiced observers agree that the Bates Road site fulfilled these conditions as ideally as could be expected in a length of road of two miles or more. No visible variation in the character of the soil could be detected; on the other hand, no positive method of establishing beyond question the lack of variation in sub-grade soil could be found.

Impact Investigations

The wide variety of pavement designs on the Bates Road offered an ideal opportunity to observe the behavior of each under carefully controlled conditions. As rapidly as the sections were completed and aged, preliminary investigations as to their action under load were conducted.

A knowledge of the wheel loads imposed by highway traffic is a fundamental requirement for rational design. It is believed that until more is known regarding the design of the economical highway transport freight unit, wheel loads must be arbitrarily limited by law, in order to safeguard the many millions of dollars already invested in pavements. In contemplating the design of a pavement, it is necessary either to assume the maximum expected wheel load or be governed by the limits set by the law. Whether or not an impact factor must be allowed is a matter of great importance. Research, therefore, was undertaken to determine this.

The impact effect of wheel loads on concrete pavements, and on pavements with concrete base only, was investigated. No suitable instrument could be found for determining the fiber deformation in the upper face of a concrete slab under moving loads; instead, an attempt was made to find a measure of the impact stresses by accurate observations of deflections. Records of rigid pavement failures seem to indicate that, in ordinary types, maximum stresses occur at corners and unbroken edges. Accordingly, impact observations were confined to such points.

Relation of Deflection Curves Due to Impact and to Static Loads.—It was thought that possibly a sudden blow, produced, for instance, by a truck wheel falling from an obstruction, might result in a deflection curve of shorter radius than that resulting from a static load giving the same total deflection at a

certain point. In order to establish the relationship of deflection curves produced by impact and by static loads, the following plan was finally devised: At intervals along the edge of the pavement slab, Ames dials were located so as to indicate the deflection of the slab at distances of 0 in., 20 in., 4 ft., 7 ft., 10 ft., 13 ft., and 16 ft. from the point of observation. The dials were actuated by metallic lugs attached to the pavement edge, and were equipped with a friction device, by which the spindle and the index pointer, having moved to the point of maximum deflection, would retain that position after the load was removed and the pavement slab had recovered its original elevation. A small bulb at each dial, electrically connected, remained lighted as long as the lug and dial were in contact. The procedure was then as follows: The spindle of each dial was adjusted to contact with the lug, each bulb, therefore, being lighted. The wheel of a loaded truck was then lifted by a hydraulic jack and allowed to fall on the pavement edge or corner at a point immediately opposite the zero dial, the wheel load and height of drop being varied to represent impact conditions up to such extremes as the slab might be expected to resist without failure. Only such loads and drops were recorded as caused an impact deflection greater than that resulting from the load at rest. The fact that the dropping of the wheel extinguished all the lights, with no subsequent flicker, indicated conclusively that the dials recorded the impact deflection only, rather than any subsequent vibratory or static load deflection. After the dials were read, a gradually increasing load was applied at the same point on the pavement, using a hydraulic jack and a loadometer, until contact again was made at the zero dial. All the dials then were adjusted to contact and readings again taken. Thus, the first set of readings defined the impact deflection curve, and the second, a static deflection curve having an equal maximum.

Tests conducted during daylight hours were not reliable, owing doubtless to temperature effects. All such tests, therefore, were made at night during periods of least sub-grade support resulting from warping of the slabs due to change in temperature, a condition which will be discussed elsewhere.

In Fig. 1 are plotted the readings of the night test that resulted in the greatest variance between the impact and static deflection curves; the average results of these tests show a close coincidence of the two graphs. This may be appreciated from the fact that although a static load of 10 000 lb. might be necessary to effect a pavement deflection sufficient to light the first bulb, yet an increase of only about 200 lb. would cause contact at all the remaining dials. In many cases, several of the bulbs would light at the same instant. Often when the first bulb showed contact, a man jumping on the edge of the pavement could make or break contact at all the dials.

The close coincidence of the impact and static deflection curves indicates that the deflection method is reasonably reliable.

Procedure for Impact Tests.—As applied to actual impact of traffic, the method was as follows: A smooth runway consisting of steel plates was laid on the surface of the pavement near the edge (Fig. 2). A loaded truck was placed on the shoulder and arranged in such a manner that a hydraulic jack, re-acting against an I-beam, which could be quickly run out from under the truck body, might be used to impose a static load of any required amount at

the point where one wheel of a moving truck would fall from the end of the runway. An Ames dial with a friction device, arranged to indicate maximum deflection, was placed at the edge of the pavement opposite the point where the wheel would strike (Fig. 3). An electric contact and light bulb was arranged so that a subsequent equal deflection would light the bulb. Electric contact points at fixed distances on the runway, and a stop-watch, afforded means for determining the speed of the truck. Immediately after the truck had passed, the hydraulic jack, together with a weighing device, was swung out, and a static load of increasing amount applied until contact was secured at the dial.

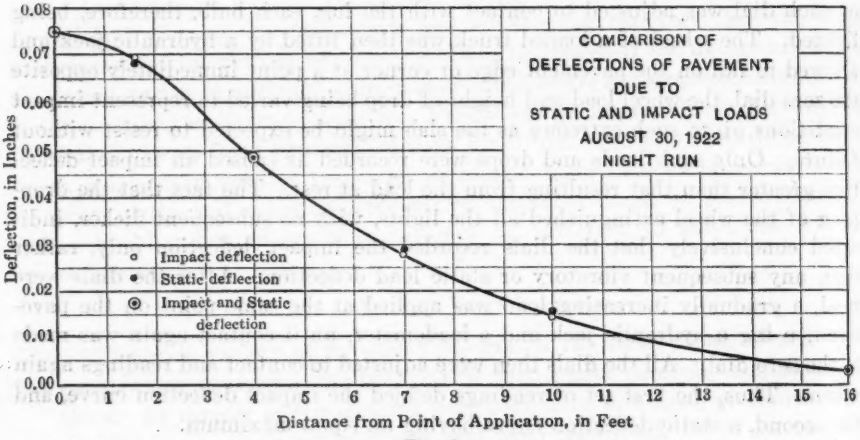

FIG. 1.

Assuming that the impact and static deflection curves are coincident in all directions and assuming also that if the radius of deflection curvature is the same, the fiber deformations and stresses are equal also, then the ratio of the static load to the moving wheel load should represent the correct impact factor for use under similar conditions.

Following a series of runs designed to determine this relationship for various speeds and height of drop, the truck was operated in the opposite direction so that the impact would be that caused by the wheel mounting the obstruction.

Results of Impact Tests.—Fig. 4 shows the results obtained for wheel loads of 4 000 lb., 6 000 lb., and 8 000 lb., for drops of $\frac{1}{8}$ in., $\frac{1}{4}$ in., $\frac{3}{8}$ in., and $\frac{1}{2}$ in., and for truck speeds varying from about 1 mile per hour to about 20 miles per hour. The unsprung weight was constant. Fig. 5 shows the results obtained under similar conditions, except that the truck moved in the opposite direction so as to mount the obstruction. The increase in wheel loads was effected by placing weights in the body of the truck and, therefore, above the springs.

These results indicate that for all those heights of drop or obstruction used, the equivalent static load or the deflection at the critical point with an increase in speed decreased to a certain minimum, then increased more or less gradually. In amount this reduction in equivalent static load shows a dis-

FIG. 2.—RUNWAY AND AUXILIARY TRUCK FOR APPLYING EQUIVALENT STATIC LOAD AT POINT OF IMPACT.

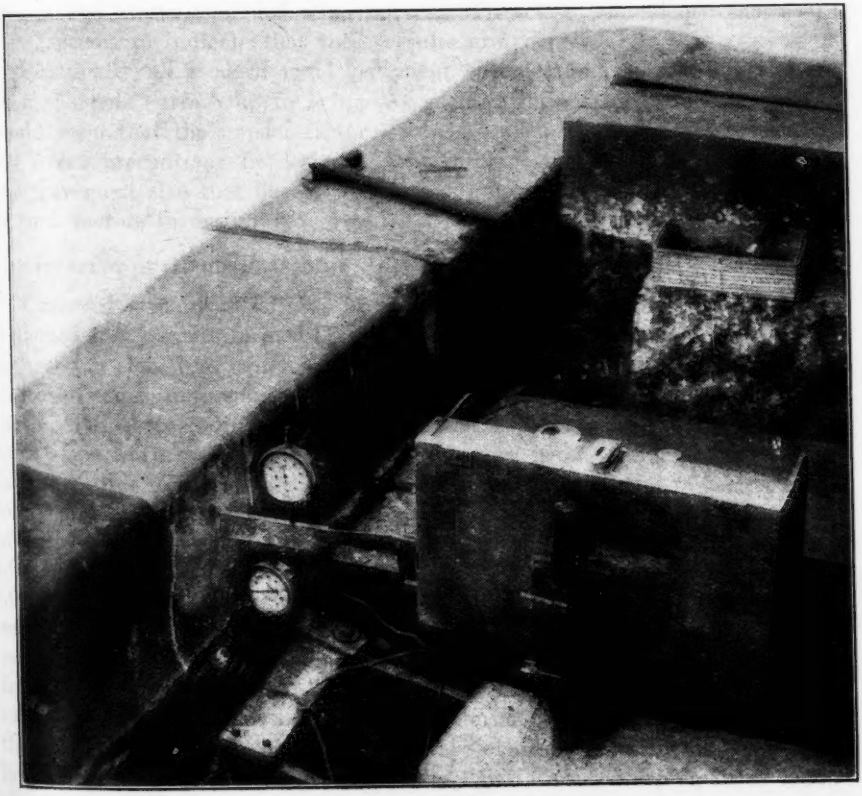

FIG. 3.—APPARATUS USED FOR RECORDING STATIC AND IMPACT DEFLECTIONS.

tinct tendency to increase with the increase of load above the springs. This is especially true in all cases of dropping load and to a less degree for the ⅛-in. and ¼-in. vertical rises. The difference between the minimum and maximum equivalent static load was not greatly affected by the change in load. For all heights of drop, this results in a lowering of the impact factor, that is, the ratio of equivalent static load to wheel load, as the load above the springs is increased.

At all speeds, for the ⅛-in. drops and the ⅛-in. rise with the truck fully loaded, the equivalent static load was less than the static load of the wheel. For the ¼-in. drops, truck fully loaded, the equivalent static load was less than the truck-wheel load until the speed of the truck exceeded about 12 miles per hour, and did not increase materially for speeds in excess of 14 miles per hour; the maximum equivalent static load for the 8 000-lb. wheel load was only a little greater than the wheel load itself. In mounting the ¼-in. obstruction, the critical speed was about 10 miles per hour and the equivalent static load did not increase materially for speeds in excess of 14 miles per hour. For the drops and rises of greater magnitude, the critical point was passed at lower speeds and the maximum impact effect was much greater.

The value of Figs. 4 and 5 as an index of the relative magnitude of impact and static load stresses depends on the equality of the shortest radii of the impact and static load deflection curves. The close coincidence shown in Fig. 1 seems to indicate that these results are correct.

Practically all modern rigid pavement specifications permit a variation from the true surface up to ¼ in. As such variations are rarely abrupt, it would seem that the impact factor is not of sufficient importance to justify any great precautions in design. Accidental obstructions, as loose boards or a pavement slab that has heaved, are so unusual as to justify the neglect of such factors in design.

Warping of Rigid Pavement Slabs, Due to Temperature Changes

Observed structural failures of existing rigid pavements had previously indicated that corners formed by the intersection of transverse cracks and the edge of the slab were points of weakness; therefore, such corners, as well as unbroken edges, were subjected to loads of varying amounts, and observations made. These proceedings soon disclosed the important fact that rigid pavement slabs warp seriously, due to daily changes in air temperature. Fig. 6 illustrates this for the corner of a 9-in. pavement slab during a 60-hour period. and shows also the deflection of the corner under a load of 6 000 lb. applied at hourly intervals throughout the period. Fig. 7 plotted from a number of simultaneous observations illustrates the warping effect of daily changes of temperature on various pavement slabs. Fig. 8 shows the air temperature, and that of the top, mid-depth, and bottom surface of a concrete slab for a 2-day period. It is to be noted that although the temperature of the top surface varied as widely as that of the air, the temperature of the under surface varied only a little. This condition being normal, the expansion and contraction of the top surface, due to temperature changes, must inevitably be followed by a corresponding warping of the slab. Corner warping of as much

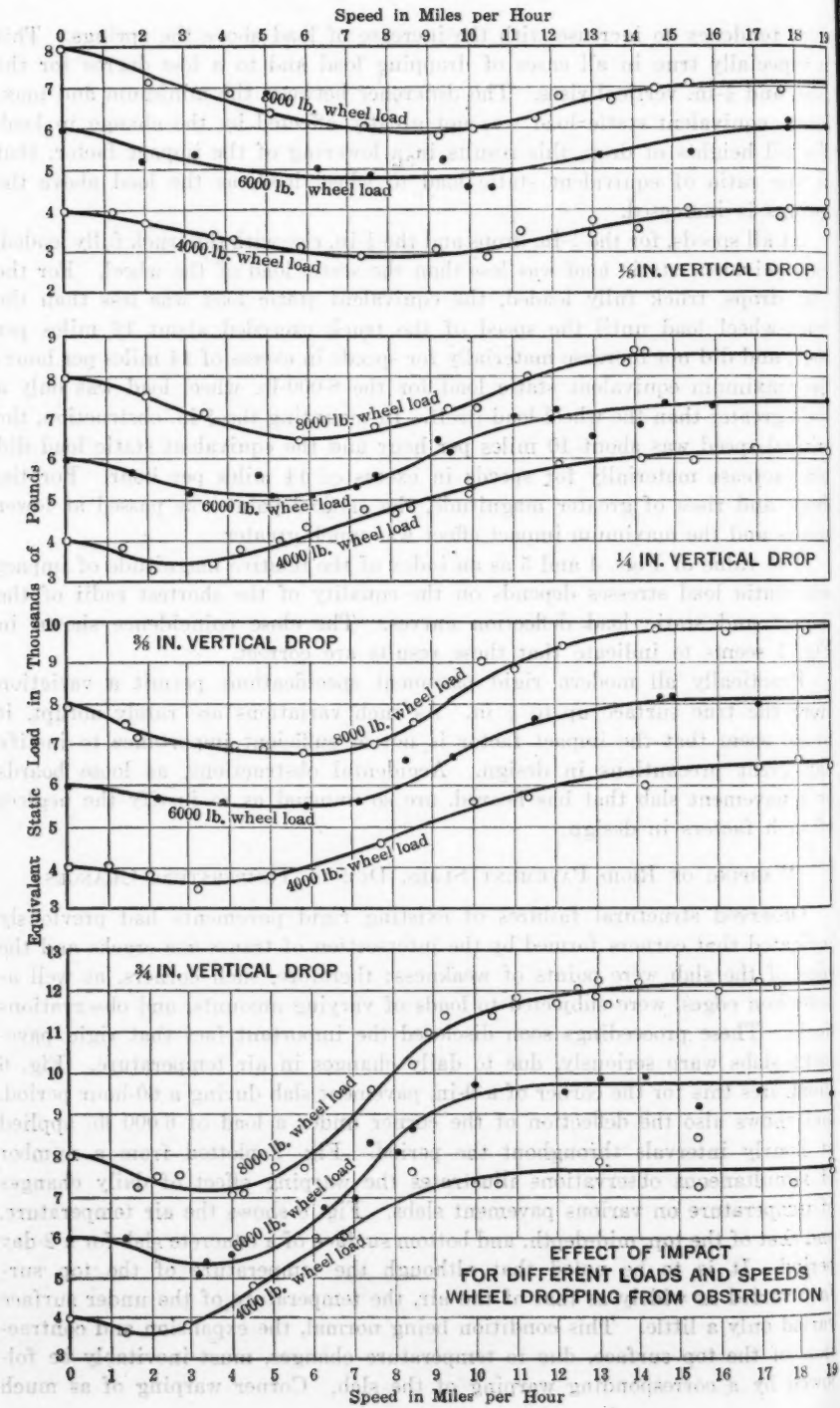
Speed in Miles per Hour
8000 lb. wheel load
6000 lb. wheel load
4000 lb. wheel load
⅛ IN. VERTICAL DROP
¼ IN. VERTICAL DROP
⅜ IN. VERTICAL DROP
¾ IN. VERTICAL DROP
Equivalent Static Load in Thousands of Pounds
EFFECT OF IMPACT
FOR DIFFERENT LOADS AND SPEEDS
WHEEL DROPPING FROM OBSTRUCTION

FIG. 4.

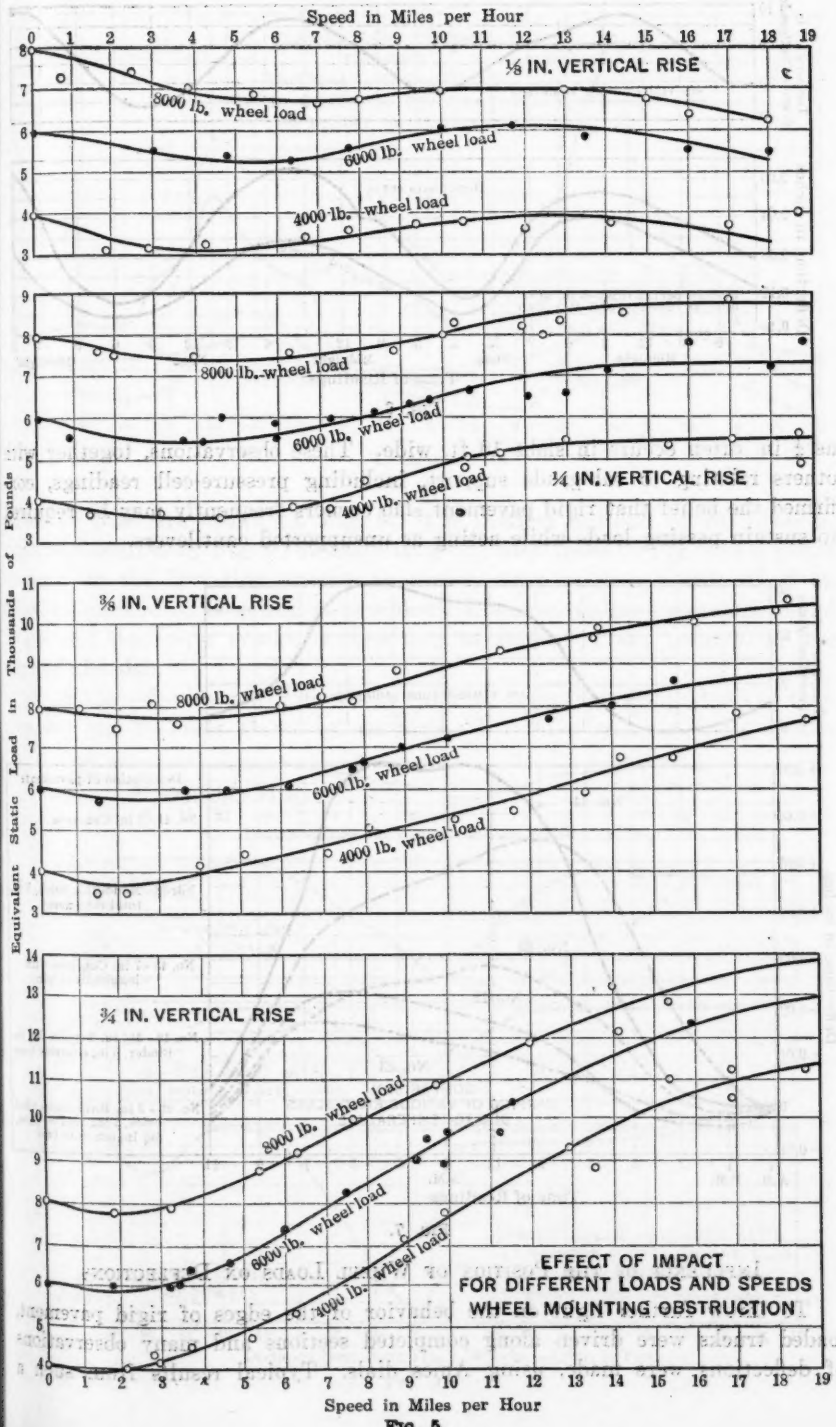
Speed in Miles per Hour
⅛ IN. VERTICAL RISE
8000 lb. wheel load
6000 lb. wheel load
4000 lb. wheel load
¼ IN. VERTICAL RISE
⅜ IN. VERTICAL RISE
¾ IN. VERTICAL RISE
Equivalent Static Load in Thousands of Pounds
EFFECT OF IMPACT
FOR DIFFERENT LOADS AND SPEEDS
WHEEL MOUNTING OBSTRUCTION
Speed in Miles per Hour

FIG. 5.

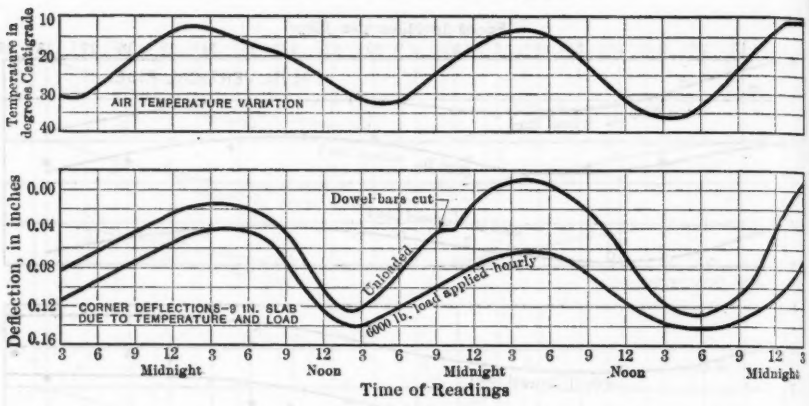

FIG. 6.

as ¼ in. often occurs in slabs 18 ft. wide. These observations, together with others relating to sub-grade support, including pressure-cell readings, confirmed the belief that rigid pavement slab corners frequently may be required to sustain passing loads while acting as unsupported cantilevers.

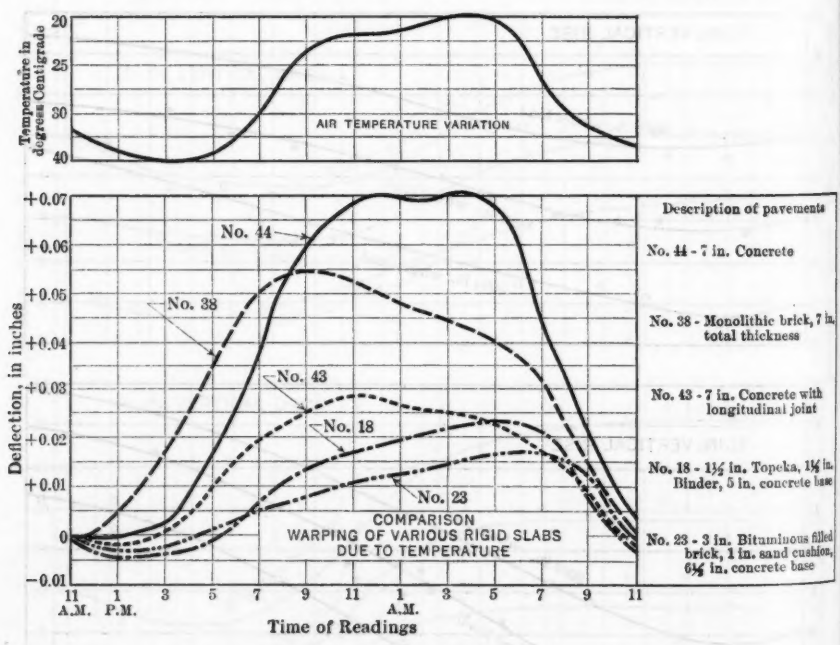

FIG. 7.

INFLUENCE OF THE POSITION OF WHEEL LOADS ON DEFLECTIONS

To throw further light on the behavior of the edges of rigid pavement, loaded trucks were driven along completed sections and many observations of deflections were made, using Ames dials. Typical results from such a

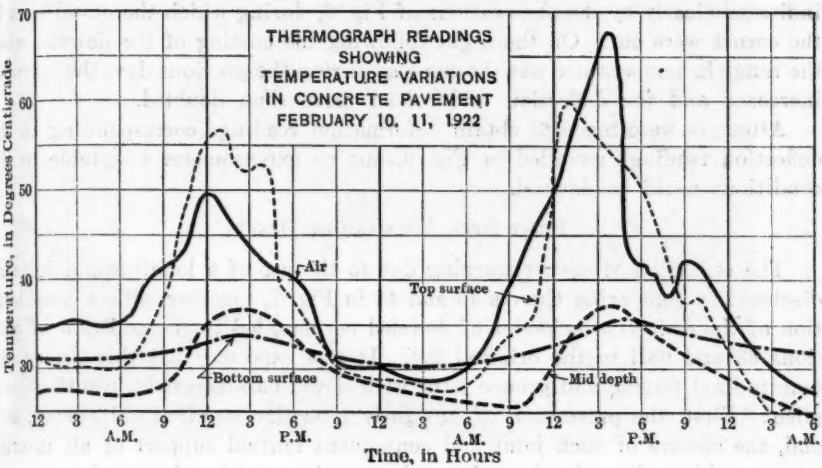

FIG. 8.

series of tests are shown on Fig. 9. The marked contrast of the observations represented by Fig. 9 (*b*) and Fig. 9 (*c*), with those of Fig. 9 (*d*), points strongly to the fact that stresses in corners may be greatly reduced if an effective method of doweling is provided. However, unless means are found to prevent transverse cracks, corners may be formed at any point along the edge of the slab.

A similar effectiveness of dowels in reducing deflections caused both by temperature and by loads, shown by comparing Fig. 9 (*c*) and Fig. 9 (*d*), is also

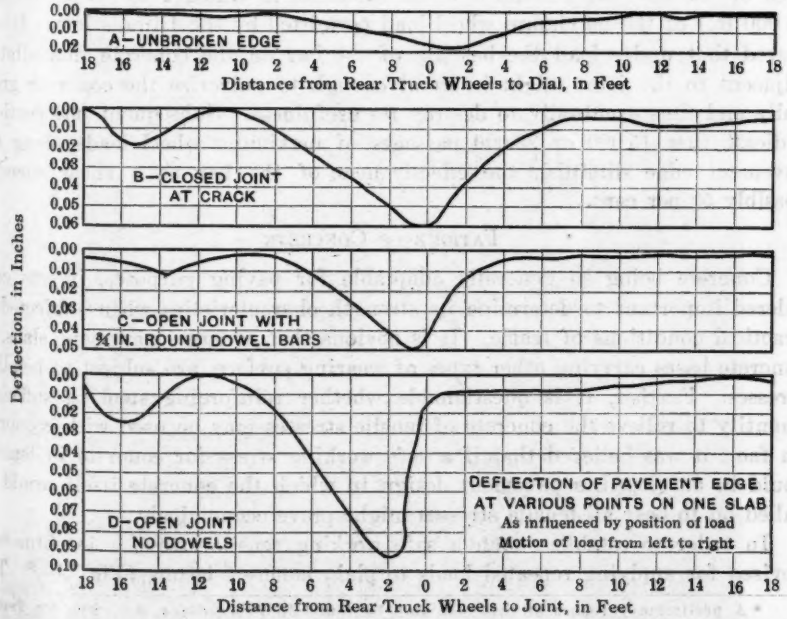

FIG. 9.

indicated clearly by the observations of Fig. 6, during which the dowel bars in the corner were cut. On the night following the cutting of the dowels, when the range in temperature was the same as during the previous day, the warping increased and the deflection under load more than doubled.

Attempts were made to obtain deformation readings corresponding to the deflection readings recorded in Fig. 9, but no extensometer adaptable to the conditions could be devised.

First Step Forward in Design

The reduction of corner warping due to the use of a longitudinal joint as disclosed by comparing Curves 43 and 44 in Fig. 7, together with a consideration of the deflection behavior of doweled corners, led to the addition of Sections 63 and 63B to the original list. It was expected that this use of the longitudinal tongue and groove joint with dowel bars across it, would accomplish: First, the prevention of unsightly irregular longitudinal cracks; second, the closure of such joint and consequent mutual support of all interior corners; third, the reduction of warping at the outside edges and corners to the minimum which might be expected in a half width slab, thus insuring the maximum possible sub-grade support during periods following a drop in temperature.

A continuous ¾-in., round, smooth bar embedded at half the depth of the slab and near each edge was included, in order that adjacent edge corners might be more or less mutually supported. This continuous dowel bar, as it might be called, was painted and oiled in order to avoid a concentration of tensile stress at cracks and joints during a general drop in temperature. The area of the bar was presumed to be sufficient to transfer by shear one-half (4 000 lb.) of the maximum wheel load permitted by the Illinois law. It was feared that under load the bearing of the bar on the concrete immediately adjacent to the joint might be great enough to pulverize the concrete gradually and thus eventually to destroy its usefulness. Subsequent observations indicate that 15 000 or 20 000 passages of maximum wheel loads along the pavement edge diminish the effectiveness of the bar as a shear member possibly 50 per cent.

Fatigue of Concrete

Concrete being so generally adaptable for paving purposes, it was considered important to determine its strength characteristics when subjected to practical conditions of traffic. It is obvious that concrete pavement slabs, or concrete bases carrying other types of wearing surface, are subject to bending stresses. Further, it is questionable whether reinforcing steel in sufficient quantity to relieve the concrete of tensile stresses may be used with economy. In fact, it was believed that if a safe working stress for concrete in tension could be developed, a pavement design in which the concrete itself would be called on to bear all tensile stresses might prove economical.

In order to establish such a safe working tensile stress, a machine was devised for applying repeated loads to plain concrete beams (Fig. 10).* The

* A preliminary report of this test may be found in *Proceedings*, Am. Soc. for Testing Materials, Vol. 22. Pt. 2, p. 408.

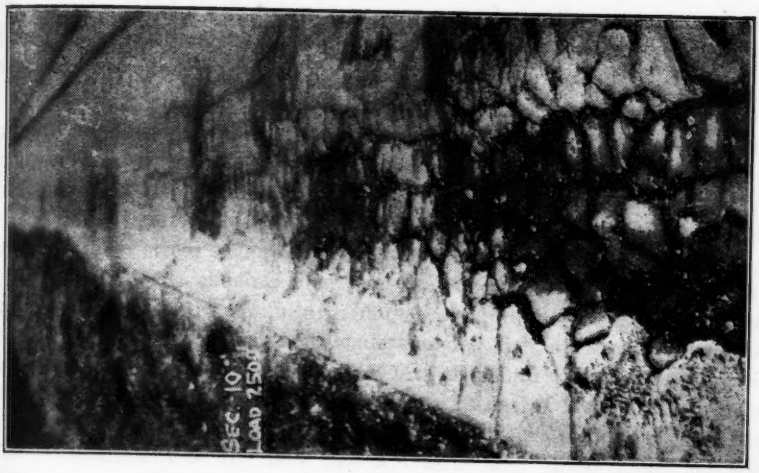

FIG. 11.—TYPICAL FAILURE OF ASPHALTIC CONCRETE SURFACING ON MACADAM BASE.

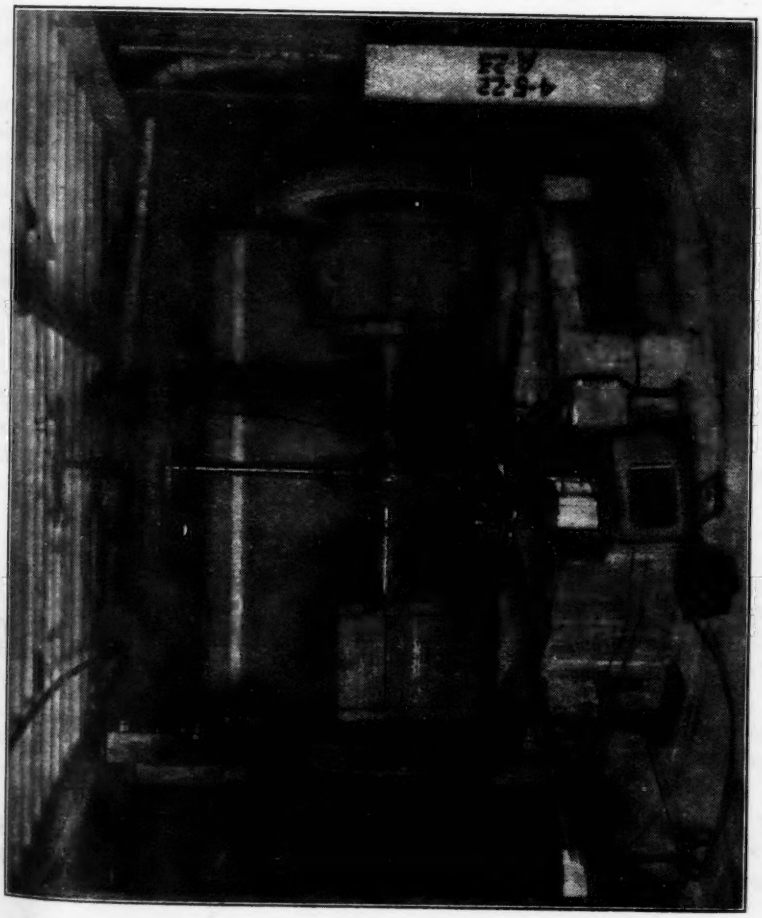

FIG. 10.—APPARATUS FOR DETERMINING FATIGUE OR ENDURANCE LIMIT OF PLAIN CONCRETE BEAMS.

data accumulated since this report was issued, confirm the tentative results given. The conclusions that may be accepted with a reasonable degree of assurance are as follows:

(*a*).—Plain concrete beams or slabs will sustain without failure from bending an indefinite number of repetitions of a load if the tensile fiber stress induced is less than 50% of the modulus of rupture. At the present time (December 1, 1923) there are in the fatigue machine test beams that have withstood without failure about 5 000 000 repetitions of a load sufficient to produce a fiber stress of approximately 50% of the modulus of rupture.

(*b*).—For loads causing fiber stress in excess of 50% of the modulus of rupture, the tendency to failure increases rapidly with the increase of this excess of stress. For instance, loads causing fiber stresses of about 60% of the modulus of rupture, repeated a few thousand times (rarely more than 30 000) will cause failure; for stresses in excess of 70% of the modulus of rupture, only a few hundred repetitions (rarely more than 5 000) are required. The establishment of the fact that a tensile fiber stress somewhat less than 50% of the modulus of rupture may be assumed as safe for a road slab, will be of great value when analytical methods for computing fiber stresses in all parts of pavement slabs are found.

The phenomenon of accelerated failure is also of importance in interpreting the behavior of existing concrete slabs under traffic. For example, a corner break in a 4-in. concrete section of the Bates Road, under a 3 500-lb. wheel load, indicated that the concrete at corners was subjected to stresses nearing or exceeding the critical 50% endurance limit. In the succeeding increment, the wheel load was increased 1 000 lb., or 28 per cent. If, therefore, the 3 500-lb. load caused fiber stresses equal to approximately 50% of the modulus of rupture, the next increment was imposing stresses of about 78 per cent. The fatigue-test results indicate that at this percentage rapid failure should follow. This proved to be the fact inasmuch as many corners of 4-in. slabs were broken and the progressive destruction was quite rapid. Similar phenomena have been noticed in connection with Illinois pavements in service, some of which have withstood normal traffic for a number of years, and then have become seriously damaged by suddenly increased highway loadings.

Sub-Grade Soil Investigations

Before any rational method may be developed for determining stresses in all parts of pavement slabs, the character of the support afforded by the sub-grade must be thoroughly understood. Research on this subject by the Illinois Highway Department has been confined thus far to what might generally be classed as clay soils.

Moisture Content.—It has been fairly well established that the bearing value of a clay soil varies with its moisture content. Attempts made to control the moisture content of the sub-grade soil are, therefore, of interest.

Under each edge of a 200-ft. section of the Bates Road was laid a tile drain 24 in. below the sub-grade, the trench back-filled with cinders, and a free outlet provided for the tile. Moisture samples were taken from the underlying soil

at various points throughout this 200-ft. section, and likewise from the adjacent undrained slabs. During a period of three years, no measurable difference in the moisture content of the sub-grade at these points has been observed. At another place, on the "Chatham Road", where clay of a different character is found, tile drains were laid 42 in. under each edge of the pavement for a distance of 1 000 ft., the trenches back-filled with cinders, and similar extended observations were made, with results as shown on Fig. 12. No attempt is made to explain why the soil underneath the section provided with tile drains has throughout the entire period contained more moisture than that under the adjacent pavement. Judging from these two examples in which tile drains were of absolutely no apparent value, it is questionable whether such attempts to control moisture are of any merit whatever in clay soils.

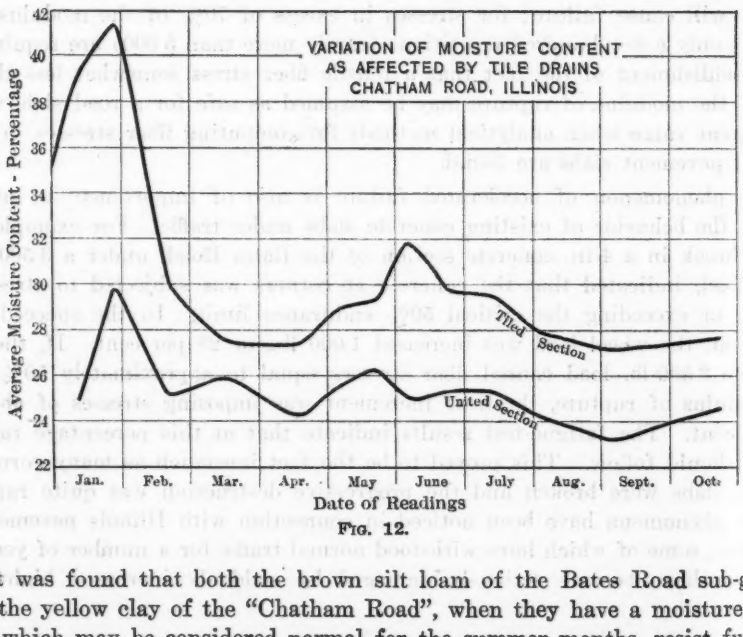

FIG. 12.

It was found that both the brown silt loam of the Bates Road sub-grade and the yellow clay of the "Chatham Road", when they have a moisture content which may be considered normal for the summer months, resist further saturation to a marked degree. Attempts to saturate the soil underneath the Bates Road failed. Water standing at sub-grade elevation for six weeks during the summer months did not cause a perceptible rise in the moisture content of the sub-grade soil at a sampling station 30 in. distant. Tests now under way on thirty samples of clay soils, gathered from different points throughout the State, indicate that this phenomenon in slightly varying degrees probably is common to all.

Another series of experiments indicate that if the moisture content of any of these clay soils is reduced to a point where the soil is dry enough to crumble readily, absorption takes place rapidly, to the point of saturation.

These two properties of clay soils may have a marked effect on the supporting power of the sub-grade under a freshly laid pavement slab; for example,

the sections of the Bates Road built in the fall of 1920 were laid on a sun-dried sub-grade, as a rainless period and hot weather had preceded the construction of the pavement. In October, 1920, the first moisture samples were taken from the underlying soil just after a three-day period of rain. At that time the sub-grade was found to be as nearly saturated as it ever became. On the other hand, Sections 64 to 68, inclusive, were laid in the fall of 1922, when the sub-grade soil contained about 25% moisture. The moisture content of the soil under these slabs remained practically constant throughout the winter months of 1922–23 and, although the spring and summer rains were heavy, it continued throughout the summer of 1923 materially below that of the remainder of the road. From this, it may be inferred that for perhaps a period of a year or more after a pavement is laid, the bearing power of a clay sub-grade soil may be affected materially by its moisture content at the time of construction.

Bearing Power.—Many attempts have been made to evaluate the bearing power of the sub-grade soil of the Bates Road, as well as that of other Illinois soils. As narrow rural pavements encourage the passage of highway loads along fairly definite paths, it was thought necessary to determine the relationship between the bearing power of sub-grade soils and repeated loads. An apparatus was devised, by which repeated loads on areas of a few square inches could be made with facility. The use of this apparatus immediately called attention to the excessive depression or permanent deformation caused by the first few applications of load. After several hundred applications, the soils in some cases seemed to become more or less stabilized, and to show decided elastic properties.

Believing that the initial excessive depression might be due to a poor contact between the metal shoe, used for imposing pressures, and the soil, and might also be affected by the small area under pressure, a number of concrete slabs, 3 ft. in diameter, were cast on the sub-grade adjacent to the edge of the Bates Road. It was thought that these slabs would have an initial bearing on the sub-grade soil at least as satisfactory as that of existing pavements. Repeated loads were applied to these slabs. Owing to the cumbersome arrangement of the apparatus used, it was not practicable to make large numbers of repetitions during periods while conditions affecting sub-grade support remained constant. Fig. 13 shows the results for Slab No. 3 of a series of tests which included ten applications of a load of 6 ft. per sq. in. repeated six times with intervening rest periods of 24 hours each. The loads were applied in each case at 15-min. intervals. The moisture content of the sub-grade (26.8%) may be considered normal for this soil during the early fall months. The principal points of interest are: The permanent depression due to the first load applied after each period of rest; the recovery of elevation during the rest periods; the resultant depression at the end of the third day; and the decreased permanent depressions on succeeding days.

Fig. 14 shows the effect of another series of load repetitions. The excessive permanent depression recorded on February 20, 1922, may be accounted for partly by the increased moisture content, but probably was due chiefly to freezing and thawing of the soil. This may be inferred from the fact that

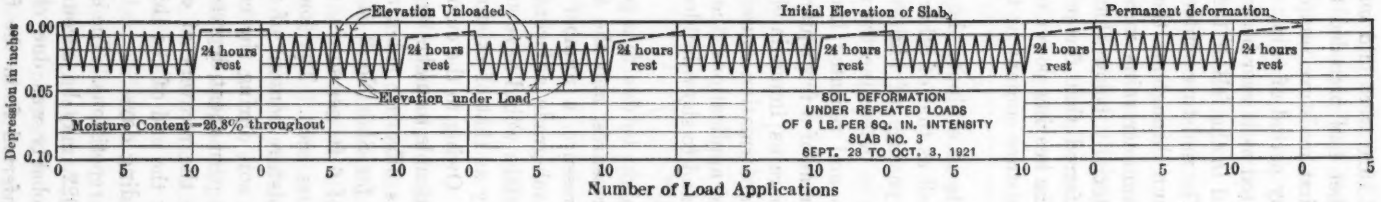
Elevation Unloaded
Initial Elevation of Slab
Permanent deformation
24 hours rest
Elevation under Load
Moisture Content=26.8% throughout
SOIL DEFORMATION
UNDER REPEATED LOADS
OF 6 LB. PER SQ. IN. INTENSITY
SLAB NO. 3
SEPT. 29 TO OCT. 3, 1921
Depression in inches
0.00
0.05
0.10
Number of Load Applications

FIG. 13.

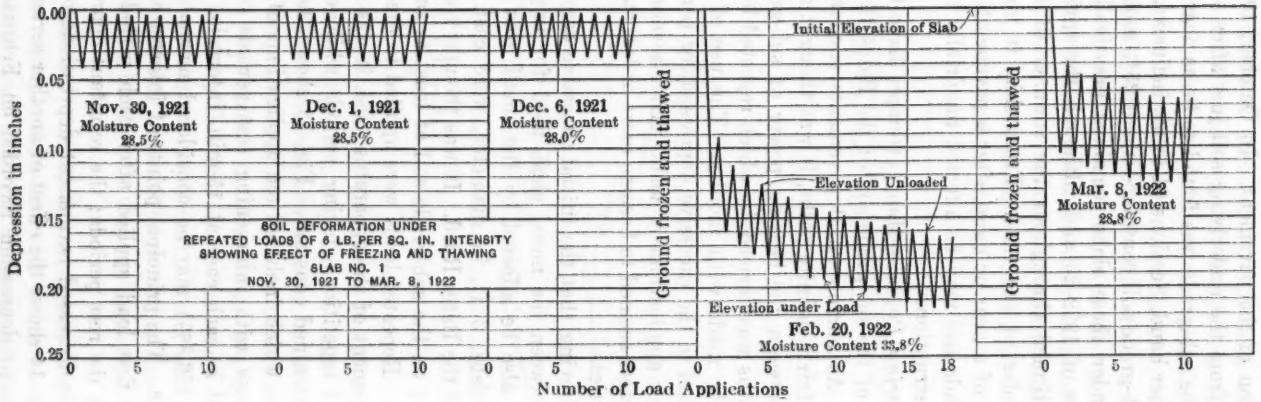
Nov. 30, 1921
Moisture Content
28.5%
Dec. 1, 1921
Moisture Content
28.5%
Dec. 6, 1921
Moisture Content
28.0%
SOIL DEFORMATION UNDER
REPEATED LOADS OF 6 LB. PER SQ. IN. INTENSITY
SHOWING EFFECT OF FREEZING AND THAWING
SLAB NO. 1
NOV. 30, 1921 TO MAR. 8, 1922
Ground frozen and thawed
Initial Elevation of Slab
Elevation Unloaded
Elevation under Load
Feb. 20, 1922
Moisture Content 33.8%
Ground frozen and thawed
Mar. 8, 1922
Moisture Content
28.8%
Depression in inches
0.00
0.05
0.10
0.15
0.20
0.25
Number of Load Applications

FIG. 14.

excessive depressions were also recorded on March 8, at which time the moisture content was practically the same as on December 1. However, the soil had been frozen and thawed once or twice between February 20 and March 8. All the other slabs used for similar observations behaved in the same manner, but in varying degree. Similar tests now are being made on thirty different types of Illinois sub-grade soils using an apparatus that will apply a large number of repeated loads at short intervals on areas of approximately 7 sq. ft. The results of these tests are not sufficiently complete to justify definite conclusions. The present indications, however, point to the probability that none of the clay soils exhibits sufficiently uniform elastic properties to justify an assumption of elastic sub-grade supporting power for use in a design formula. It is certain that for purposes of pavement design, it is not safe to place reliance on a bearing-power test involving only a single application of load.

Effect of Truck Traffic Tests on the Bates Road

The entire Bates Road was laid out on a tangent. The artificial truck traffic consisted of Liberty B trucks driven west along the north side, and east along the south side. Inasmuch as the probability of edge weakness had been established, the east-bound traffic was made to follow a guide line painted on the pavement surface so as to bring the path of the center of the outer rear wheels 6 in. from the pavement edge. The edge of these wheels traveled practically flush with the edge of the pavement on all sections, except those having a macadam base. The west-bound traffic was likewise guided, the path being parallel to and 36 in. from the north edge of the pavement, except on the macadam base sections. On the sections having macadam bases, the wheels of both west-bound and east-bound traffic traveled about 18 in. from the edge of the pavement. The operation of the west-bound traffic was intended to approximate conditions that would normally apply on wide rural pavements and city streets.

In Table 2 will be found details of the wheel loads and the number of round trips for each increment of loading.

An attempt to give complete details of the behavior under truck traffic of each of the sections, or even of each of the groups of sections, would be impracticable. Only the characteristics believed to be of the greatest importance as affecting principles of design will be discussed.

Brick and Asphaltic Wearing Surfaces on Macadam Base.—Fig. 15 is typical of a large series of cross-sections taken as the traffic loading progressed, at many points along the macadam base sections having a brick wearing surface. The last cross-section indicates the condition of the test section when failure had progressed to such an extent that the section could no longer be considered as representing a serviceable highway.

Fig. 16 is typical of a large series of macadam base, asphaltic concrete top, cross-sections, illustrating the particular section of this type which proved most satisfactory. Other tests illustrated the fact, that an increase of total thickness is not necessarily a direct measure of serviceability under truck traffic.

TABLE 2.—DETAILS OF WHEEL LOADS USED AND NUMBER OF ROUND TRIPS FOR EACH INCREMENT OF LOADING.

Increment number.	Load, in pounds, on each rear wheel.	Load, in pounds, on each front wheel.	Gross load.	Net carried or live load, in pounds.	Number of Round Trips.	
					Day.	Night.
1922.						
1	2 500	2 250	9 500	.....	1 000	.....
2	3 500	2 150	11 300	.....	2 167	1 033
3	4 500	2 000	13 000	1 700	2 000	1 000
4	5 500	1 900	14 800	3 500	2 000	1 000
5	6 500	1 800	16 600	5 300	2 000	1 000
6	8 000	1 930	19 860	8 560	5 000	5 000
1923.—Original Sections (Excluding Section 63):						
1	4 500	1 800	12 660	1 300	2 000	1 000
2	6 000	1 600	15 200	3 900	2 000	1 000
3	6 500	1 600	16 200	4 900	2 000	1 000
4	8 000	1 600	19 200	7 900	2 000	1 000
5	9 000	1 700	21 400	10 100	2 000	1 000
6	10 000	2 000	24 000	12 700	2 000	1 000
7	11 000	2 600	27 200	15 900	2 000	1 000
8	12 000	2 600	29 200	17 900	2 000	1 000
9	13 000	2 500	31 000	19 700	2 000	1 000
1923.—New Sections (and Including Section 63):						
1	6 500	1 800	16 600	5 300	2 000	1 000
2	8 750	1 700	20 900	9 600	2 000	1 000
3	8 000	1 600	19 200	7 900	7 000	3 000
4	10 000	2 000	24 000	12 700	2 000	1 000
5	11 000	2 600	27 200	15 900	2 000	1 000
6	12 000	2 600	29 200	17 900	2 000	1 000
7	13 000	2 500	31 000	19 700	2 000	1 000

General Results of Tests on Macadam Base Sections.—In general, the failure of all macadam base sections took the form of rutting along the wheel paths (Fig. 11). In the better sections having an asphaltic concrete top, the serious ruts were not always continuous, but sometimes took the form of elongated depressions. The full series of cross-sections indicates the probability that the entire surface may, during the test, have changed in elevation due to a general swelling or shrinking of the sub-grade. The fact that the sub-grade soil in the wheel paths sometimes flowed horizontally, causing bulging between wheel paths, is evident. The entire series of cross-sections also shows that a progressive permanent depression of the sub-grade occurred along the wheel paths of all sections.

It seems justifiable to conclude that none of the surfaces reduced the pressure transmitted to the sub-grade sufficiently to render harmless the progressive depression or flow of the sub-grade soil under the loads applied.

It is worthy of note that the traffic was purposely confined to well defined paths. Experience indicates that on rural pavements of the common width used for a double line of traffic and where the traffic is sufficiently continuous to cause vehicles to keep habitually to one side of the road, fairly definite

lanes inevitably will be followed. Evidently, in pavements of this type, it is necessary to use thicknesses or other factors of design adapted to reduce the pressure on the sub-grade soil to that which it will bear without material permanent displacement.

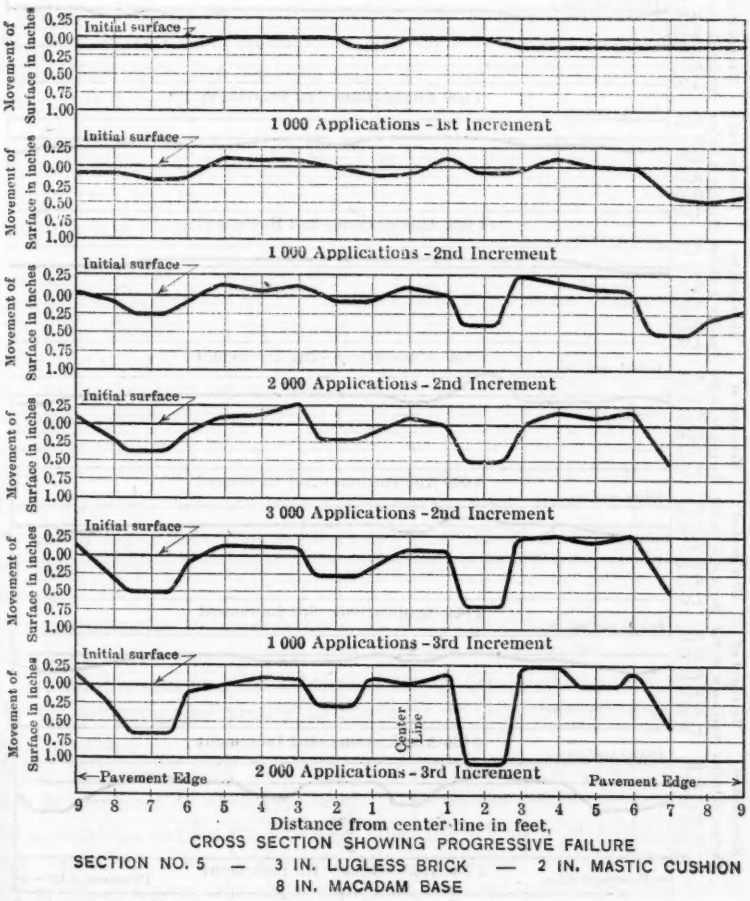

CROSS SECTION SHOWING PROGRESSIVE FAILURE
SECTION NO. 5 — 3 IN. LUGLESS BRICK — 2 IN. MASTIC CUSHION
8 IN. MACADAM BASE

FIG. 15.

It would also appear plain that the serviceability of pavements of this type would be greatly increased if they were built wide enough to avoid the necessity of vehicles following definite wheel paths. Under conditions favoring the spreading of traffic, a depression caused by one load would be filled sooner or later by the flow of soil from an adjacent wheel path.

Pressure-cell readings under the section having a 10-in. macadam base and 2-in. Topeka top are of decided interest. A 4-ton wheel load standing over a pressure cell of this section before the truck traffic was started resulted in a pressure of about 12 lb. per sq. in. After 1 000 round trips had been made by the trucks, the reading had increased to about 26 lb. per sq. in. Apparently,

vibration caused by the traffic had loosened the mechanical bond originally secured by rolling the foundation courses. The suggestion is made that a bituminous binder would help to counteract this effect.

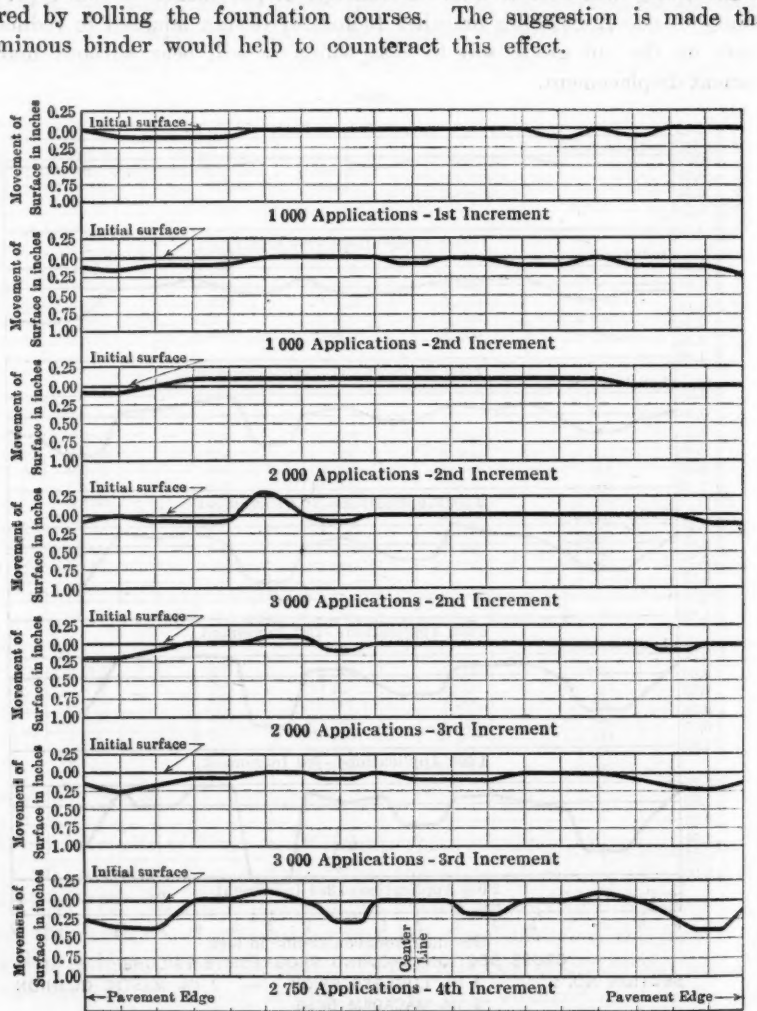

FIG. 16.

Asphaltic Concrete Top on Concrete Base.—Almost invariably the failures of this type started by breaking a small corner involving an area of only 2 or 3 sq. ft. Subsequent loads, because of the excessive bearing pressure, caused a depression of the broken corner. This resulted in excessive impact on the depressed corner itself and on the edge of the adjacent unbroken slab as the truck wheels mounted it. The progressive breaking down of the pavement in the direction of the flow of traffic followed as a logical sequence. Dis-

integration often occurred in the reverse direction. All sections of this type were provided with an integral concrete curb equal to the thickness of the asphaltic top. In addition to corner breakage, cracks through the curb, extending to the bottom surface of the slab, were frequently observed. Whether or not these curb cracks represented transverse cracks extending across the entire width of the pavement could not be determined. The plotted points in Fig. 17 (*a*) show the relation between the loads causing critical corner breaks and base thicknesses for various types of construction. The curve passes through points determined by the formula:

$$d = \sqrt{\frac{3\,W}{S}}, \text{ or } W = \frac{1}{3}\,S\,d^2.$$

This formula is evolved from the well known equation, $S = \frac{M\,c}{I}$, the assumptions being as follows: That the load, W, is applied at the extreme point of a right-angled corner formed by the intersection of an open transverse crack or joint with the edge of the pavement slab; that the corner is entirely unsupported by the sub-grade and, therefore, acts as a simple cantilever; and that fiber stresses are uniform on any section normal to a line bi-secting the corner angle. The average modulus of rupture of the test specimens corresponding with that particular concrete slab being substituted for S, the value of W should represent, under the conditions assumed, the theoretical breaking load.

These diagrams indicate that the formula, when used in connection with the design of rigid pavement slabs of fairly constant cross-section and having no special provision for edge strengthening, may be used with considerable confidence.

It was distinctly noticeable that, in all paving sections of this type, the initial corner break was not immediately followed by rapid progressive destruction. No doubt, this may be attributed to the fact that the asphaltic concrete top by its cohesion and ability to diminish the abruptness of the depression helped materially to reduce excessive impact.

Brick Surfacing with Bituminous Joint Filler on Concrete Base.—The failure of sections of this type was of much the same character as in the group of sections having an asphaltic concrete top on a concrete base. Failure always started at a south side corner. Progressive failure after the initial corner break, however, was more rapid. These sections were provided with an integral curb having a depth equal to the combined thickness of the brick surfacing and the sand cushion. The thickness used in plotting Fig. 17 (*b*) does not take into account the presence of the curb.

Monolithic Brick.—The term monolithic brick is applied to all sections having a brick surface laid on a fresh concrete base, the cement grout joint filler being poured in as far as possible before the base concrete had attained initial set. In Fig. 17 (*c*), the plotted points show the wheel loads causing the initial serious corner failure of all sections of this type, the ordinates in this case being the total thickness of the pavement. In a true monolith, the total thickness should be a measure of strength. Inasmuch as failure was caused in all cases by loads much less than those which might be expected, a

consideration of the actual behavior of these sections is of interest. At many points along the edges and adjacent to all corners, it was observed that, under load, the brick surfacing became distinctly separated from the concrete base. This seemed to indicate that the pavement was acting as two separate slabs rather than as a monolith. In Fig. 17 (*d*), abscissas were used which represent the thickness of a concrete slab computed as having transverse strength equal to the transverse strength of two superimposed independent slabs, each assumed to have a modulus of rupture equal to that of the test specimens cast at the time the base was poured and a thickness equal to that of the top and base courses. It is noticeable that by the use of this method for computing breaking loads, a reasonable agreement between the actual and theoretical failures obtains.

Concrete Sections.—In Fig. 17 (*e*), the plotted points show the loads causing critical corner failure in all plain concrete sections, and in sections considered as equivalent to plain concrete. These points include two sections of plain concrete, to which had been added 10% of hydrated lime; and two sections containing 42-lb. wire mesh placed at about the neutral axis. Considering the quantity and location of the steel in these sections, it would afford little, if any, relief of tensile stresses in the concrete.

In Fig. 17 (*f*) are shown the loads causing critical corner failure in all concrete sections which were provided with transverse joints spaced at 25-ft. intervals. These joints were formed by ordinary corrugated metal sheets placed on edge, the corrugations running horizontally. The concrete was poured against these metal sheets, no provision being made for expansion. This construction merely resulted in a transverse crack having a corrugated cross-section. The inclusion of these test sections was based on the assumption that possible intermediate transverse cracks would not be formed; that contraction would occur only at the joints; and that, because of the corrugations, more or less mutual support would be afforded by adjacent slabs, thus making corner failure less probable. All the plotted points in this diagram represent sections in which ¾-in. steel marginal bars were used. The position of the plotted points indicates that the presence of the transverse corrugated joints had little effect in increasing resistance to structural failure.

It is worthy of note that two plain concrete sections, divided also by transverse joints of the same type and spacing, but having no marginal reinforcing bars, withstood the entire traffic tests without failure although the thickness was 7 in. and 8 in., respectively. From this, it may be inferred that the use of marginal steel was also of doubtful value.

In Fig. 17 (*g*), the plotted points represent the loads causing critical corner failures in all sections of rigid type. These points were plotted in the same position relative to the curve determined by the formula, $D = \sqrt{\frac{3\,W}{S}}$ (using for S the average modulus of rupture of all test specimens), as they appear in Fig. 17 (*a*) to (*e*). In this diagram, attention is called to the grouping of the plotted points about the curve representing the theoretical breaking load as determined by the formula given. It will be noted that the lower curve, in which 50% of

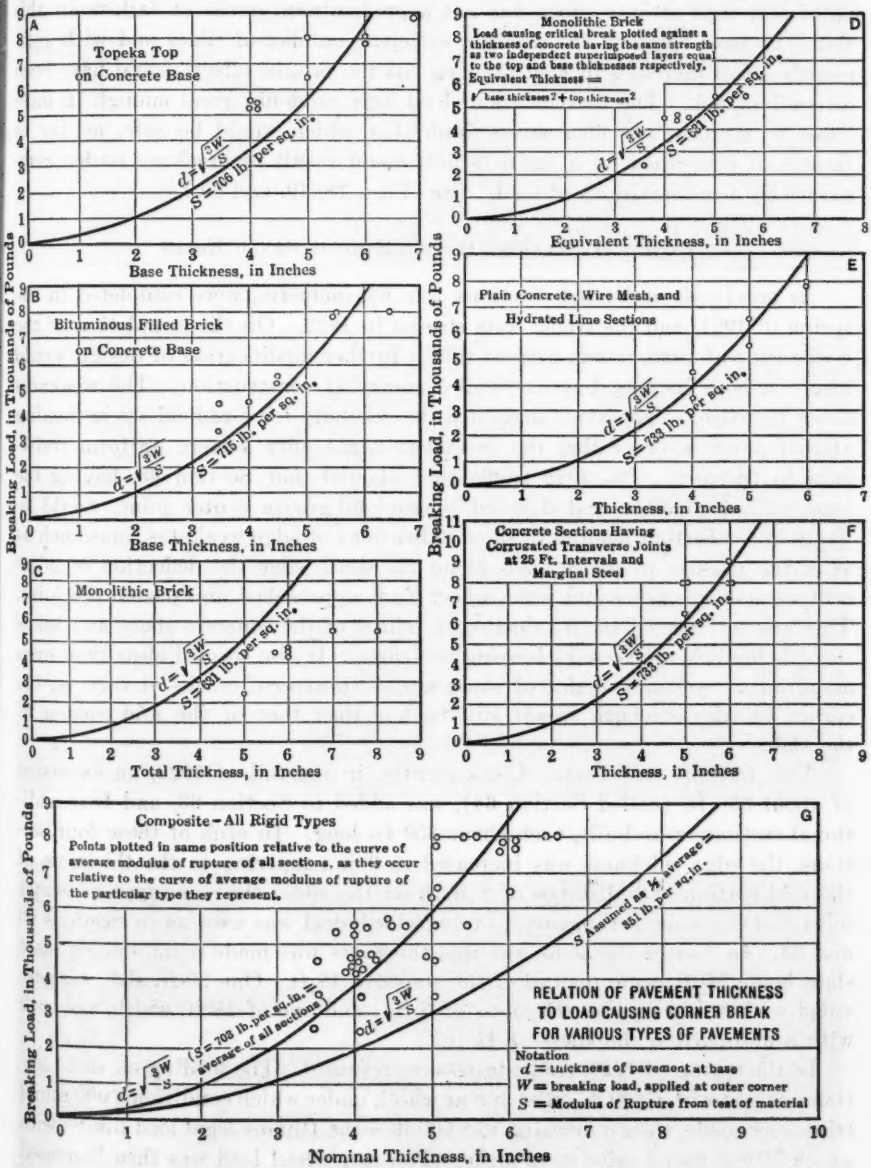
A
Topeka Top
on Concrete Base
$d=\sqrt{\frac{3W}{S}}$
S = 706 lb. per sq. in.
Base Thickness, in Inches
B
Bituminous Filled Brick
on Concrete Base
$d=\sqrt{\frac{3W}{S}}$
S = 715 lb. per sq. in.
Base Thickness, in Inches
C
Monolithic Brick
$d=\sqrt{\frac{3W}{S}}$
S = 681 lb. per sq. in.
Total Thickness, in Inches
D
Monolithic Brick
Load causing critical break plotted against a thickness of concrete having the same strength as two independent superimposed layers equal to the top and base thicknesses respectively.
Equivalent Thickness = $\sqrt{\text{base thickness}^2 + \text{top thickness}^2}$
$d=\sqrt{\frac{3W}{S}}$
S = 631 lb. per sq. in.
Equivalent Thickness, in Inches
E
Plain Concrete, Wire Mesh, and
Hydrated Lime Sections
$d=\sqrt{\frac{3W}{S}}$
S = 733 lb. per sq. in.
Thickness, in Inches
F
Concrete Sections Having
Corrugated Transverse Joints
at 25 Ft. Intervals and
Marginal Steel
$d=\sqrt{\frac{3W}{S}}$
S = 733 lb. per sq. in.
Thickness, in Inches
Breaking Load, in Thousands of Pounds
G
Composite – All Rigid Types
Points plotted in same position relative to the curve of average modulus of rupture of all sections, as they occur relative to the curve of average modulus of rupture of the particular type they represent.
S = 703 lb. per sq. in. = average of all sections
S Assumed as ½ average = 351 lb. per sq. in.
$d=\sqrt{\frac{3W}{S}}$
RELATION OF PAVEMENT THICKNESS
TO LOAD CAUSING CORNER BREAK
FOR VARIOUS TYPES OF PAVEMENTS
Notation
d = thickness of pavement at base
W = breaking load, applied at outer corner
S = Modulus of Rupture from test of material
Nominal Thickness, in Inches

FIG. 17.

the modulus of rupture was used, gives safe values for all cases causing critical failure.

The grouping of the points about the theoretical breaking load curve indicates also that fatigue effect was not a predominant cause of failure in this test. To have operated the trucks a sufficient number of times and with sufficiently small increases in load to bring out the fatigue effect, would have been an endless task. The increments of load were no doubt great enough in most cases to increase the fiber stress from that which would be safe, as far as fatigue is concerned, to a figure which would result in breakage under comparatively few repetitions of load. (See Figs. 18, 19, and 20.)

Concrete Sections Having Strengthened Edges

As previously indicated, Sections 1 to 63, inclusive, were completed in the spring of 1921, and the traffic tests started in 1922. On the completion of the traffic runs of 1922, it was evident that a further modification of design would result in both increased service and economy of construction. The weakness along the edge, so apparent, suggested the necessity for a radical strengthening at that point in order that the pavement might offer a more uniform resistance to fracture. The 1922 traffic runs showed that Section 63, having the longitudinal edge-bar and doweled tongue-and-groove center joint, would be likely under further loading to show indications of edge weakness, inasmuch as after the passage of many loads along the south edge the deflection of adjacent corners was not equal when wheel loads approached and passed the joint. This was interpreted as an evidence of failure of the concrete above and below the side bar due to excessive bearing pressures. It also seemed clear that, even assuming a perfect transfer of shear across transverse cracks at corners, the corner or edge strength would still be less than that of the mid-portion of the slab.

New Designs and Tests.—Consequently, in the fall of 1922, an extension of about 350 ft. (called Section 64), was added to Section 63, and four additional sections were built, each about 350 ft. long. In each of these four sections, the edge thickness was increased to 9 in., tapering to the thickness of the mid-portion at a distance of 2 ft. from the edge; the same type of center joint and the same arrangement of embedded steel was used as in Sections 63 and 64. In two of the slabs, the mid-thickness was made 6 in., one of these slabs being 20 ft. wide instead of the standard 18 ft. One 20-ft. slab was provided with a mid-portion thickness of 5 in.; and one of 18-ft. width was built with a mid-portion thickness of 4½ in.

In the spring of 1923, traffic tests were resumed. The loading on these sections started with 6 500 lb. on each rear wheel, under which condition 3 000 round trips were made, then increasing to 8 000 lb.—the Illinois legal load limit—with which 10 000 round trips were made. The rear wheel load was then increased successively to 8 750 lb., 10 000 lb., 11 000 lb., 12 000 lb., and 13 000 lb., and 3 000 round trips were made with each increment. As in previous traffic runs, the wheel path along the south side of the pavement imposed the loads practically on the edge of all these slabs, except those having the 20-ft. width. On the

FIG. 18.—TYPICAL CORNER BREAK IN A CONCRETE SECTION.

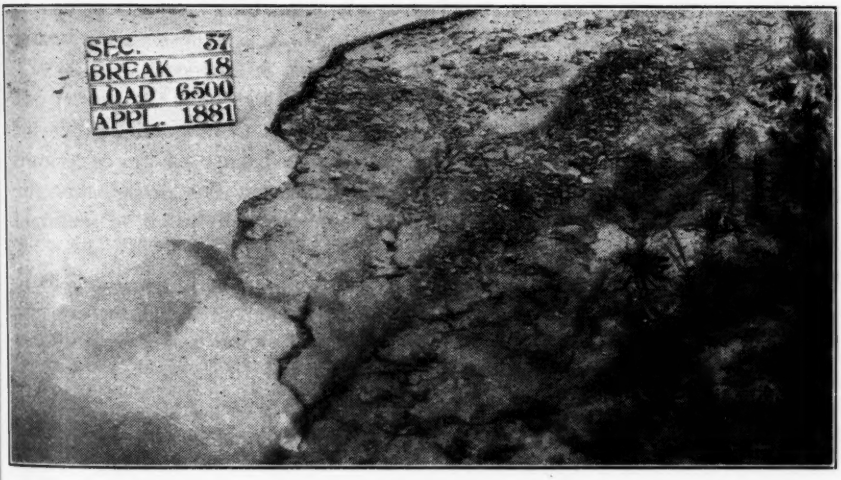

FIG. 19.—EARLY STAGES OF PROGRESSIVE DESTRUCTION FOLLOWING CORNER BREAK.

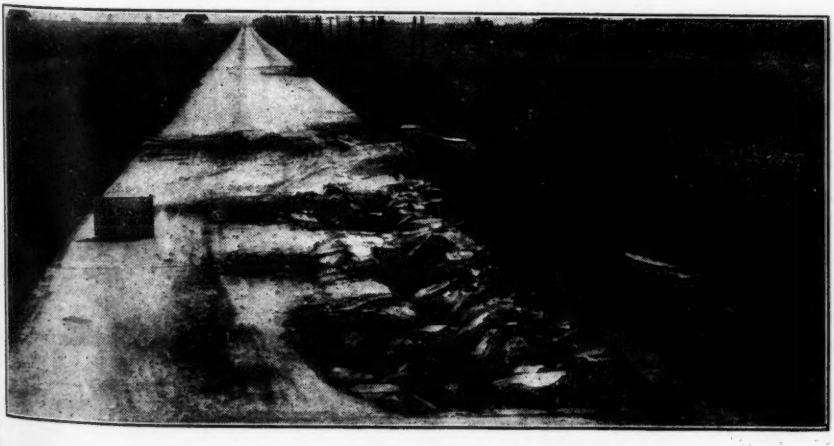

FIG. 20.—ADVANCE PROGRESSIVE DESTRUCTION.

20-ft. sections, the center of the wheel path was 1 ft. 6 in. from the edge of the pavement.

Results of Tests.—In Fig. 21 is shown a cross-section of Section 64 and a record of the damage caused to this section by the traffic. In this, and in the succeeding diagrams, the dotted lines show contraction and check cracks, the solid straight lines show longitudinal and transverse construction joints, and the irregular solid lines show cracks caused by traffic. Obviously, the corner break at *A* was due to faulty construction, the double corner break at *B*, to a normal structural failure, and the transverse cracks lettered *C* to traffic rather than to temperature contraction.

It will be noted that the broken corners at *A* and *B* withstood extensive heavy traffic before they became pulverized, and that even at the end of the test they had not suffered serious progressive failure. This is attributed to the fact that the continuous edge bar prevented the corners from becoming immediately depressed, thus relieving temporarily the excessive impact, which, under prolonged traffic, would no doubt eventually have caused serious progressive destruction.

Fig. 22 shows in the same way the effect of truck traffic on Section 65. The letters, *AA*, indicate the location of very short cracks that appeared early but showed no extension as the loading continued. The letters, *BB*, indicate transverse cracks caused by traffic. At the end of the tests, this section was not damaged in any way that would cause interference with traffic service or increase the maintenance cost.

Section 65 withstood the traffic test better than Section 64, as no failure of the nature indicated at Point *B* in Section 64 occurred to jeopardize the service value. A pavement of the design shown by Section 65 represents 195.5 cu. yd. less concrete per mile than that of Section 64.

Fig. 23 shows similar information for Section 66, which has the same type of cross-section as Section 65, the width, however, being 20 ft. The number of cubic yards of concrete per mile is the same as for Section 64. A considerable number of shrinkage or check cracks appeared in this section immediately after the slab was laid and before traffic loading was started. Most of these cracks were only discernible on very careful inspection. A short longitudinal crack started at *A*, but did not progress throughout the test. The somewhat diagonal transverse crack shown at *B* did not result in the destruction of the pavement between the crack and the end of the section, the area of this part evidently not being sufficiently small to cause an abnormal increase of bearing pressure on the sub-grade soil.

Fig. 24 illustrates the behavior of Section 67, having a width of 20 ft. and edge thickness of 9 in. tapering to 5 in. at a point 2 ft. from the edge, the mid-portion of the slab having a uniform thickness of 5 in. A considerable number of check cracks appeared in this section also. A short longitudinal crack appeared at *A* which did not progress. A number of transverse cracks appeared under traffic. At the end of the traffic test, this section also remained in perfect condition as far as service to traffic is concerned; and no damage occurred which would cause additional maintenance cost.

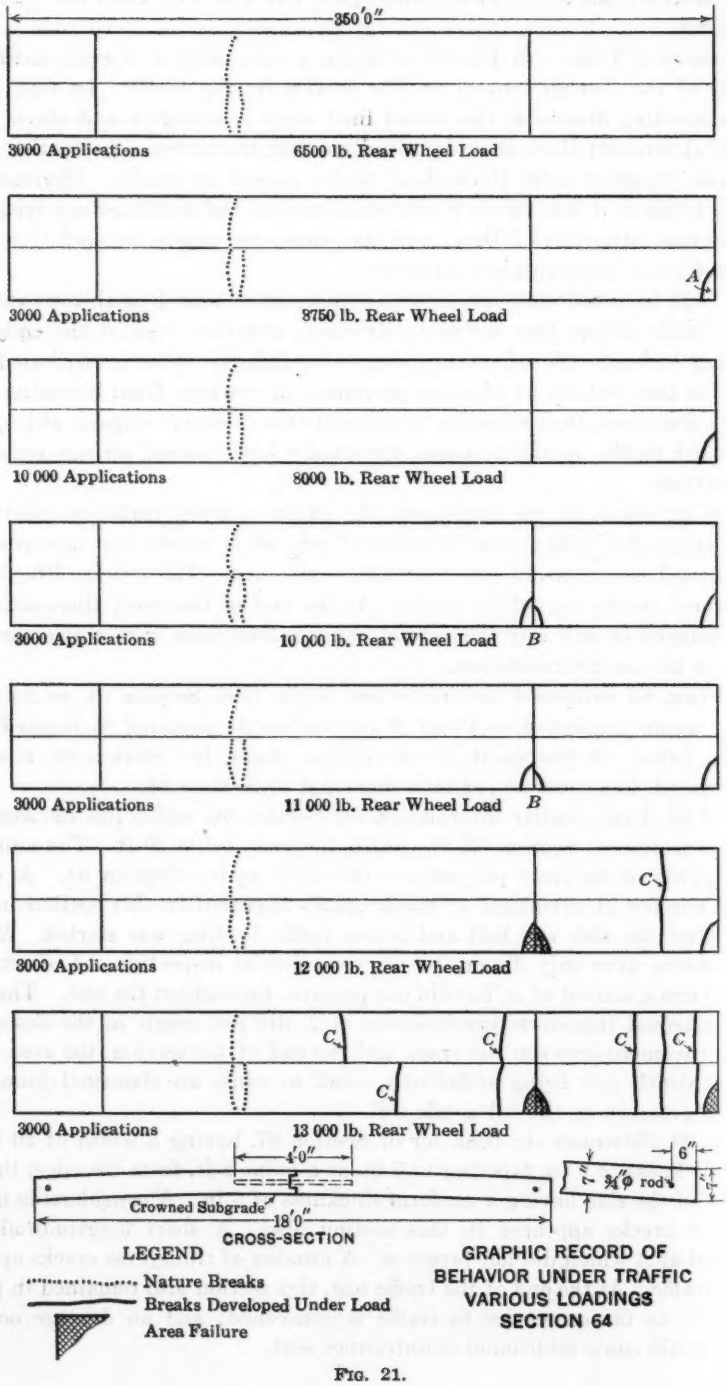
350'0"
3000 Applications
6500 lb. Rear Wheel Load
A
3000 Applications
8750 lb. Rear Wheel Load
10 000 Applications
8000 lb. Rear Wheel Load
3000 Applications
10 000 lb. Rear Wheel Load
B
3000 Applications
11 000 lb. Rear Wheel Load
B
C
3000 Applications
12 000 lb. Rear Wheel Load
C
C
C
C
C
3000 Applications
13 000 lb. Rear Wheel Load
4'0"
Crowned Subgrade
18'0"
CROSS-SECTION
6"
¾"ϕ rod
LEGEND
Nature Breaks
Breaks Developed Under Load
Area Failure
GRAPHIC RECORD OF
BEHAVIOR UNDER TRAFFIC
VARIOUS LOADINGS
SECTION 64

FIG. 21.

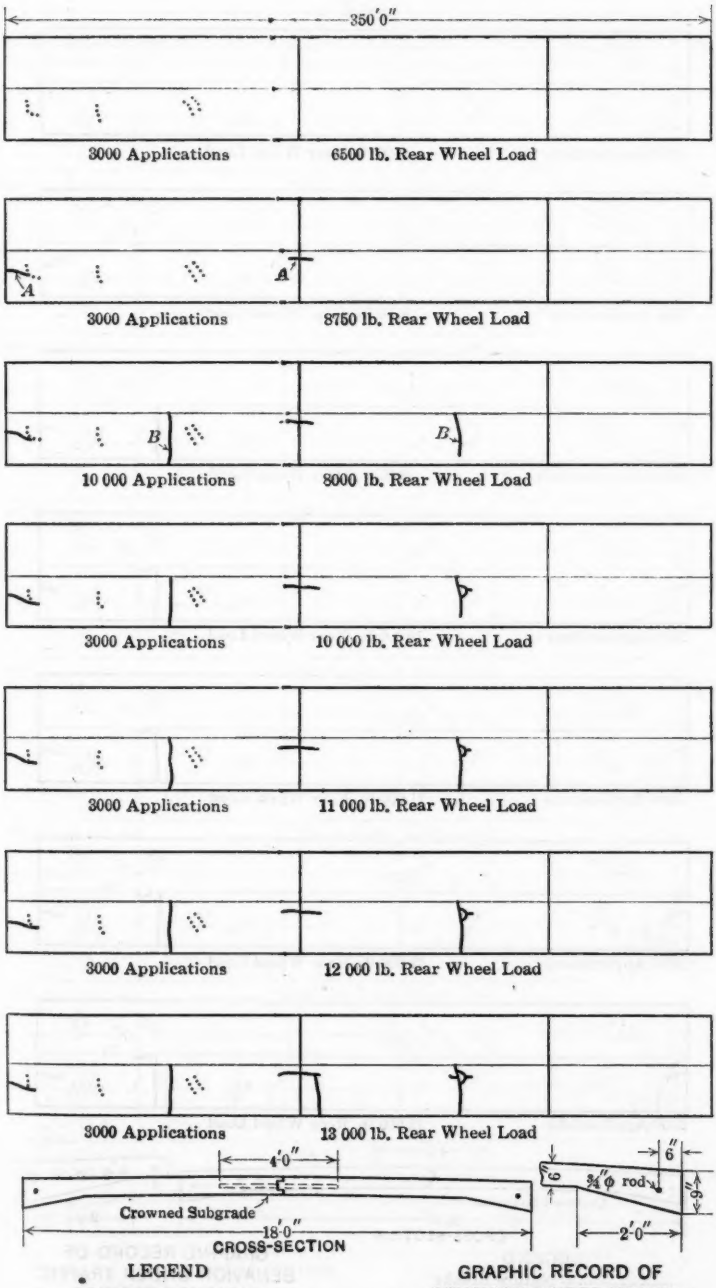
350'0"
3000 Applications
6500 lb. Rear Wheel Load
A
A'
3000 Applications
8750 lb. Rear Wheel Load
B
B'
10 000 Applications
8000 lb. Rear Wheel Load
3000 Applications
10 000 lb. Rear Wheel Load
3000 Applications
11 000 lb. Rear Wheel Load
3000 Applications
12 000 lb. Rear Wheel Load
3000 Applications
13 000 lb. Rear Wheel Load
4'0"
Crowned Subgrade
18'0"
CROSS-SECTION
6"
¾"ϕ rod
9"
2'0"
LEGEND
Nature Breaks
Breaks Developed Under Load
GRAPHIC RECORD OF
BEHAVIOR UNDER TRAFFIC
VARIOUS LOADINGS
SECTION 65

FIG. 22.

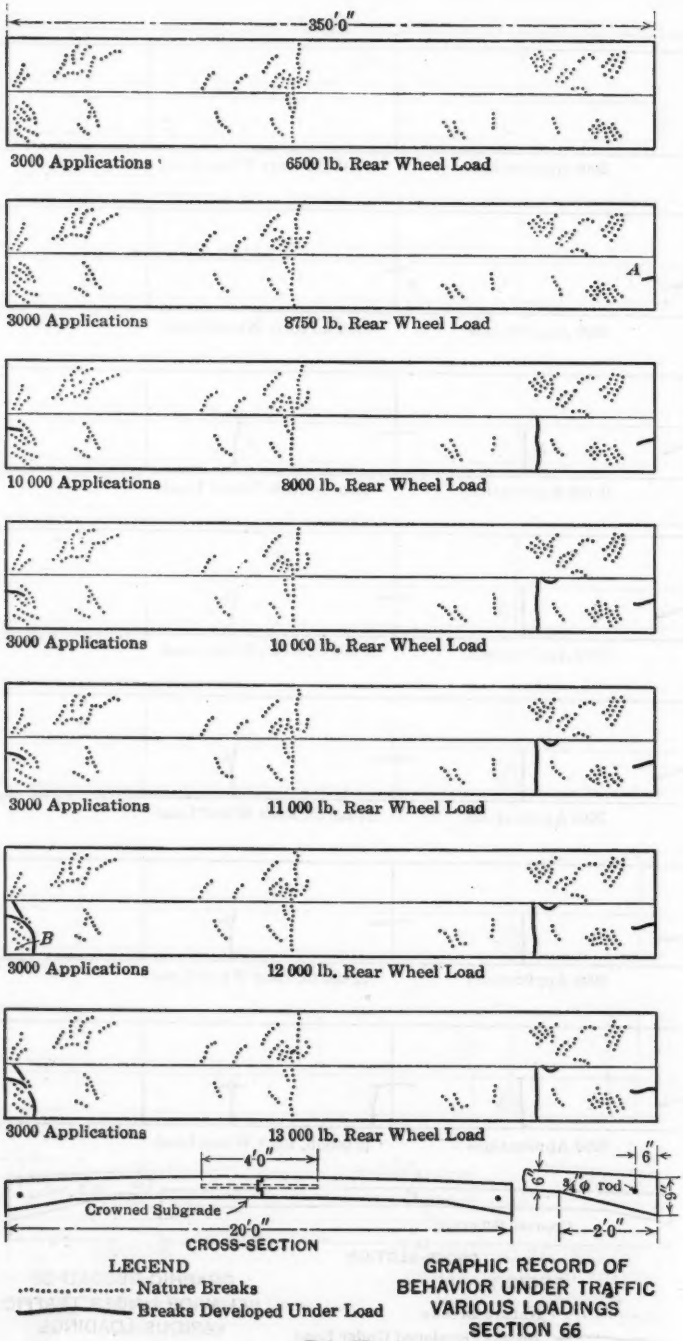
350'0"
3000 Applications
6500 lb. Rear Wheel Load
A
3000 Applications
8750 lb. Rear Wheel Load
10 000 Applications
8000 lb. Rear Wheel Load
3000 Applications
10 000 lb. Rear Wheel Load
3000 Applications
11 000 lb. Rear Wheel Load
B
3000 Applications
12 000 lb. Rear Wheel Load
3000 Applications
13 000 lb. Rear Wheel Load
4'0"
Crowned Subgrade
20'0"
CROSS-SECTION
6"
¾" ϕ rod
2'0"
LEGEND
Nature Breaks
Breaks Developed Under Load
GRAPHIC RECORD OF
BEHAVIOR UNDER TRAFFIC
VARIOUS LOADINGS
SECTION 66

FIG. 23.

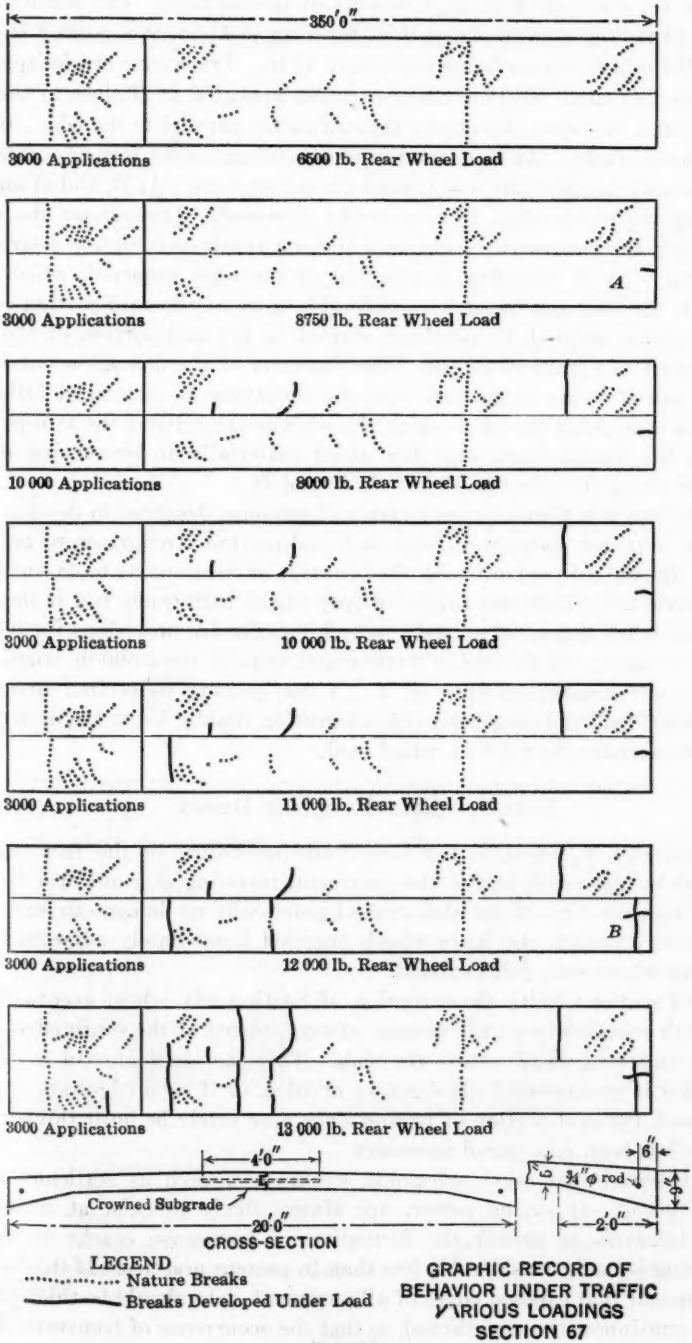
350'0"
3000 Applications
6500 lb. Rear Wheel Load
A
3000 Applications
8750 lb. Rear Wheel Load
10 000 Applications
8000 lb. Rear Wheel Load
3000 Applications
10 000 lb. Rear Wheel Load
3000 Applications
11 000 lb. Rear Wheel Load
B
3000 Applications
12 000 lb. Rear Wheel Load
3000 Applications
13 000 lb. Rear Wheel Load
4'0"
Crowned Subgrade
20'0"
CROSS-SECTION
6"
¾" ϕ rod
2'0"
LEGEND
Nature Breaks
Breaks Developed Under Load
GRAPHIC RECORD OF
BEHAVIOR UNDER TRAFFIC
VARIOUS LOADINGS
SECTION 67

FIG. 24.

Section 68, shown in Fig. 25, is worthy of special note. The width of this section is 18 ft., the edge thickness 9 in. tapering to 4½ in. at a point 2 ft. from the edge, the mid-thickness being uniformly 4½ in. Transverse cracks appeared early in the test run. Short transverse cracks appeared at *B* close to the construction joint, and soon also cracks approximately parallel to the edge, joining the transverse cracks. At *A*, a number of transverse cracks formed, beginning at the edge and running part way toward the center joint. At *D*, and at another point along the south edge, similar cracks appeared. Throughout the traffic test, however, the transverse cracks at *A* did not result in complete destruction of this area. At *B*, complete destruction of the edge occurred, which later resulted in the destruction of a considerable area of the mid-portion of the slab. At points marked, *C*, breakage started in the mid-portion of the slab, and developed to a marked extent. The character of the damage occurring at Points *B* and *C* seems to indicate that the resistance to structural failure of this section was about the same along the edge as throughout the mid-portion. No doubt the longitudinal edge bar aided materially in preventing earlier destruction along the edges at Points *A*, *B*, and *D*.

It is unfortunate that a larger number of sections, designed to develop more completely a proper balance of edge and mid-portion strength were not constructed. By way of contrast with the behavior of Sections 64 to 68, inclusive, that of Section 54 which was subjected only to the 1922 traffic run is shown in Fig. 26, this being typical of all sections lacking effective provisions for increasing edge strength. At the end of 3 000 round trips of the 5 500-lb. wheel load, distinct corner breaks appeared at *A*. These corners pulverized under the 6 500-lb. wheel load and progressive disintegration rapidly led to the destruction of the section under the 8 000-lb. wheel load.

Notes on Rigid Pavement Design

Dimensions.—No mention has been made heretofore of the fact that the wheel loads on the north half of the pavement, traveling at a uniform distance of 36 in. from the edge of the slab, caused practically no damage to any of the test sections, although the inner wheels traveled immediately adjacent to the center joint where such joint existed.

In rigid sections (with the exception of Section 68), where eventually the entire width was destroyed, the damage always started at the south edge of the pavement and progressed across the slab. This fact indicates in a striking manner that if unsupported edges can be avoided, or if such edges are properly strengthened, the mid-portion of paving slabs may safely be built thinner than heretofore has been considered necessary.

It is believed that local sub-grade weaknesses, such as settlements and irregularities of supporting power, are always likely to exist at sufficiently frequent intervals to permit the formation of transverse cracks unless the joint spacing is made considerably less than in present practice. If this be true, it would appear that exposed edges of all pavement slabs should be thickened, or otherwise continuously strengthened, so that the occurrence of transverse cracks would not result in weak corners.

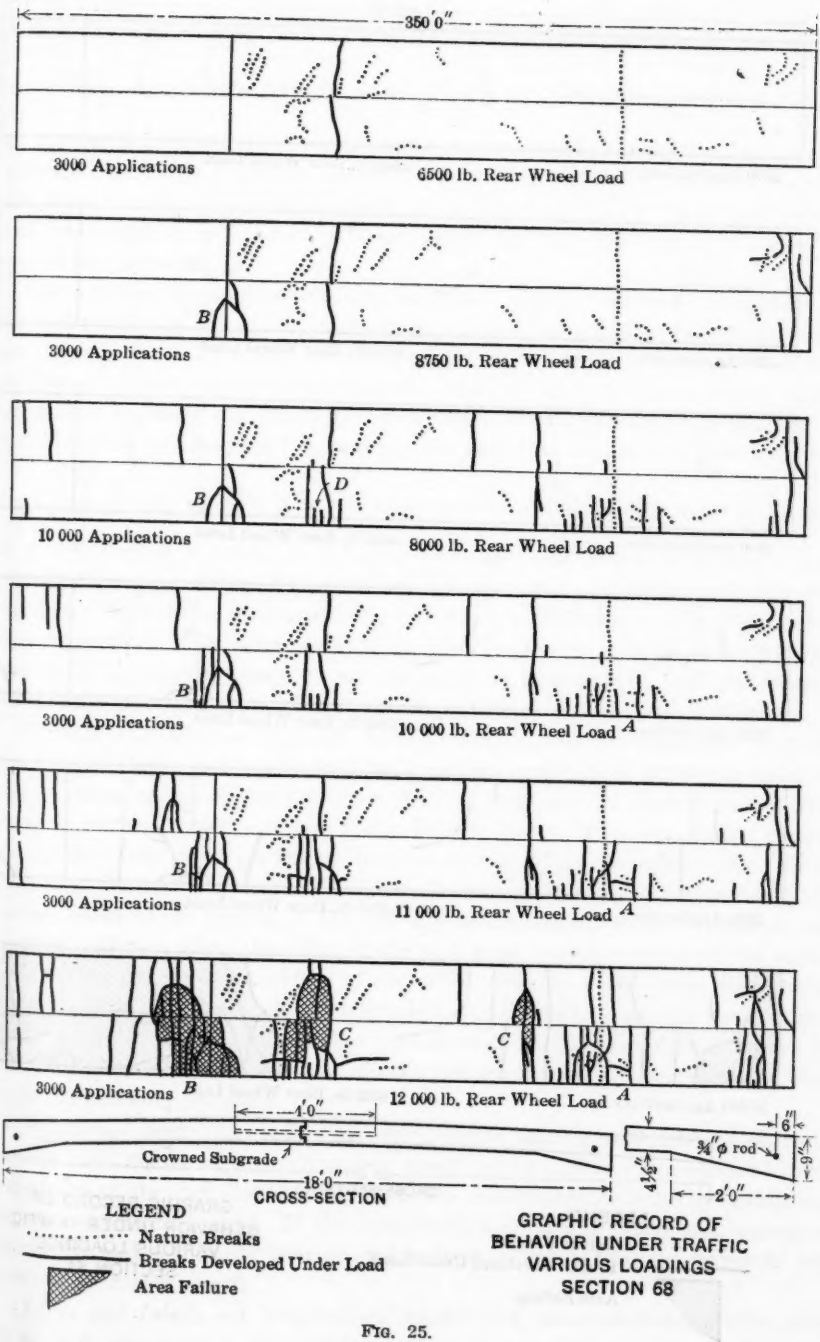
350'0"
3000 Applications
6500 lb. Rear Wheel Load
B
3000 Applications
8750 lb. Rear Wheel Load
B
D
10 000 Applications
8000 lb. Rear Wheel Load
B
3000 Applications
10 000 lb. Rear Wheel Load
A
B
3000 Applications
11 000 lb. Rear Wheel Load
A
C
C
3000 Applications
B
12 000 lb. Rear Wheel Load
A
1'0"
Crowned Subgrade
18'0"
CROSS-SECTION
6"
¾" ϕ rod
9½"
4½"
2'0"
LEGEND
Nature Breaks
Breaks Developed Under Load
Area Failure
GRAPHIC RECORD OF
BEHAVIOR UNDER TRAFFIC
VARIOUS LOADINGS
SECTION 68

FIG. 25.

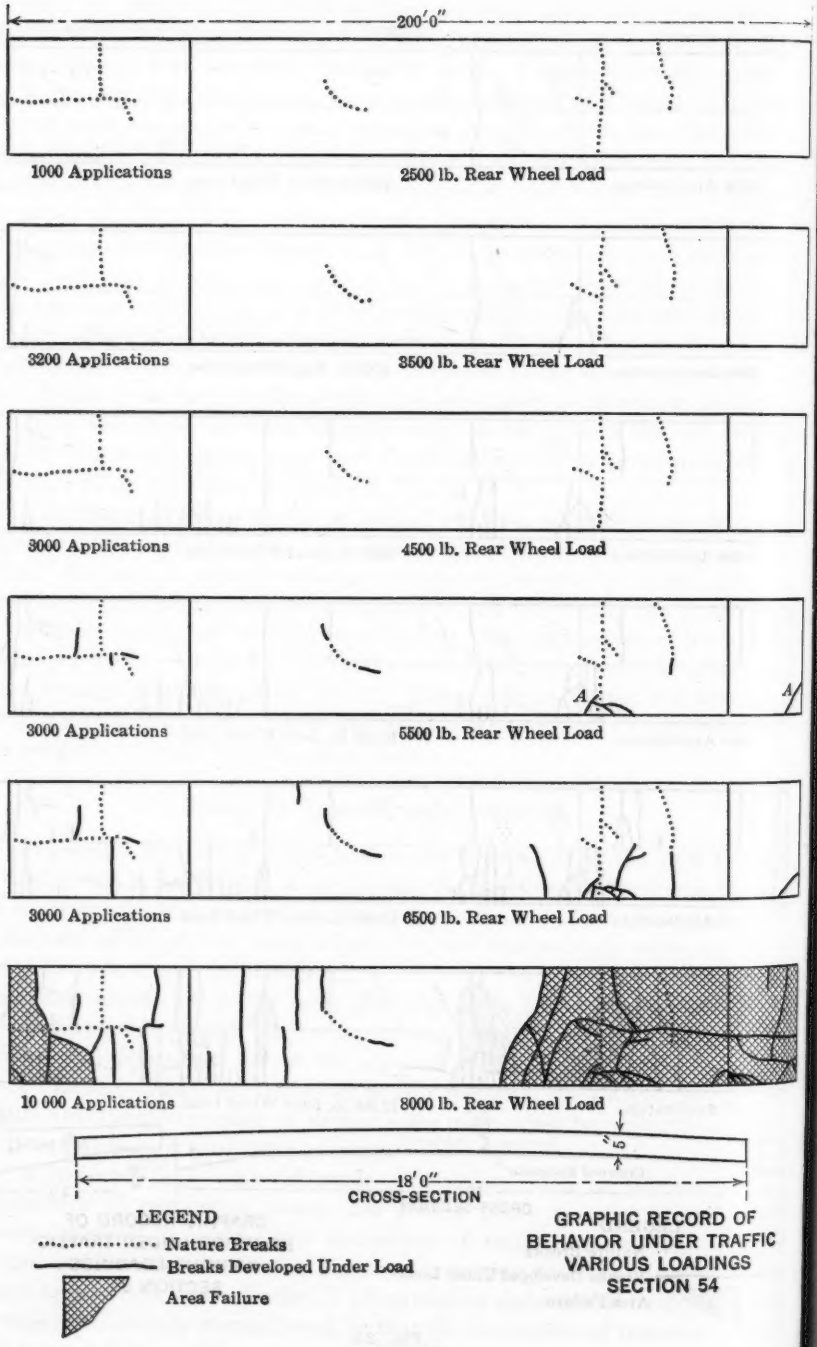
200'0"
1000 Applications
2500 lb. Rear Wheel Load
3200 Applications
3500 lb. Rear Wheel Load
3000 Applications
4500 lb. Rear Wheel Load
A
A
3000 Applications
5500 lb. Rear Wheel Load
3000 Applications
6500 lb. Rear Wheel Load
10 000 Applications
8000 lb. Rear Wheel Load
18'0"
CROSS-SECTION
LEGEND
Nature Breaks
Breaks Developed Under Load
Area Failure
GRAPHIC RECORD OF
BEHAVIOR UNDER TRAFFIC
VARIOUS LOADINGS
SECTION 54

FIG. 26.

Self-supporting edge corners may be insured by proportioning the thickness of slab edges by the formula, $d = \sqrt{\frac{3\ W}{S}}$, in which the value of S should be not greater than one-half of the modulus of rupture of the concrete used. It is suggested that this thickness should be maintained for a distance of at least 2 ft. from the edge and then decreased in another 2 ft. to the mid-portion thickness, inasmuch as initial corner breaks rarely extend more than 2 ft. from the edge of the pavement.

No very definite conclusions may be drawn as to the necessary thickness of the mid-portion of the slab. It is suggested that inasmuch as deflection measurements indicate that the deflection of the mid-portion of slabs of uniform thickness is about one-third of that at the edge, the mid-portion thickness might tentatively be made such that the transverse strength calculated as a beam be one-third that of the edge. A mid-portion thickness obtained by the formula, $d = \sqrt{\frac{W}{S}}$, would provide a mid-thickness corresponding with that of Section 68 which showed a fairly even balance of edge and mid-portion traffic supporting capacity. As the design of this one section only, conformed with this provision, this method of determining mid-portion thickness is advanced merely as a suggestion. The behavior of Section 67 seems to indicate that the mid-portion of a concrete pavement may be made as thin as 5 in., and yet sustain wheel loads amounting to at least 8 000 lb. with a reasonable factor of safety.

Contact of Pavement and Sub-Grade.—The special investigations relating to sub-grade depression under load indicate that under rigid pavement slabs, as well as under so-called flexible types, distinct ruts may be formed in the sub-grade if the wheel paths follow fairly definite lines. This was shown clearly during the traffic tests on Bates Road, especially along the south edge, where numerous shallow excavations were made for the purpose of observing the contact between the bottom of the slab and the sub-grade as the trucks passed. Even at mid-day, when the edges of the slab were warped downward the maximum amount, the bottom surface of the slab at the edge never appeared to be in contact with the sub-grade except when deflected by the passing of a heavy wheel load. At night, this condition was pronounced. A similar state of affairs in all probability existed under the wheel path on the north side, although this could not be easily observed.

Moisture.—Many clay soils when dry, readily take up sufficient moisture to cause a high degree of saturation, but absorb water slowly when moist; hence, sub-grades of dry clay should be moistened to a considerable depth by sprinkling before a pavement is laid. If the construction is on a dry clay soil, excessive saturation and minimum bearing values may occur before the concrete has attained normal strength.

Edges and Joints.—A longitudinal tongue-and groove-doweled center joint in an 18-ft. pavement is apparently effective in preventing longitudinal cracks as well as in reducing temperature warping. During the past three years,

about 1 500 miles of Illinois rural pavements have been built with this type of center joint, and no longitudinal cracks have appeared to date. The corners formed at the intersection of transverse joints or cracks with the center joint did not appear to be points of weakness in the Bates Road. This was no doubt due chiefly to the effectiveness of the tongue-and-groove joint in transmitting by shear one-half of the loads to the adjacent slab.

Longitudinal contraction in cold weather must always result in open transverse cracks or joints in rigid pavements, even when using a wearing surface other than concrete. Edge corners, therefore, must either be effectively doweled or be made self-supporting. Dowel bars, to be of value, should be continuous in order to provide for corners formed by unexpected transverse cracks and should have sufficient bearing area to minimize bearing pressures on the concrete immediately adjacent to cracks and joints.

Asphaltic concrete surfaces and bituminous filled brick surfaces apparently do not add materially to the strength of the base, but by lessening excessive impact at small broken corners, they give considerably increased resistance to progressive destruction.

Continuous longitudinal shear bars along the edges of concrete slabs aid materially in the mutual support of the adjacent edge corners for a more or less prolonged period, depending on the volume of traffic, and, in addition, are of marked advantage in preventing rapid progressive destruction in case corner breaks do occur.

Any design in which reinforcing steel is expected to relieve the concrete of all tensile stresses should take into account the possible formation of corners at any point along the edge of the slab.

Impact.—An examination of Fig. 17 indicates, by the relative position of the points representing initial structural failure and the breaking load curves based on static loads, that, in the test road, either impact was not an important factor in causing initial failure, or the increase of stress due to impact was very closely counterbalanced by some other factor. These diagrams also show that, in all probability, the strength of pavement slabs in service varies as the square of the thickness. Impact stresses are presumably directly in proportion to the thickness. If, therefore, impact was an important factor, the plotted points in the diagrams mentioned should fall at least approximately along a straight line passing through the zero point.

These considerations, strengthened by the impact deflection investigations previously described, lead to the belief that no allowance for impact need be made in the design of a pavement the nature of which makes practicable the construction and maintenance of a reasonably smooth surface.

Future Research.—The development of instruments suitable for determining fiber deformations in the surface of the pavement under traffic would aid greatly in a better understanding of stress distribution as well as magnitude. Progress in the design of such a device is being made by the U. S. Bureau of Public Roads. The development and use of this sort of instrument is exceptionally difficult, owing to the fact that the gauge length must be short, the

observations taken under rapidly moving wheel loads, and deformations of less than 0.001 in. recorded with accuracy.

In view of the vast expenditures annually being made for paved roads, the lack of more complete scientific knowledge of pavement design is a challenge to engineers which should be answered as soon as possible by intense research activity.

IMPROVED TYPE OF MULTIPLE-ARCH DAMS

Discussion*

By Messrs. L. F. Harza and L. Standish Hall.

L. F. Harza,† M. Am. Soc. C. E. (by letter).‡—The writer has read with much interest Mr. Noetzli's paper and the discussions on multiple-arch dams. In the abstract, a multiple-arch dam is an ideal type of structure, and it is hoped that its design will be rapidly developed such that it will be understood sufficiently to gain consideration wherever it is applicable and economically advantageous.

Concrete is a material primarily adapted to withstand compressive stresses and in the ideal multiple-arch dam all the material is in compression. In a gravity dam, much of the concrete has no value except weight, and concrete is expensive material for furnishing weight alone. A gravity dam judged from this point of view is, therefore, an uneconomical structure.

If every cubic yard of concrete in a multiple-arch dam is used to its full capacity in taking compressive stresses, and if these stresses are no greater than those which would be taken by the concrete in a gravity dam along the down-stream face where the compression is greatest, the reason for the economy in material of the multiple arch becomes apparent. It is merely a question of designing so that all the concrete will be active instead of merely a small proportion of it along the down-stream face. It might also be argued that to have all the concrete active to its full working compressive strength is as safe as to have only a small part of it in action, and that by so doing the factor of safety is not diminished.

The multiple-arch dam, however, introduces other new problems of design, which must be solved before it can be considered as safe as a gravity dam. Most of these questions, such as effect of temperature changes, arch shortening, etc., have been fully covered by the author and other discussors.

The writer will emphasize some other points which, perhaps, have not received their full share of importance in the paper or in the discussions. He questions whether a multiple-arch dam is ever justified on a yielding foundation, even if the engineer believes the design is such that "no irregular settlement will occur", as referred to by the author. It is impossible to be certain that a foundation will yield uniformly, and a very small unequal settlement of the buttresses of a multiple-arch dam might introduce stresses in the arches far in excess of those due to temperature or arch shortening, and of unknown direction and magnitude. On a yielding foundation, the flat-slab type of hollow dam seems to offer advantages in that the buttresses might

* Discussion on the paper by Fred A. Noetzli, Assoc. M. Am. Soc. C. E., continued from January, 1924, *Proceedings*.

† Cons. Hydro-Elec. and Hydr. Engr., Chicago, Ill.

‡ Received by the Secretary, November 23, 1923.

settle unequally without seriously changing the stresses in the facing slab. This type of dam is, however, not applicable to heights as great as the multiple arch.

The author has referred to the advantage of having the buttresses designed so that in case of the failure of one arch the thrust of the adjacent arches would not overturn the two buttresses subjected to unequal thrust. The writer does not think there is any merit in this feature of the author's design. He cannot conceive of the possibility of these two buttresses remaining intact in case of a failure of the arch. If the reservoir was filled at the time of failure, the depth of the water in the opening caused by the wrecked arch would be about two-thirds of that in the reservoir, and the two adjacent buttresses would be subjected to a lateral hydrostatic pressure which no possible economical design could be made to withstand. This is not a serious criticism, however, as no dam should be designed to fail.

In the practical application of the author's theory, the writer would suggest that the intrados of the arches be kept uniform from bottom to top of the dam. The cost of a multiple-arch dam is largely influenced by cost of forms. For a high dam, such as that proposed by the author, with arch spans of 60 ft. or more, the cost of arch centering or forms supported from the ground would be almost prohibitive. The application of the multiple arch to high dams necessitates a form which would consist of trusses spanning between the previously built buttresses and one which could be moved upward along the buttresses as the pouring advances. For a 50 or 60-ft. span, these trusses would carry heavy loads and would have to be built of steel. To vary the span of the arch would almost prohibit the practical use of this type of dam.

There are three ways in which the arch spans and the intrados can be kept constant: (1) By battering the buttresses on the inside surfaces of the exterior walls, instead of on the outside, as shown by the author's design for the Paradise Verde Dam, keeping the exterior faces of the buttresses parallel from top to bottom; (2) by using diverging buttresses, shown by the author, with the divergence chosen to compensate for the batter; and (3) by curving the dam up stream sufficiently to cause the spacing of the buttresses at the up-stream toe to equal that at the crest. This last method would not be generally applicable, because it would usually be necessary to locate the dam, in plan, from other considerations.

There is another important element of weakness to be guarded against in the multiple-arch or in any hollow dam, as compared with the gravity dam, that is, the inherent uncertainty of concrete. Engineers who perfunctorily specify a 1 : 2 : 4, or a 1 : 3 : 5, or other similar mixtures of concrete are resting under a false sense of security in thinking that a specification of this type has much bearing on the quality of concrete. The more concrete the writer builds and tests, first from theoretical proportions, then from the material as discharged from the mixer, and lastly from the material as finally deposited in the forms, the more he is inclined to believe that good concrete is principally dependent on good workmanship. For example, the designing engineer may add a large excess of cement to the concrete mixture and the contractor by careless handling, excess water, and segregation during transportation and

in the forms, can lower the theoretical strength of the concrete far more than was added by surplus cement. Engineers are just beginning to learn how to build dependable concrete; only within the last few years has the effect of surplus water and other conditions, to which the concrete is very sensitive, been determined.

The writer is of the opinion, therefore, that a multiple-arch dam should be designed with conservative unit stresses and, perhaps, be built by force-account under the direct supervision of the designing engineer who appreciates the importance of good concrete, because control of the quality of contract work sufficiently to satisfy the rigid requirements of this type of structure is difficult to realize.

Failures of reinforced concrete structures have attended the development of the art throughout its history, although, fortunately, they are becoming less frequent as more is learned about the fickle nature of concrete. These failures usually do little harm and are soon forgotten. As the failure of a dam, however, usually results in a great catastrophe, safety is demanded.

The writer believes there is much merit in the author's type of hollow buttress. It is undoubtedly the most stable form of buttress for a given quantity of concrete, the most economical section of high structure for resisting unequal lateral stresses, and offers possibilities of greatly improved architectural treatment over a thin buttress with its multiplicity of bracing.

Hollow spaces and interior surfaces of buttresses are much more cheaply constructed than lateral ribs or other irregularities on the exterior surfaces. Internal cavities can be formed with the roughest and cheapest of lumber left in place, if desirable, whereas external irregularities, such as ribs, would require relatively expensive form work and careful surface treatment, in addition to being weaker structurally against lateral deflection than the H-section proposed by the author.

The writer recently investigated the possibility of using a multiple-arch dam, about 270 ft. high, at a site where the cost of a gravity concrete dam would have defeated the project economically. The local conditions were such as to require the excavation of a quantity of rock for a flood channel sufficient to build a rock-fill dam. It was felt that a rock-fill dam with ample spillway, conservative slopes, and highly reinforced concrete sheet on the up-stream face could be relied on with confidence and could be built for less than the multiple-arch dam. The result was a decision in favor of the rock-fill dam for this site.

In connection with this project, Ing. Guido Semenza, of Milan, Italy, reported on the extent to which the multiple-arch dam has been built in Italy, as this type has received more favorable consideration there than in any other country. It was found that no dams of importance had yet been completed (early in 1923), the most important one of which information is available being only 69 ft. high, considerably less than existing dams in this country. The chief available information on each important Italian dam now under construction or projected is as follows:

The Tirso Dam in Sardinia.*—This dam was the furthest advanced of any, and since the report was made, has been completed and has been in quite successful operation for several months. It has a length of 740 ft., and the span of each arch is 49 ft. Its maximum height is 208 ft., and it has a maximum head of 198 ft. The buttresses are of rubble masonry and the arches are of reinforced concrete.

In the electrification program of the State Railways, there are now two dams under construction for storage or power purposes, one at Pavana and one at Castrola, and another dam, the Suviana, is projected by the same Department.

The Pavana Dam.—This structure has a maximum height of 154 ft., and a water head of 148 ft. It is 394 ft. long, and the inclination of the axis of the arches to the horizon is 60 degrees.

The Castrola Dam.—The maximum height of this dam is 226 ft., with a head of water of 218 ft. There are eleven arches and the dam is 680 ft. long, the spacing of the buttresses being 52 ft.

The Suviana Dam.—This dam is not yet under construction, but it will have a height of 279 ft., with a head of water of 262 ft., and a length of crest of 590 ft.

The regulations of the State Railways Department, which is building these three dams, call for a factor of safety of 8 in concrete, which is higher than that recommended by the author. As this factor of safety is considered to be unnecessarily high, the opinion is not unanimous in the Italian State Railways Department in regard to continuing its use, as it largely reduces the economic advantage of this type of dam over the ordinary gravity dam.

Other projected Italian dams of multiple-arch type are the Gleno, 165 ft. high; the Val Tidone, 181 ft. high; and the Val d'Arda, 138 ft. high. At least ten other multiple-arch dams of lesser importance are also said to be projected in Italy.

The Italian practice of the rubble masonry buttresses is probably best suited to conditions in that country because of the experience of Italian laborers in laying this kind of masonry, but it does not indicate that this type of buttress would be economical under American labor conditions.

The Italian engineers, at least those in charge of the State Railways electrification, seem to have satisfied themselves of the safety and economy of this type of dam, as shown by the fact that they already have under construction and projected three dams, two of which will be the highest of this type in the world. This program of high dams was launched without the experience or precedent of a single completed dam of comparable magnitude to guide their judgment and confidence.

The multiple-arch dam is distinctly a problem of structural design. After the assumptions are made, it probably yields as closely to mathematical analysis as most structures. The assumptions can be made with accuracy as great as that for the design of a gravity dam, and probably much greater, for

* *Transactions*, Am. Soc. C. E., Vol. LXXXIV (1921), and *Engineering News-Record*, May 10, 1923.

the enormous uncertainty involved in uplift at the base and in horizontal joints is eliminated.

The author deserves credit for a distinct contribution to the advancement of this type of dam and its application to higher heads.

L. STANDISH HALL,* ASSOC. M. AM. SOC. C. E. (by letter).†—The author has solved the problem of proper stiffening for the buttress walls of multiple-arch dams in a satisfactory and ingenious manner. This type of design is more pleasing than the usual spandrel beam bracing, although the latter may be more economical for dams of moderate height.

Engineers in recent years have devised several methods of reducing the cost of dam construction by the use of either the single or multiple-arch type. Many of these innovations appear safe and conservative, and it is hoped that opportunity may be afforded to try them in actual construction. However, as the final approval of such structures during recent years has been placed more and more in the hands of Federal or State authorities, it becomes very difficult to introduce innovations in design, because, as a rule, these bodies are ultra-conservative. Unsafe designs should be rejected, but the introduction of conservative innovations should not be prohibited.

It often happens in the case of arch dam design, where the approval of both the State and the Federal Government is necessary, that, after the requirements of both of these authorities are satisfied, the cost is so increased by thickening the base and the top, or by carrying the abutments farther into the rock, that it is cheaper to build a structure of gravity type.

A trace of this conservatism is brought out by the author in reference to the design of the Horseshoe Multiple-Arch Dam on the Rio Verde, where the United States Reclamation Service required that the sliding factor between buttresses and bed-rock be not more than 0.65. Where a dam is constructed on solid rock and the foundations well "keyed", it is difficult to see how sliding can occur until crushing or shearing has taken place. That other designers have taken advantage of this additional factor of safety against sliding, is shown in the references of the author, indicating that dams have been constructed with a sliding factor as high as 0.80.

With regard to sliding along construction joints, the author suggests that the joints be stepped and inclined so as to form an angle equal to the angle of the coefficient of friction. Although, in general, this suggestion is a good one, the writer prefers a modification by reducing the angle to one-half the angle of the coefficient of friction. The reason is that, if the joints were inclined so as to neutralize slipping with the reservoir full, there would be a tendency for the structure, when the reservoir was empty, to slide back into the reservoir along these joints.

---

* Asst. Engr., H. L. Haehl, San Francisco, Calif.

† Received by the Secretary, December 15, 1923.

OCEAN BEACH ESPLANADE, SAN FRANCISCO, CALIFORNIA

Discussion*

By Lynn Perry, M. Am. Soc. C. E.

Lynn Perry,† M. Am. Soc. C. E. (by letter).‡—This paper presents authentic information concerning the design and construction of one of the largest recent structures for shore protection known to the writer. Its importance and cost warranted considerable investigation and study before the final design was determined. The paper, however, contains very little information, concerning tides, the nature of the sand, the direction of prevailing winds at times of maximum erosion, the extent of this erosion, and the quantity of littoral drift.

Unprotected beaches are subject to erosion and accretion, and a great deal of money has been spent in attempts to protect water-fronts from such erosion and even to promote accretion. This construction and the results recorded have supplied considerable information concerning what may be expected under certain conditions. A few examples will serve to illustrate the point.

In 1858, Atlantic Avenue was the beach front street in Atlantic City, N. J., and considerable anxiety was felt concerning the progressive erosion taking place at that time. In order to save a light-house at the northern end of the island, the Government built a breakwater (about 1875) at right angles to the shore line and about 200 ft. in length. This brought about immediate and permanent relief, the shore line already having receded about ½ mile. Other similar structures, as well as the piers, have caused continued accretion. Fig. 8 shows what occurred at Longport, N. J., a few miles away, during these years. It is the original map of the Borough, with the shore line as it was in 1914 outlined thereon. Conservative estimates indicate a loss of more than 180 acres in this recession of about ¾ mile. Most of the ocean front of Longport is now protected by a sea-wall, of which Fig. 9 is a vertical cross-section.

Given a free hand and ample funds, an engineer often can protect a beach from destructive erosion by using a combination of sea-walls and groins. A sea-wall, if well built and judiciously located above the high-water line, will protect the shore line, which protection is frequently necessary. At the same time, it intensifies the scouring action, lowering the beach level and too frequently undermining the sea-wall—an annoying condition. To offset this action, a system of groins may be used to prevent the swirling action of the receding water from carrying away the beach sand. Experience indicates

* This discussion (of the paper by M. M. O'Shaughnessy, M. Am. Soc. C. E., published in *Proceedings* for November, 1923, but not presented at any meeting of the Society) is printed in *Proceedings* in order that the views expressed may be brought before all members for further discussion.

† Asst. Prof., Hydr. and San. Eng., Lafayette Coll., Easton, Pa.

‡ Received by the Secretary, December 7, 1923.

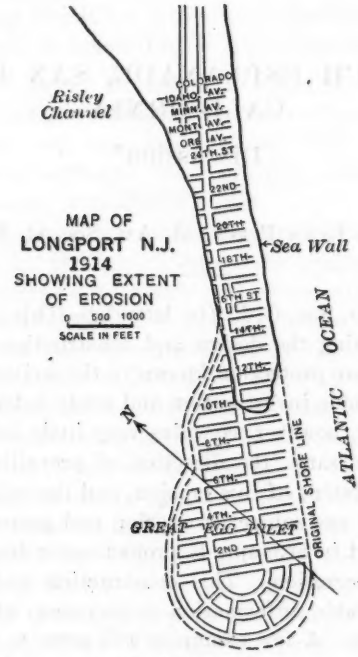
Risley Channel
COLORADO AV.
IDAHO AV.
MINN. AV.
MONT. AV.
ORE. AV.
24TH. ST
22ND
20TH
18TH
16TH ST
14TH
12TH
10TH
8TH
6TH
4TH
2ND
MAP OF
LONGPORT N.J.
1914
SHOWING EXTENT
OF EROSION
0 500 1000
SCALE IN FEET
Sea Wall
OCEAN
ATLANTIC
ORIGINAL SHORE LINE
GREAT EGG INLET

FIG. 8.

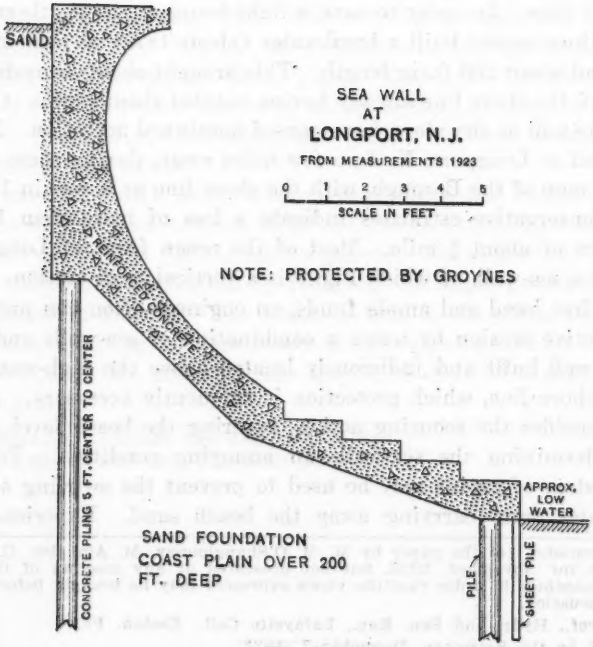
SAND
SEA WALL
AT
LONGPORT, N.J.
FROM MEASUREMENTS 1923
0 1 2 3 4 5
SCALE IN FEET
NOTE: PROTECTED BY GROYNES
REINFORCED CONCRETE
CONCRETE PILING 5 FT. CENTER TO CENTER
APPROX. LOW WATER
SAND FOUNDATION
COAST PLAIN OVER 200
FT. DEEP
PILE
SHEET PILE

FIG. 9.

that groins are a dependable defense against undermining. Short sections of sea-walls often have been destroyed by the flanking action of the sea during storms, and, therefore, when sea-walls are built, they should be continuous for reasonably long stretches.

The stepped section of the sea-wall presents many advantages over some of the older sections built in England and along Continental beaches. Case states that the wall should present an elliptical front, the eccentricity depending on the slope of the beach. Laboratory observations, however, indicate that a compound circular face could be designed to present the same advantages and obviate some of the disadvantages of construction.

The groins or jetties should be: (*a*) tight; (*b*) protected with rip-rap; (*c*) begin at the wall and extend well beyond the low-water mark; (*d*) project 2 or 3 ft. above the beach; (*e*) be spaced at a distance apart equal to their length; and (*f*) be built normal to the shore line. If they are built of wood, the wood should be treated with creosote, and all spikes and fittings should be well galvanized. The most serious objection to systems of groins is their unsightly appearance.

For a shore protective structure, a rigid system of inspection and repair should be maintained. Too many municipal structures have been permitted to depreciate on account of poor systems of upkeep. If not diligently maintained, this type of structure is subject to serious damage or destruction.

MEMOIRS OF DECEASED MEMBERS

NOTE.—Memoirs will be reproduced in the volumes of *Transactions*. Any information which will amplify the records as here printed, or correct any errors, should be forwarded to the Secretary prior to the final publication.

HIRAM FRANCIS MILLS, Hon. M. Am. Soc. C. E.*

DIED OCTOBER 4, 1921.

Hiram Francis Mills, a son of Preserved Brayton and Jane Lunt Mills, was born in Bangor, Me., on November 1, 1836. His father was a prominent physician of the Thompsonian system and was highly esteemed in the community.

Hiram Francis Mills was educated in the public schools of Bangor from which he entered the Rensselaer Polytechnic Institute, at Troy, N. Y., and was graduated with the degree of B. S., in the Class of 1856. Among his classmates were other noted engineers, including the late Joseph Phineas Davis, Charles Cyril Martin, and John Allston Wilson, Members, Am. Soc. C. E.

Before commencing independent professional work, Mr. Mills resolved to have ten years' experience with the ablest engineers in the United States on important works then in progress, and during this period he was associated with such eminent men as the late James P. Kirkwood, William E. Worthen, and James B. Francis, Past-Presidents, Am. Soc. C. E., Charles S. Storrow, Hon. M. Am. Soc. C. E., and others. This experience was sought, for the opportunity of association with such engineers, without regard to salary. In pursuance of this plan, Mr. Mills served on the Bergen Tunnel of the Brooklyn Water-Works with Mr. Kirkwood; on water-power measurements and distribution of power at Cohoes, N. Y.; on water measurements and construction of mills at Lowell, Mass.; and on experiments at North Billerica, Mass., on the Concord River, in connection with the drainage of the adjacent lowlands. While on this work, he came in contact with Mr. Storrow, one of the Commissioners for the State, with whom he formed a lasting acquaintance and friendship that led ultimately to his engagement at Lawrence, Mass.

In 1863, Mr. Mills was Resident Engineer at the east end of the Hoosac Tunnel, when he designed and built the State dam in the Deerfield River. Three years later, he designed a stone dam on the Penobscot River at Bangor, Me., and made plans for the development of a water supply.

About 1868, he opened an office in Boston, Mass., for professional work, making a specialty of hydraulic engineering and difficult foundations. In 1869, he conducted a series of tests on water turbine wheels at the Canal of the Wamesit Power Company, at Lowell, Mass., to determine their efficiency in the use of water and power. These turbines included the Swain wheel, the Risdon, Leffel, Bodine, and other runners which have been superseded by improved and higher class wheels. The writer assisted as an observer on these tests and thereafter was associated with Mr. Mills during the remainder of his life.

* Memoir prepared by Richard A. Hale, M. Am. Soc. C. E.

In 1869, Mr. Mills accepted the position of Chief Engineer of the Essex Company, at Lawrence, Mass., which had developed a large water power on the Merrimac River twenty years previous and had founded the City of Lawrence. Mr. Charles S. Storrow who had designed and developed the power and had laid out the city, was Treasurer of the Company. Mr. Mills began extensive hydraulic experiments in connection with the development of methods and instruments for the daily measurement of water leased to the various mills at Lawrence.

Among his studies was one which resulted in the improvement of the Pitot tube for convenient and accurate gauging purposes and brought the instrument to a high degree of efficiency. It has never been placed on the market as a commercial venture, as it was always Mr. Mills' idea that the profession should receive the benefit of the results. In April, 1878, he contributed an interesting paper on the subject of piezometers to the American Academy of Arts and Sciences.

Between 1870 and 1885, Mr. Mills had a large outside practice in the development of hydraulic power in New England and the West, and was closely connected with the construction of a number of mills, including difficult foundations.

Soon after the death in 1892 of James B. Francis, Past-President, Am. Soc. C. E., who had been in charge of the Lowell Water Power for many years, Mr. Mills was called to assume its direction and, later, was made Chief Engineer of the Locks and Canals Company, which position he held until shortly before his death. He also retained his connection with the Essex Company until his death.

In 1886, Mr. Mills was appointed a member of the newly organized Massachusetts State Board of Health and was elected by his associates to be Chairman of its Committee on Water Supply and Sewerage, serving as such until the Board was legislated out of existence in 1914. His devotion to this work and to the interests of the State has seldom been equalled and never surpassed in Massachusetts. He organized an extensive system of water sampling and analysis of all the supplies and of the important rivers of the Commonwealth and began extensive experiments on the purification of water and sewage. Although there was no salary attached to his position, and his labors were solely for the public welfare, the excellent and earnest character of the work soon commanded the respect of the Legislature and resulted in unusually liberal appropriations being placed at the disposal of Mr. Mills. In this way, the famous Lawrence Experimental Station was developed, which, all things considered, is probably the leading laboratory in the world devoted solely to the study of the purification of water and sewage. His services, in conjunction with those of Dr. Henry P. Wolcott, Chairman of the old State Board, and the other members, gave the organization an excellent reputation. Deaths from consumption for the whole State dropped from 45 per 100 000 persons to about 5 when the Board was abolished, while the death rate from all causes, for the State as a whole, dropped during the period of Mr. Mills' membership, from about 20 per 100 000 to 14.9.

Among the important public enterprises with which Mr. Mills was connected in a position of the highest responsibility may be mentioned the preliminary studies for the improved sewerage and drainage of the Boston Metropolitan District, the water supply of the Boston Metropolitan District, the damming of the Charles River, and various investigations in connection with the general subject of public health. None of these is more thoroughly characteristic of his public spirit, however, than the construction of the water filter at Lawrence. As long ago as 1875, when the public water-works were built in that city, Mr. Mills doubted the expediency of drawing a supply from the polluted Merrimac River, for he did not believe in the theory of the rapid self-purification of running streams, which at that time was held strongly in England.

As opportunity offered, he investigated the typhoid epidemics along the river and eventually became an earnest advocate of the filtration of this supply for domestic use. After a great deal of opposition had been overcome, an appropriation for a filter was made by the City authorities, and the direction of the work was left to Mr. Mills, as he had agreed to assume all responsibility for design and construction, without expense to the city. This was the most noted filter in the United States for many years, and its effect on the death rate was marked.

Although the death rate in Lawrence from typhoid fever was greater than in most cities before the filter was put in operation, since then the rate has remained below the normal. The vital statistics show that probably about sixty lives annually have been saved by this work, not to mention the many cases of sickness from which recoveries are made. In this undertaking, as in many others of a public nature, Mr. Mills served entirely without compensation and often against considerable opposition, in order to achieve results which he considered to be of general advantage. It is only among men who have worked under him that the importance of his labors for the profession and the public are fully recognized.

Mr. Mills was granted the degree of Master of Arts by Harvard University in 1889. He was elected a Fellow of the American Academy of Arts and Sciences in 1877, and a member of the Corporation of the Massachusetts Institute of Technology in 1885.

He published many professional papers, among which are the following: "Experiments Upon Piezometers Used in Hydraulic Experiments"; "Water Power of the United States"; "Experiments Upon Central Discharge Water Wheels"; "Protection of the Town of Westfield from Future Floods"; "Construction of the Pacific Mills Chimney"; "The Protection of the Purity of Inland Waters"; "Purification of Sewage by Applying It to Land"; "Report of The State Board of Health Upon the Sewerage of the Mystic and Charles River Valleys"; "A Classification of the Drinking Waters of the State"; "Report of The State Board of Health on Filtration of Sewage and of Water and Chemical Precipitation of Sewage"; "Purification of Sewage and of Water by Filtration"; "The Filter of the Water Supply of the City of Law-

rence and Its Results"; as well as memoirs of John C. Hoadley, James B. Francis, and Charles S. Storrow, leaders in the engineering world.

In 1917, Mr. Mills resigned his position at Lowell and removed to Hingham, Mass., where he resided until his death. He had been busy, as his health permitted, in completing various hydraulic formulas in connection with his life work.

He was married on October 8, 1878, to Miss Elizabeth Worcester, who died on August 23, 1917, at Hingham, shortly after leaving Lowell. They had no children. Mr. Mills is survived by two nephews and two nieces, the children of his brother, James Mills, a prominent mining engineer who died many years ago.

With prudent management and wise investments, he had accumulated considerable property unknown to his most intimate friends. His will, containing many bequests of public interest, showed his usual careful consideration and thoughtfulness. No finer expression of the ideas and lessons drawn from the will can be found than the following comment from a prominent writer in one of leading engineering publications of New York, under the title, "Will of a Great Engineer":

"For reasons only too well known to most of our readers the last will and testament of an engineer is rarely of interest outside his family circle. An exception rare as to the sum total bequeathed and notable because of the beneficiaries named, the evident thought put upon their selection and the restrictions and explanations relating to the residuary estate, is afforded by the will of the late Hiram F. Mills, which has just been made public. Of the public bequests of specified amounts, two are outstanding because of their objects and conditions. A large cancer research fund bequeathed to Harvard University speaks volumes, coming as it does from a man who, through his thirty years of devoted work on the State Board of Health of Massachusetts, contributed so much to the reduction of the mortality rate in general and to the typhoid rate in particular. Some decades ago, it is conceivable that Mr. Mills might have established a fund to combat typhoid. That is no longer an urgent need. A fund to aid in the reduction of the general death rate would not have that directness of aim to be expected from an engineer like Mr. Mills. What more natural, familiar as he was with the major causes of disease, suffering, and death, still awaiting successful attack, than that Mr. Mills should select that widespread, baffling, and dreaded disease, cancer?

"The minor public bequests, it may be noted in passing, show discrimination. The gifts are small, but they will prove helpful materially and, in some respects, more important yet, because of the appreciative recognition given to these institutions in the will of a great and thoughtful engineer.

"Most directly human of all the gifts, and perhaps most characteristic of the giver, is the bequest of the residue of Mr. Mills' estate for the benefit of the needy of Lawrence and Lowell, particularly the mill workers. This gift, as stated in the will, springs from Mr. Mills' half century of professional work in making the most of the water power on the Merrimac River and upbuilding the cities of Lawrence and Lowell. The gift shows an appreciation of the human as well as the mechanical factor in the growth of these communities.

"Mr. Mills' bequests prove anew that a man's deeds are his best monument. They also show that a last will and testament may be the most self-revealing of the documents a man leaves among the written memorials of his life work and his deepest and most heartfelt aspirations."

Mr. Mills was elected an Honorary Member of the American Society of Civil Engineers on November 30, 1909.

HERBERT CLARENDON ALDEN, M. Am. Soc. C. E.*

DIED NOVEMBER 9, 1922.

Herbert Clarendon Alden was born in Newark, N. J., on October 28, 1859. After receiving his preliminary education, he entered New York University from which he was graduated in 1881 with high honors, receiving the degree of B. S. He stood at the head of his class during his entire term in college in all subjects relating in any way to mathematics. Later, Mr. Alden took a post-graduate course at the School of Mines, Columbia University, from which he was graduated in 1884 with the degree of E. M.

On February 1, 1885, he entered the service of the Aqueduct Commissioners of the State of New York as a Rodman on the construction of the difficult tunnel driven about 300 ft. under the Harlem River to form part of what at that time was known as the New Croton Aqueduct. On May 9, 1887, Mr. Alden was appointed an Assistant Engineer on this work, in which position he remained until April 15, 1893, when, the Harlem River Tunnel having been completed, he was transferred to the Engineer Corps of the Aqueduct Commissioners then engaged on the construction of the Carmel Reservoir on the West Branch of the Croton River. Mr. Alden remained on this work until it was completed in the fall of 1897, when he was transferred to the Engineer Corps in charge of the construction of the Jerome Park Reservoir in the Borough of The Bronx.

In connection with Mr. Alden's work with the Aqueduct Commissioners, Edward Wegmann, M. Am. Soc. C. E., writes as follows:

"While in the service of the Aqueduct Commissioners, Mr. Alden was for more than nine years a member of the Engineer Corps, of which I had charge as Division Engineer, and I got to know him, therefore, quite intimately. He was very intelligent, quick, exceedingly zealous and efficient in the performance of his duties, and absolutely honest".

On January 19, 1905, the work on the Jerome Park Reservoir having been completed, Mr. Alden was transferred to the Office of the President of the Borough of The Bronx, in which office he served until his death on November 9, 1922.

While in the employ of the President of the Borough of The Bronx, he was assigned to various works for which his unusual qualifications fitted him. He was connected with the construction of the Storm Relief Tunnel, from Webster Avenue to the Harlem River, which was built to relieve the overcharged condition of the Webster Avenue sewer. This tunnel sewer was equivalent in size to a circle about 12 ft. in diameter, and the work was carried on at certain points under somewhat difficult conditions. While engaged on this work, Mr. Alden found time to make a careful study of the geology of the material through which the tunnel was constructed, and after its completion, he prepared an interesting and comprehensive report of this feature of the work.

During his connection with the Office of the President of the Borough of The Bronx, he also had charge of various important public works and designed several of the large sewers built in the Borough.

* Memoir prepared by Josiah H. Fitch, M. Am. Soc. C. E.

Mr. Alden was unusual in that after having been graduated from college, he maintained, by constant study, his familiarity with higher mathematics, chemistry, geology, and languages. He spoke and read German, French, Italian, and Spanish, and was one of the most widely informed men in the service of the city. He had written books on higher mathematics; no mathematical problem was too deep or too involved for him to solve. He was an expert chemist and toward the latter part of his term of service, his knowledge of chemistry was utilized continually in the testing of all asphalts used for paving in the Borough of The Bronx. For this work a laboratory had been equipped in Borough Hall for his personal use.

Aside from his engineering work, Mr. Alden had a hobby of making, in his leisure hours, musical instruments, such as violins, mandolins, guitars, etc. He was very successful at this work and made instruments of excellent tone.

He had devoted a great deal of his spare time to military service of the State and the United States. He enlisted in the New York National Guard as a Private in the 4th Separate Company, Yonkers, N. Y., on December 27, 1900, and served, subsequently, as Corporal and Sergeant until January 7, 1907. He was appointed First Lieutenant and Battalion Quartermaster of the 10th Infantry, on June 7, 1907, but due to the re-organization of the State forces, he was made a Second Lieutenant of the 10th Infantry, on February 20, 1908. He was appointed a Captain of the Coast Artillery Corps, on December 10, 1910, and assigned to the 8th Coast Defense Command, but, again, due to re-organization, he was appointed First Lieutenant on September 29, 1913, and as such was mustered into the Federal Service on July 15, 1917. He served at Forts Totten and Schuyler until the termination of the World War, and was honorably discharged in 1919.

Mr. Alden's loss to the Engineering Corps in the office of the President of the Borough of The Bronx, City of New York, is one that can never be replaced. There was no subject connected with mathematics, chemistry, geology, or general engineering that, if referred to him, did not receive conscientious study, followed by a comprehensive, intelligent, and complete report.

He died with his lifetime of service to the city, the State, and the country known only to a few intimate associates, but he left a lasting memory of his many wonderful qualities in the hearts of the fortunate few who knew him well.

Mr. Alden was elected an Associate Member of the American Society of Civil Engineers on March 1, 1893, and a Member on February 2, 1909.

AUGUSTUS ELLSWORTH BACHERT, M. Am. Soc. C. E.*

DIED JULY 11, 1922.

Augustus Ellsworth Bachert, the son of William Miller and Suzanna (Messersmith) Bachert, was born in Tamanend, Pa., on August 14, 1862.

* Memoir prepared from information on file at the Headquarters of the Society.

After receiving his preliminary education, Mr. Bachert was employed from 1874 to 1876 as Chainman and Instrumentman on property surveys in Schuykill, Carbon, and Luzerne Counties, Pennsylvania, as well as surveys to settle disputed boundaries between the Philadelphia and Reading Railroad Company, H. A. Weldy and Company, and others, in Schuykill County. From 1876 to 1885, he attended the Millersville Normal School and the Ohio Northern University at Ada, Ohio, from which he was graduated in March, 1885, with the degree of Civil Engineer. During his vacations, Mr. Bachert worked on property surveys, some of which were for the Pennsylvania Railroad Company.

In 1885 and 1886, he was employed as Chainman on surveys on Division III of the South Pennsylvania Railroad, under Gaylord Thompson, M. Am. Soc. C. E., and the late Frank H. Clement, M. Am. Soc. C. E.

In 1886, he accepted the position as Assistant to the late Thomas S. McNair, M. Am. Soc. C. E., Resident Engineer for the Lehigh Valley Railroad Company, on the location and construction of 13 miles of railroad from Hazleton to Delano, Pa. Mr. Bachert had charge of the maintenance of way of the Hazleton, Beaver Meadow, and Mahanoy Divisions of the Lehigh Valley Railroad. He also constructed reservoirs at Hazleton, Park Place, and Delano, and was engaged in mining engineering in Luzerne County, Pennsylvania.

From 1890 to 1895, he held the position of Resident Engineer and Land Agent for the East Broad Top Railroad, the Rockhill Iron and Coal Company, the Broad Top Improvement Company, and the Broad Top Semi-Anthracite Coal Company. His work in this connection consisted of the survey and construction of 7½ miles of extension for the East Broad Top Railroad Company and the construction of Woodvale Shaft for the Coal Companies.

During 1895-96, Mr. Bachert was engaged in architectural work and contracting at Hazleton, McAdoo, and other places in Pennsylvania. In 1896, he again accepted a position as Assistant Engineer to the late Mr. McNair, Chief Engineer for the Cranberry Improvement Company, the Black Creek Improvement Company, the Union Improvement Company, and the Highland Coal Company of Luzerne County, Pennsylvania, and, in this position, he was engaged in railroad, mining, and hydraulic engineering. In 1900, he entered the employ of the H. C. Frick Coke Company as Division Engineer, in charge of the Leisenring Division, in Fayette County, Pennsylvania, consisting of Leisenring Nos. 1, 2, and 3, Trotter, Adelaide, Rist, Henry Clay, Davidson, Youngstown, and Bitner Mines.

On January 1, 1905, Mr. Bachert was appointed Chief Engineer of the Ellsworth Coal Company, at Ellsworth, Pa., and, in April of the same year, he was made General Superintendent of the Rockhill Iron and Coal Company, the Broad Top Improvement Company, and the Broad Top Semi-Anthracite Coal Company, at Robertsdale, Pa. In addition, on January 1, 1907, Mr. Bachert accepted the appointment of Chief Engineer of the East Broad Top Railroad Company, holding both positions until 1909.

For two years following, he was engaged in private practice as a Civil and Mining Engineer. In 1911, Mr. Bachert was appointed Geologist and Mining

Engineer for the Pennsylvania Railroad Company, retaining this position until his death on July 11, 1922.

He was the author of monographs entitled "Huns *versus* American Indian" and "Albigenses, Waldenses and Vaudois Huguenots".

On September 18, 1885, Mr. Bachert was married to Miss Ada E. Weaver who, with two daughters, survives him.

He was a member of Iota Kappa Delta, the American Association for the Advancement of Science, a Fellow of the Royal Society of Arts, a Mason, and a Knight of Malta.

Mr. Bachert was elected a Member of the American Society of Civil Engineers on June 3, 1908.

GEORGE THOMAS BARNSLEY, M. Am. Soc. C. E.*

DIED OCTOBER 23, 1909.

George Thomas Barnsley was born in Montgomery County, Pennsylvania, on January 23, 1864. His paternal ancestors were of good English and French Huguenot stock, who settled on the Delaware River, above Philadelphia, Pa., in 1756. His education was received in the public and private schools of that locality. He entered Swarthmore College with the Class of 1887.

On leaving college, Mr. Barnsley entered the service of the Norfolk and Western Railway Company as Rodman, and rose to the position of Resident Engineer of Construction during the following six years. This and other railroad construction occupied his attention until 1898, when he went to the Pittsburgh District.

After serving about a year in charge of construction of a section of the Buffalo, Rochester, and Pittsburgh Railway, he transferred to the Pennsylvania Railroad in 1899, and was in charge of important surveys and construction work in Western Pennsylvania for the next two years.

In 1901, he was selected to take charge of the construction of the famous Pittsburgh Terminal of the Wabash System. The entry of the Wabash Railway into Pittsburgh, Pa., was a notable achievement. The opportunity here offered to play an important part in carrying out a project surrounded by many physical difficulties, was grasped by Mr. Barnsley, and the line was brought into the heart of the city in spite of the combined opposition of powerful railroad and other interests. Notwithstanding all the physical and financial difficulties, during the following four years the many necessary bridges and tunnels were completed. Emerging from a long tunnel under Mt. Washington, traffic crosses the great cantilever bridge over the Monongahela River, and reaches the extensive passenger and freight terminal at an elevation high above the city streets. Thus are seen at a glance the monuments of skill and enterprise which will long endure and commemorate the notable contest by which a new trunk line secured entrance into Pittsburgh.

* Memoir prepared by Philip W. Price, Assoc. M. Am. Soc. C. E.

After serving as Chief Engineer of the Eastern Extension of the Wabash System, Mr. Barnsley resigned to become Chief Road Engineer of Allegheny County, Pennsylvania, in January, 1906. This position he held until stricken with heart failure while at his desk on October 23, 1909. During this brief period, the work of road improvement in Allegheny County progressed to a marked degree. The system of up-to-date roads in this County was already well and favorably known. The County Commissioners, however, desired to extend and improve the existing road system and selected to take charge of this work the best engineer available. The record for energy and achievement so recently won by Mr. Barnsley made his selection for this task eminently fitting. His untimely death occurred in the midst of a program that contemplated a network of 600 miles of road constructed according to the best standards of that day.

Mr. Barnsley had a host of friends, his kindly and earnest manner winning them rapidly, and holding them thereafter. His interest in the younger members of the profession was marked. The fact that he was always willing to assist them, has kept his memory fresh in the minds of many of the present generation. Deep interest in his fellows led him at an early age to membership in many engineering and other societies. He took a very active part in his local Society—the Engineers' Society of Western Pennsylvania—of which he was President at the time of his death. He was also a member of the following organizations: Engineers' Club of Philadelphia, The Franklin Institute, The American Association for the Advancement of Science, and the Art Society of Pittsburgh.

Mr. Barnsley resided at Oakmont, Pa., for many years, and he was a member of St. Thomas Memorial Protestant Episcopal Church of that place. In 1890, he was married to Susa G. Jones, of Olney, Md., and is survived by his wife and one son, George T. Barnsley, Jr., who reside in Pittsburgh.

Mr. Barnsley was elected a Junior of the American Society of Civil Engineers on May 31, 1892, an Associate Member on May 7, 1894, and a Member on February 6, 1906.

SAMUEL CLARENCE ELLIS, M. Am. Soc. C. E.*

DIED JANUARY 21, 1912.

Samuel Clarence Ellis was born on September 8, 1833, in Oxford, Ohio, where his parents were located temporarily. He was the son of Samuel Ellis and Caroline (Little) Ellis, and a brother of the late General Theodore Granville Ellis, F. Am. Soc. C. E. During his childhood, Mr. Ellis lived in the historic Frankland Mansion, in North Square, Boston, Mass., which had long been the home of his father and grandfather. His mother was the daughter of William Little, an old-time merchant, who lived in the famous Hutchinson Mansion, also in North Square.

Early in life, Mr. Ellis worked as a Civil Engineer on railroad construction. In the spring of 1856, he entered the office of the City Engineer of Boston,

* Memoir prepared by Frank O. Whitney, M. Am. Soc. C. E.

where he remained until the breaking out of the Civil War, when he enlisted and served with the Forty-fifth Massachusetts Regiment. When he left the service, he held the commission of Captain.

Returning to Boston, Mr. Ellis re-entered the office of the City Engineer, where he remained until 1867. He was then assigned to the Surveying Department as Assistant, serving until June, 1891, at which time, he became Chief Engineer of the Boston Board of Survey.

During his service in the City Engineer's office, Mr. Ellis performed many responsible duties in connection with the water-works and bridges. He also had charge of the making of the Public Garden.

In the Surveying Department, he had charge of many important surveys, including the street changes in the Burnt District, after the great fire in 1872; the extension of Washington Street to Haymarket Square, the raising and improving of the Suffolk Street, Church Street, and Northampton Street Districts, as well as the development of the Back Bay.

As Chief Engineer of the Board of Survey, he carried on a systematic co-ordinate survey of the city, including a comprehensive platting of an up-to-date street system.

Mr. Ellis retired from active practice of his profession in July, 1895. He continued his residence in Boston, however, until his death, which occurred on January 21, 1912.

Mr. Ellis was never married. He was a member of the Boston Society of Civil Engineers. He was also a Veteran Member of the Cadets, a member of Post 113, G. A. R., and of the Loyal Legion.

He was elected a Member of the American Society of Civil Engineers, on August 7, 1872.

FREDERICK GIDDINGS, M. Am. Soc. C. E.*

DIED DECEMBER 13, 1922.

Frederick Giddings was born in Bristol, England, on April 29, 1842. He came to this country when he was twenty-one years old, and completed extensive studies in the Canadian Military School, at Toronto, Ontario, afterward engaging in the work which became his profession, Civil Engineering, as follows:

1866, Rodman on the Winona and St. Peter Railroad, in Minnesota, and the La Crosse, Trempeleau and Prescott Railroad, in Wisconsin; 1867, on the construction of the Flint and Pere Marquette Railroad, in Michigan; 1869, Instrumentman and Assistant to the Division Engineer on the construction of the Missouri River, Fort Scott, and Gulf Railroad, in Kansas; 1870 to 1872, Assistant Engineer on the construction of the Leavenworth, Lawrence, and Galveston Railroad, in Kansas; 1872, Engineer on the Sheboygan and Fond du Lac Railroad, in Wisconsin; January, 1873, to December, 1880, Engineer

* Memoir prepared by C. M. Rathburn, Pres., Atchison Union Depot & R. R. Co., Atchison, Kans.

on the Atchison and Nebraska Railroad, extending from Atchison, Kans., to Lincoln, Nebr.; as Chief Engineer, Mr. Giddings had charge of the construction of an extension of this road from Lincoln to Columbus, Nebr., known as the Lincoln and Northwestern Railway; 1881-82, with the St. Paul, Minneapolis and Manitoba Railway, as Assistant Engineer in charge of bridges, buildings, and water stations; later, he had charge of the construction of the line from St. Cloud to Hinckley, Minn.; 1883, in private practice, at Atchison, Kans.; 1884-85, Assistant Engineer in charge of a division on the reconstruction of the St. Joseph and Des Moines Railroad, in Missouri; April, 1885, to date of his retirement (except one year), City Engineer of Atchison, Kans.; during this period, he also served as County Surveyor of Atchison County for five years, and as County Bridge Engineer for about ten years.

On January 28, 1879, Mr. Giddings was married to Miss Mary Taliaferro of Atchison, Kans., the wedding taking place in Trinity Protestant Episcopal Church, of which Mr. Giddings was always an active member, serving successively as First Vestryman, Junior Warden, and Senior Warden.

Mr. Giddings was a member of the American Society for Municipal Improvements, having served one year as Vice-President and one year as President.

He was a 32d Degree Scottish Rite Mason, a Shriner, and a Charter Member of the Atchison Benevolent Protective Order of Elks, of which he was Exalted Ruler for one year.

Mr. Giddings died in Charlotte, N. C., on December 13, 1922, and is survived by two daughters, Mrs. Christine G. Hereford, of Charlotte, N. C., and Mrs. Edwynne G. Allen, of Albuquerque, N. Mex. He was buried in Mt. Vernon Cemetery, Atchison, Kans.

During the last few years of his life, Mr. Giddings was prominent as a Consulting Engineer. He was a man of splendid ability in his profession, of the highest integrity, strict in all his business relations, and possessed of a most kindly disposition and charming personality.

Mr. Giddings was elected a Member of the American Society of Civil Engineers, on June 6, 1906.